NASA TM X-390

TECHNICAL MEMORANDUM

X-390

INVESTIGATION AT MACH NUMBERS OF 0.60 TO 3.50 OF BLENDED WING-BODY COMBINATIONS WITH CAMBERED AND TWISTED WINGS WITH DIAMOND, DELTA AND ARROW PLAN FORMS

By George H. Holdaway and Jack A. Mellenthin

Ames Research Center
Moffett Field, Calif.

NATIONAL AERONAUTICS AND SPACE ADMINISTRATION
WASHINGTON

October 1960
Declassified September 1, 1961

NATIONAL AERONAUTICS AND SPACE ADMINISTRATION

TECHNICAL MEMORANDUM X-390

INVESTIGATION AT MACH NUMBERS OF 0.60 TO 3.50 OF BLENDED WING-BODY COMBINATIONS WITH CAMBERED AND TWISTED WINGS WITH DIAMOND, DELTA, AND ARROW PLAN FORMS

By George H. Holdaway and Jack A. Mellenthin

SUMMARY

This investigation is a continuation of the experimental and theoretical evaluation of blended wing-body combinations. The basic diamond, delta, and arrow plan forms which had an aspect ratio of 2 with leading-edge sweeps of 45.00°, 59.04°, and 70.82° and trailing-edge sweeps of -45.00°, -18.43°, and 41.19°, respectively, are used herein as standards for evaluating the effects of camber and warp. The wing thickness distributions were computed by varying the section shape along with the body radii (blending process) to match the prescribed area distribution and wing plan form. The wing camber and warp were computed to try to obtain nearly elliptical spanwise and chordwise load distributions for each plan form and thus to obtain low drag due to lift for a range of Mach numbers for which the velocities normal to the wing leading edge are subsonic. Elliptical chordwise load distributions were not possible for the plan forms and design conditions selected, so these distributions were somewhat different for each plan form. The models were tested with transition fixed at Mach numbers from 0.60 to 3.50 and at Reynolds numbers, based on the mean aerodynamic chord of the wing, of roughly 4,000,000 to 9,000,000.

At speeds where the velocities normal to the wing leading edges were supersonic, an increase in the experimental wave-drag coefficients due to camber and twist was evident, but this penalty decreased with increased sweep. Thus the minimum wave-drag coefficients for the cambered arrow model were almost identical with the zero-lift wave-drag coefficients for the uncambered arrow model at all test Mach numbers.

With each plan form the camber and twist resulted in a reduction in drag due to lift at all Mach numbers below the design speed (different for each plan form). At test Mach numbers greater than the design values, the camber and twist did not cause increases or penalties in drag due to lift. Near the design Mach numbers the theoretical reductions in drag due to lift were experimentally realized best for the cambered delta model and only partially realized for the cambered arrow model. With each plan form the camber and twist were very effective in reducing the drag due to lift at transonic speeds. The effects of camber and twist on the other aerodynamic parameters were generally slight. The experimental results for the cambered models were most accurately predicted with linear theory for the cambered delta model.

INTRODUCTION

The investigation reported in references 1, 2, and 3 on the evaluation of blended wing-body combinations has been extended herein to similar models with the wings altered to have camber and twist. The procedure used to design the load distribution of the wings is based on the theory of reference 4 and is described briefly here and in more detail in appendix B. In reference 4 a triangular wing was designed to have approximately elliptical load distributions in both the spanwise and chordwise directions to approach the minimum drag due to lift as suggested in reference 5 for narrow wings lying near the center of the Mach cone. The plan forms previously selected in the investigation were not considered to be optimum for the procedures of reference 4, but rather as useful in demonstrating design variables. Although the spanwise load distributions were designed to be approximately elliptical for each plan form, the chordwise distributions could not be, so the smoothest chordwise distribution which approached an elliptic distribution was selected in each case. The symbols used in the report are listed in appendix A.

MODELS AND TESTS

Representative wing sections and other geometric details of the cambered and twisted models are illustrated in figures 1(a) through 1(c). The radii of the bodies used for the cambered and twisted models are listed in table I and are identical with those of reference 2. As in the previous part of the total investigation, the delta models are evaluated without the rearward body bump and thus have the different area distributions shown in figure 2.

Photographs showing the three basic plan forms of the models are presented in figure 3. The coordinates and thicknesses of the cambered

wings are listed in tables II through IV and may also be used to define the coordinates of the basic or symmetrical configurations which are defined fully in reference 2. These wing thickness distributions were computed by varying the section shape along with the body radii (blending process) to match the prescribed area distribution and wing plan form. The symmetrical wings were formed by straight-line elements perpendicular to the model center line forming triangular spanwise sections. Straight-line elements at constant percent chord stations were used to design wing camber and twist. Thus the wing twist and camber were introduced such that the wing plan forms and thickness distributions were unaltered at the reference spanwise stations and for regions of the wing with little sweep of the percent chord lines. For other regions of the wings (between reference spanwise stations) the straight-line fairing between constant percent chord points usually resulted in a slight thickening of the cambered wings relative to the symmetrical wings. The details of the design of the cambered models are given in appendix B; however, the similarity and differences in the selected design conditions for the different plan forms are summarized in the following table:

	$\eta = m\sqrt{M^2-1}$	M	$C_{L_{opt}}$	$C_{D_i}/C_L{}^2$
Cambered diamond	0.9	1.345	0.19	0.253
Cambered delta	.9	1.805	.15	.353
Cambered arrow	.9	2.773	.12	.444

The similarity in design is identified by the constant value of η, less than 1, which defines subsonic leading-edge conditions in each case.

The wing sections of the arrow models were designed with blunt trailing edges as discussed in references 2 and 3. For wing cross sections perpendicular to the body center line, the trailing-edge thicknesses of the arrow wings were half the ridge-line thickness except near the body juncture and the model center line ($y \sim 0$) as shown in tables VI and VII. The wing sections had an average value of maximum thickness of about 4 percent of the local chords in a streamwise direction with the greater thickness ratios inboard.

The models were tested at the Ames Research Center in the 14-Foot Transonic Wind Tunnel, and in the 9- by 7-foot and 8- by 7-foot supersonic test sections of the Ames Unitary Plan Wind Tunnel. Representative photographs of some of the models in the high-speed test regions of the wind tunnels are presented in figures 4(a) through 4(c). The ranges of the test variables in each facility are shown in the following table:

Wind tunnel throat	Models	M	R/ft	α, deg	Transition
14-Foot	All	0.60 to 0.80	3,500,000 to 4,000,000	-2 to 12	Fixed 0.04 in. grit
14-Foot	All	0.80 to 1.20	4,000,000	-2 to 9	
9- by 7-Foot	All	1.55 to 2.35	3,000,000	-2 to 13	
8- by 7-Foot	All except the diamond models	2.50 to 3.50	2,000,000	-3 to 15	
8- by 7-Foot	Diamond model	2.50 to 3.00	4,000,000	-2 to 12	
8- by 7-Foot	Diamond model	3.00 to 3.50	3,000,000	-2 to 12	

The cambered diamond model was also tested in the 9- by 7-foot supersonic test section with a smaller transition grit (0.023 in. average).

Three-component aerodynamic forces and moments were measured and corrected by standard procedures. For the model sizes and shapes, the force corrections for blockage and buoyancy were generally found to be negligible. At all Mach numbers, the drag coefficients were adjusted by equating the body base pressures to free-stream static pressures. All aerodynamic coefficients are based on the complete plan-form area of the wings of 800 square inches. The pitching-moment coefficients were computed about longitudinal centers as shown in figures 1(a) through 1(c). These moment centers were selected to give approximately a 10-percent static longitudinal stability margin at M=0.60 for each model.

Transition was fixed with one grit size and one location, the same as used for the tests of references 1 and 2, in order to prevent a secondary effect from influencing the basic results of this test. The grit average height was about 0.040 inch and the grit was located 1.13 inches rearward of the wing leading edges (upper and lower surfaces) and of the body nose in a streamwise direction. All the data presented are with transition fixed and include a drag-coefficient penalty attributed to the grit of about 0.0003 which was not due to fixing transition.

RESULTS

The basic test data for the cambered models are presented jointly with previously obtained results for the symmetrical models in figures 5(a) through 12(c), so that direct evaluations of the effects of the camber and twist can be made. The results for the diamond models are presented

first and are grouped as to the test facility (transonic and then supersonic to M=2.35). The aerodynamic data for the delta and arrow models follow in order and are presented in a manner similar to that used for the diamond models; however, the data are presented at Mach numbers up to 3.50.

There are two results presented in these basic plots which will not be apparent in the following cross plots and should be noted. The results of figure 6(d) show that almost doubling the grit size had very little effect on the drag coefficients of the cambered diamond model. Attention is next directed to figures 7(d), 8(c), and 9(c) which show that the cambered delta model was self trimming at lift coefficients which decreased from 0.12 at M=0.60 to 0.01 at M=3.50.

Cross plots of the variation in the aerodynamic parameters with Mach number will be presented when discussed in the following sections of the report. In order to clarify the differences in the test Reynolds numbers with Mach number, figure 13 is presented. Also note that for Mach numbers above 2.50 the diamond model was generally tested at higher Reynolds numbers than the other models; however, the effects of the Reynolds number changes were not large as was discussed in reference 2.

DISCUSSION

The discussion is presented in two parts. The first section is concerned with the drag characteristics as a function of Mach number (wave drag, drag due to lift, and base drag), and the second portion is concerned with the variation with Mach number of maximum lift-drag ratios, lift-curve slopes, and aerodynamic-center locations as indicated by theory and experiment. In each case the presentations are made in a form to illustrate directly the combined effects of the camber and twist on the aerodynamic characteristics of each plan form. No effort is made to compare plan forms as was done in reference 2.

Drag Characteristics

The experimental zero-lift wave-drag coefficients for the symmetrical models are presented in figure 14 with the minimum wave-drag coefficients for the cambered models. The similarity between these wave-drag coefficients of the symmetrical and cambered models at transonic speeds indicate that at these speeds there is only a slight penalty due to the camber and to the slight increase in thickness of the cambered models. At speeds where the velocities normal to the wing leading edges are supersonic, a greater penalty in wave drag due to

camber is evident; but this penalty decreased with increased sweep. Thus the minimum wave-drag coefficients for the cambered arrow model are almost identical with the zero-lift wave-drag coefficients for the arrow model.

In figures 15(a) through 15(c) experimental values of the drag due to lift parameter, C_{D_i}/C_L^2, for the symmetrical and cambered models are compared with similar theoretical values for flat plate wings of the same plan form with and without leading-edge thrust. The theoretical results for the flat-plate wings have been previously presented in reference 2 and are based on reference 6. The camber and twist for the diamond plan form resulted in reductions in the drag due to lift parameter at all test Mach numbers up to 2.35, the limit of the comparisons, although at Mach numbers above the design value of 1.345 the improvements were slight. The camber and twist was very successful in reducing the drag due to lift of the delta plan form; the reductions were equally as great as indicated by theory (M=1.805, fig. 15(b)). As with the cambered diamond models the cambered delta model showed less improvement in the drag due to lift parameter at Mach numbers above its design value of 1.805. The camber and twist of the arrow plan form was effective in reducing the drag due to lift parameter, relative to the symmetrical model, over the entire Mach number range as shown in figure 15(c). However, at the design Mach number of 2.773, the calculated reduction in drag due to lift (relative to the theory without leading-edge thrust) was only partially realized experimentally by cambering the arrow wing. Greater reductions in drag due to lift might have been realized at lower Mach numbers if the design Mach numbers were lower (e.g., $\eta = 0.5$); however, such an approach would have reduced the range of Mach numbers for which improvements would be important and, in each case, the present designs were very effective in reducing the drag due to lift at transonic Mach numbers.

The experimental and theoretical variation with Mach number in wing and body base-drag coefficients for the arrow and cambered arrow models are presented in figure 16. The theoretical base-drag coefficients have been discussed relative to the arrow model in reference 2. Of course, at all Mach numbers, the drag coefficients were adjusted by equating the body (not the wing) base pressures to free-stream static pressures. The wing camber and twist had a negligible effect on the wing base-drag coefficients for the arrow wing as presented in reference 2.

Other Aerodynamic Variables

The maximum lift-drag ratio is the aerodynamic parameter of primary interest in evaluating the usefulness of a cambered wing design. Trends with Mach number of the maximum lift-drag ratios, lift-curve

slopes, and aerodynamic center locations for the diamond and cambered diamond models as indicated by experiment and theory are presented in figures 17(a) through 17(c). Similar results for the delta models are presented in figures 18(a) through 18(c) and for the arrow models in figures 19(a) through 19(c).

The agreement between experiment and theory is quite good for the symmetrical models as was discussed in reference 2. For the cambered models the theoretical predictions (at the design Mach number) were best for the cambered delta models (figs. 18(a) and 18(b)). With each plan form the camber and twist had little effect on the lift-curve slopes and the aerodynamic-center position, but resulted in improvements in maximum lift-drag ratios at transonic speeds. However, at the higher Mach numbers up to 3.50 the effects on the maximum lift-drag ratios were slight. At Mach numbers from 2.50 to 3.50 the maximum lift-drag ratios for the cambered delta model (fig. 18(a)) were consistently lower than corresponding values for the delta model. This result can be directly attributed to the higher minimum wave drag coefficients for the cambered delta model shown in figure 14(b) and discussed previously (supersonic leading-edge conditions). The equally powerful effect of the zero-lift (or minimum) wave-drag coefficients, relative to the drag due to lift, on the maximum lift-drag ratios was also noted and discussed in references 2 and 3. The need for further improvement or reduction in zero-lift wave-drag coefficients (particularly at supersonic leading-edge conditions for the diamond model) has been made evident in all parts of the total investigation and prompted the analytical investigation presented in the appendix of reference 3.

The previous discussion has covered most of the parameters considered in the design of the cambered wings except the optimum lift coefficient. Thus for comparison with the selected design conditions presented in the models and test section of this report, the experimental results of the optimum lift coefficients near the design Mach numbers are included in the following table:

		M	C_{D_i}/C_L^2	$C_{L_{opt}}$
Cambered diamond model	Experiment	1.20	0.242	0.184
	Theory	1.345	0.253	0.190
	Experiment	1.55	0.327	0.228
Cambered delta model	Experiment	1.55	0.257	0.187
	Theory	1.805	0.353	0.150
	Experiment	1.95	0.352	0.146
Cambered arrow model	Experiment	2.70	0.520	0.133
	Theory	2.773	0.444	0.120

Note that the experimental results for the cambered delta model at M=1.95 are better than would be expected from the theory and the experimental variations with Mach number.

CONCLUDING REMARKS

The following statements apply to the combined effects of the specific camber and twist investigated with blended wing-body combinations at Mach numbers up to 3.50 with transition fixed.

With each plan form the camber and twist resulted in a reduction in drag due to lift at all Mach numbers below the design speed (different for each plan form). At test Mach numbers greater than the design values, no increases or penalities in drag due to lift were obtained. Near the design Mach number the theoretical reductions in drag due to lift were best realized experimentally for the cambered delta model and only partially realized for the cambered arrow model. With each plan form the camber and twist was very effective in reducing the drag due to lift at transonic Mach numbers.

At speeds where the velocities normal to the wing leading edges were supersonic, an increase in experimental wave drag due to camber and twist was evident; but this penalty decreased with increased sweep. Thus the minimum wave-drag coefficients for the cambered arrow models were almost identical with the zero-lift wave-drag coefficients for the arrow model at all test Mach numbers.

With each plan form the camber and twist resulted in significant improvements in the maximum lift-drag ratios at transonic speeds; however, at the higher Mach numbers the effects were generally slight and reflected the previously discussed drag characteristics.

Ames Research Center
National Aeronautics and Space Administration
Moffett Field, Calif., June 7, 1960

APPENDIX A

SYMBOLS

A	aspect ratio
A_{bb}	body base area
A_{wb}	wing base area projected on a plane perpendicular to the conventional x axis
b	wing span
$C_{1\cdots4}$	arbitrary constants of the lifting-pressure distribution
C_D	drag coefficient (All aerodynamic coefficients are based on the total wing area.)
$C_{D_{bb}}$	body base-drag coefficient
$\frac{C_{Di}}{C_L^2}$	drag due to lift parameter
$C_{D_{wb}}$	wing base-drag coefficient
C_L	lift coefficient
$C_{L_{opt}}$	lift coefficient at $\left(\frac{L}{D}\right)_{max}$
C_{L_α}	lift-curve slope, per deg
C_m	pitching-moment coefficients computed about centers shown in figures 1(a) through 1(c)
c	local wing chord
c_d	wing section drag coefficient
c_l	wing section lift coefficient
c_R	center line on wing-root chord
$\bar{c}$	mean aerodynamic chord
k	$\frac{m}{m_1}$

$\left(\frac{L}{D}\right)_{max}$	maximum lift-drag ratio
L.E.	wing leading edge
l	model length
M	Mach number
m	cotangent of sweepback angle of wing leading edge
m_1	cotangent of sweepback angle of wing trailing edge
N	total number of terms or harmonics used in computing ΔC_{D_o}
P	pressure coefficient
q	dynamic pressure
R	Reynolds number
r	body radius
r_b	body base radius
S_w	total wing area
t	wing thickness
X	airfoil percent thickness term in NACA 65(06)A00X airfoil designation
x,y,z	conventional body axes measured from the model or wing section nose
x_1	x station measured from leading edge of wing center-line chord
V	volume
α	angle of attack
β	$\sqrt{M^2-1}$
$\Delta C_{D_{o_{min}}}$	minimum wave-drag coefficient
ΔC_{D_o}	zero-lift wave-drag coefficient
η	$m\sqrt{M^2-1}$ or βm

θ roll angle of a cutting plane tangent to a Mach cone as measured between the z axis and the intersection of the cutting plane with the y,z plane

Λ angle of sweepback

λ wing taper ratio

ξ $\frac{x_1}{c_R}$

σ $\frac{|y|}{b/2}$

APPENDIX B

DESIGN OF THE CAMBER AND TWIST OF THE WINGS

The lifting pressure distribution over the assumed wings of zero thickness was taken to have the same form as that used in reference 4:

$$\frac{P}{C_L} = \frac{C_1}{C_L} + (1-k)\frac{C_2}{C_L}\xi + \frac{C_3}{C_L}\sigma - \frac{C_4}{C_L}\sigma^2 \qquad (1)$$

The spanwise load distribution was computed in reference 4 to be approximately elliptical for all pointed wings if three of the arbitrary constants were defined as follows:

$$\left.\begin{aligned} \frac{C_1}{C_L} &= \frac{4k}{(1+k)\pi} + \frac{1-k}{1+k}\frac{C_3}{C_L} \\ \frac{C_2}{C_L} &= \frac{4}{(1+k)\pi} - \frac{2}{1+k}\frac{C_3}{C_L} \\ \frac{C_4}{C_L} &= 6 - \frac{16}{\pi} \end{aligned}\right\} \qquad (2)$$

The selection of the fourth constant C_3 may be taken to define a trim condition or a chordwise load distribution.

The chordwise lifting-pressure distribution was computed at a series of wing stations ξ by performing spanwise integrations as follows (made dimensionless by the wing semispan, b/2):

$$\frac{\text{local lift}}{\text{total lift}} = \frac{2\sigma C_2(\xi)q}{S_w C_L q} = 2\int \frac{P}{C_L}\, d\sigma \qquad (3)$$

With the resulting equations derived for each plan form the chordwise load distributions were investigated for various values of C_3/C_L for the following design conditions:

Camber and twist design parameters	Diamond	Delta	Arrow
Λ_{LE}	45.80°	59.04°	70.82°
Λ_{TE} (Values for diamond arbitrarily selected to make acceptable theoretical computations)	-42.00° (-45° actual)	-18.43°	41.19°
$m = \cot \Lambda_{LE}$	1.0000	0.6000	0.3478
$m_1 = \cot \Lambda_{TE}$	-1.1111	-3.0000	1.1430
$k = \frac{m}{m_1}$	-0.900	-0.200	0.3043
$\eta = m\sqrt{M^2-1}$ (Selected as the acceptable maximum)	0.9	0.9	0.9
M (design)	1.345	1.803	2.773
C_{D_i}/C_L^2 (design)	0.253	0.353	0.444
$C_{L_{opt}}$ (design)	0.19	0.15	0.12
M for sonic leading edge	1.414	1.944	3.044
M for sonic trailing edge	1.414 (actual) 1.345 (comp.)	1.054	1.329

The variations in the shape of the chordwise load distributions with C_3/C_L are shown in figure 20 for each wing plan form. For the plan forms and conditions selected, elliptic chordwise distributions were not possible; however, the smoothest chordwise distribution which roughly approached an elliptic distribution was selected in each case with the resultant design curves shown in figure 21.

With the numerical values of the constants C_1 through C_4 selected, table I of reference 4 was used to compute the dimensionless shapes of the mean camber lines as shown in figures 22(a) through 22(c). To obtain the wing ordnates the wings were first rotated in a negative α direction so that the chord line of the camber line at $\sigma = 0.10$ was zero. Next the dihedral was largely eliminated to permit easier fabrication; this was suggested as permissible in moderation in reference 4 (i.e., the wing shape may be altered by a set of ordinates which depend only on σ and not on x). Then the design lift coefficients ($C_{L_{opt}}$ previously listed) were computed in three steps and mechanically integrated as follows:

$$\frac{c_{d_m}}{c_R C_L^2} = \int \frac{z}{c_R} \frac{m}{C_L} d\left(\frac{P}{C_L}\right) \tag{10}$$

$$\frac{C_{D_i}}{C_L^2} = \frac{2c_R(b/2)}{mS_w} \int_0^1 \frac{c_{d_m}}{c_R C_L^2} d\sigma \tag{11}$$

$$C_{L_{opt}} = \sqrt{\frac{C_{D_o}}{C_{D_i}/C_L^2}} \tag{12}$$

The estimated values of C_{D_o} used in equation (12) to determine the design lift coefficients did not include the drag of the grit used to fix transition or the wing base drag in the case of the cambered arrow model. The design lift coefficients were used to determine the actual z values of the mean camber lines.

Finally the wing thickness and camber ordinates were combined, which involved some compromise in the definition of the wing elements. The camber lines were defined at percent chord locations and the wing thicknesses were defined by straight-line elements perpendicular to the model center line. Thus the wing twist and camber were introduced such that the wing plan forms and thicknesses were unaltered at the reference spanwise stations (σ = 0, 0.1, 0.2, 0.4, 0.6, 0.7, 0.8, 0.9, 0.95 and 1.0) and for the regions between where the percent chord lines had little sweep. For other regions of the wings (between reference spanwise stations) the straight-line fairing between constant percent chord points usually resulted in a few thousands of an inch thickening of the cambered wings. The experimental wave-drag results of figure 14 indicate that the effect of the increased thickness of the cambered wings was negligible.

REFERENCES

1. Holdaway, George H., Mellenthin, Jack A., and Hatfield, Elaine W.: Investigations at Mach Numbers of 0.20 to 3.50 of a Blended Diamond Wing and Body Combination of Sonic Design But With Low Wave-Drag Increase With Increasing Mach Number. NASA TM X-105, 1959.

2. Holdaway, George H., and Mellenthin, Jack A.: Investigation at Mach Numbers of 0.20 to 3.50 of Blended Wing-Body Combinations of Sonic Design With Diamond, Delta, and Arrow Plan Forms. NASA TM X-372, 1960.

3. Holdaway, George H., and Mellenthin, Jack A.: Evaluation of Blended Wing-Body Combinations With Curved Plan Forms at Mach Numbers up to 3.50. NASA TM X-379, 1960.

4. Tucker, Warren A.: A Method for the Design of Sweptback Wings Warped to Produce Specific Flight Characteristics at Supersonic Speeds. NACA Rep. 1226, 1959. (Supersedes NACA RM L51F08)

5. Jones, Robert T.: The Minimum Drag of Thin Wings in Frictionless Flow. Jour. Aero. Sci., vol. 18, no. 2, Feb. 1951, pp. 75-81.

6. Mueller, James N., and Grimaud, John E.: Effects of Twist and Camber and Thickness on the Aerodynamic Characteristics of a 75° Swept Arrow Wing at a Mach Number of 2.91. NASA TM X-138, 1959.

7. Puckett, A. E., and Stewart, H. J.: Aerodynamic Performance of Delta Wings at Supersonic Speeds. Jour. Aero. Sci. vol. 14, no. 10, Oct. 1947, pp. 567-578.

8. Love, Eugene S.: Base Pressures at Supersonic Speeds on Two-Dimensional Airfoils and on Bodies of Revolution With and Without Fins Having Turbulent Boundary Layers. NACA TN 3819, 1957.

9. Holdaway, George H., and Mersman, William A.: Application of Tchebichef Form of Harmonic Analysis to the Calculation of Zero-Lift Wave Drag of Wing-Body-Tail Combinations. NACA RM A55J28, 1956.

TABLE I.- COORDINATES FOR BODIES, INCHES

Diamond and cambered diamond		Delta and cambered delta			Arrow and cambered arrow		
x	r	x		r	x		r
0	0						
.375	.079						
.750	.148						
1.500	.258						
2.250	.356						
3.000	.449						
3.750	.542						
4.500	.623						
5.250	.693						
6.000	.761						
6.750	.830						
7.500	.903						
8.250	.976						
9.000	1.042						
9.750	1.116						
10.500	1.179						
11.250	1.238						
12.000	1.296						
12.750	1.353						
13.125	1.388						
13.875	1.448						
14.625	1.509						
15.375	1.570						
16.125	1.630						
16.875	1.688						
17.500	1.733						
18.000	1.762						
19.000	1.823						
19.300	1.860						
20.000	1.874						
21.000	1.825						
22.000	1.712						
24.000	1.471						
24.800	1.392						
26.000	1.347						
26.400	1.360						
28.000	1.405						
29.600	1.447						
31.200	1.487						
32.800	1.522						
33.600	1.539						
34.400	1.554						
35.200	1.569						
36.000	1.582						
36.800	1.594						
37.600	1.605						
38.400	1.614						
39.200	1.621						
40.000	1.625						
51.000	1.625						
52.000	1.657						
53.000	1.730						
54.000	1.827						
55.000	1.878						
55.640	1.860						
55.875	1.846						
56.625	1.795						
57.300	1.747						
57.600	1.728						
57.900	1.709						
58.200	1.692						
58.500	1.677						
58.800	1.662						
59.100	1.649						
59.400	1.637						
59.700	1.629						
60.000	1.625						
		10.683		1.190	10.400		.739
		11.000		1.210			
		12.000		1.216	12.000		.816
		13.000	Blended body	1.169			
		14.000		1.099	13.600		.890
		15.000		1.057	15.200		.960
		16.000		1.035			
		16.800		1.026	16.800		1.026
		18.400		1.089	18.400		1.089
		19.200		1.119	19.200		1.119
		20.000		1.149	20.000		1.149
		20.800		1.178	20.800		1.178
		21.600		1.206	21.600		1.206
		23.200		1.260	23.200		1.260
		24.800		1.311	24.800		1.311
		26.400		1.360	26.400		1.360
		28.000		1.405	28.000		1.405
		29.600		1.447	29.600		1.447
		31.200		1.487	31.200		1.487
		32.800		1.522	32.800		1.522
		33.600		1.539	33.600		1.539
		34.400		1.554	34.400		1.554
		35.200		1.569	35.230		1.570
		36.000		1.582	36.000		1.620
		36.800		1.594	37.000		1.660
		37.600		1.605	38.000		1.690
		38.400		1.614			
		39.200		1.621	39.000		1.705
		40.000		1.625	40.000		1.718
					40.500		1.725
					41.000		1.735
					41.532		1.751
					42.000		1.776
					43.000		1.821
					45.000	Blended body	1.906
					47.000		1.975
					49.000		2.011
					51.000		2.000
					53.000		1.942
		54.100		1.625			
		54.500		1.637			
		55.000	Fairing	1.655	55.000		1.872
		56.000		1.688	56.000		1.825
		57.000		1.711	57.000		1.767
		57.600		1.728	57.500		1.732
					57.600		1.728

[1]Body equivalent to design area curve

[2]Part of a von Kármán ogive (l = 40 in. and r_b = 1.626 in.)

TABLE II.- COORDINATES FOR THE CAMBERED DIAMOND WING, INCHES

(a) Inboard portion of wing panel

x	y = 0			y = 2			y = 4			y = 8		
	Ordinates		t	Ordinates		t	Ordinates		t	Ordinates		t
	Top	Lower		Top	Lower		Top	Lower		Top	Lower	
17.500	0	0	0									
18.000	.470	-.470	.940									
18.500	.685	-.685	1.370									
19.000	.824	-.824	1.648									
19.500	.926	-.926	1.852	0.001	0.001	0						
20.000	1.010	-1.010	2.020	.225	-.179	.404						
20.500	1.047	-1.047	2.094	.387	-.311	.698						
21.000	1.070	-1.070	3.140	.509	-.409	.918						
21.500	1.089	-1.089	2.178	.604	-.486	1.090	-0.095	-0.095	0			
22.000	1.098	-1.098	2.196	.675	-.545	1.220	.052	-.192	.244			
23.000	1.086	-1.086	2.172	.766	-.616	1.382	.258	-.334	.592			
24.000	1.050	-1.050	2.100	.806	-.648	1.454	.390	-.418	.808			
25.000	.996	-.996	1.992	.810	-.650	1.460	.466	-.464	.930			
25.500										-0.087	-0.087	0
26.000	.925	-.925	1.850	.784	-.630	1.414	.502	-.478	.980	-.007	-.115	.108
27.000	.858	-.858	1.716	.750	-.604	1.354	.516	-.476	.992	.109	-.161	.270
28.000	.799	-.799	1.598	.714	-.580	1.294	.520	-.470	.990	.188	-.192	.380
29.000	.755	-.755	1.510	.684	-.564	1.248	.519	-.465	.984	.245	-.215	.460
30.000	.724	-.724	1.448	.659	-.557	1.216	.520	-.464	.984	.288	-.234	.522
31.000	.702	-.702	1.404	.642	-.554	1.196	.521	-.467	.988	.318	-.254	.572
32.000	.685	-.685	1.370	.627	-.555	1.182	.520	-.472	.992	.343	-.271	.614
33.000	.677	-.677	1.354	.617	-.563	1.180	.524	-.480	1.004	.364	-.292	.656
34.000	.670	-.670	1.340	.609	-.569	1.178	.526	-.490	1.016	.379	-.311	.690
35.000	.661	-.661	1.322	.598	-.572	1.170	.524	-.496	1.020	.390	-.328	.718
36.000	.640	-.640	1.280	.580	-.562	1.142	.512	-.492	1.004	.389	-.337	.726
37.000	.612	-.612	1.224	.554	-.544	1.098	.494	-.478	.972	.379	-.343	.722
37.500	.594	-.594	1.188	.539	-.531	1.070	.481	-.469	.950	.370	-.342	.712
38.000	.610	-.610	1.220	.550	-.544	1.094	.489	-.481	.970	.369	-.351	.720
39.000	.631	-.631	1.262	.564	-.562	1.126	.496	-.494	.990	.358	-.358	.716
40.000	.643	-.643	1.286	.569	-.569	1.138	.496	-.496	.992	.338	-.360	.698
41.000	.649	-.649	1.298	.570	-.570	1.140	.491	-.493	.984	.313	-.355	.668
42.000	.650	-.650	1.300	.566	-.566	1.132	.481	-.483	.964	.284	-.346	.630
43.000	.649	-.649	1.298	.560	-.560	1.120	.469	-.471	.940	.250	-.332	.582
44.000	.655	-.655	1.310	.562	-.554	1.116	.463	-.459	.922	.216	-.318	.534
45.000	.667	-.667	1.334	.572	-.548	1.120	.460	-.448	.908	.178	-.302	.480
46.000	.683	-.683	1.366	.588	-.540	1.128	.457	-.433	.890	.136	-.280	.416
47.000	.710	-.710	1.420	.614	-.536	1.150	.459	-.421	.880	.088	-.250	.338
48.000	.744	-.744	1.488	.644	-.530	1.174	.459	-.403	.862	.027	-.207	.234
49.000	.787	-.787	1.574	.680	-.524	1.204	.456	-.378	.834	-.051	-.143	.092
49.500										-.101	-.101	0
50.000	.845	-.845	1.690	.721	-.519	1.240	.445	-.343	.788			
51.000	.924	-.924	1.848	.766	-.514	1.280	.421	-.291	.712			
51.500	.970	-.970	1.940	.788	-.506	1.294	.397	-.249	.646			
52.000	1.020	-1.020	2.040	.806	-.492	1.298	.361	-.195	.556			
52.500	1.048	-1.048	2.096	.803	-.455	1.258	.303	-.117	.420			
53.000	1.061	-1.061	2.122	.781	-.399	1.180	.222	-.004	.226			
53.500	1.065	-1.065	2.130	.743	-.323	1.066	.116	.116	0			
54.000	1.060	-1.060	2.120	.682	-.226	.908						
54.500	1.045	-1.045	2.090	.595	-.101	.696						
55.000	1.011	-1.011	2.022	.468	.064	.404						
55.500	.942	-.942	1.884	.286	.286	0						
56.000	.842	-.842	1.684									
56.500	.712	-.712	1.424									
57.000	.500	-.500	1.000									
57.500	0	0	0									

TABLE II.- COORDINATES FOR THE CAMBERED DIAMOND WING, INCHES - Concluded

(b) Outboard portion of wing panel

x	y = 12			y = 14			y = 16			y = 18			y = 19			y = 20		
	Ordinates		t	Ordinates		t	Ordinates		t	Ordinates		t	Ordinates		t	Ordinates		t
	Top	Lower		Top	Lower		Top	Lower		Top	Lower		Top	Lower		Top	Lower	
29.500	-0.079	-0.079	0															
30.000	-.022	-.080	.058															
31.000	.060	-.096	.156															
31.500				-0.075	-0.075	0												
32.000	.120	-.116	.236	-.022	-.070	.048												
33.000	.168	-.138	.306	.051	-.081	.132												
33.500							-0.071	-0.071	0									
34.000	.202	-.164	.366	.105	-.099	.204	-.022	-.062	.040									
35.000	.227	-.189	.416	.143	-.121	.264	.046	-.068	.114									
35.500										-0.066	-0.066	0						
36.000	.240	-.210	.450	.168	-.144	.312	.089	-.083	.172	-.019	-.053	.034						
36.500													-0.064	-0.064	0			
37.000	.241	-.229	.470	.180	-.167	.347	.113	-.102	.220	.040	-.054	.094	-.018	-.050	.032			
37.500	.238	-.238	.476	.181	-.175	.356	.126	-.112	.238	.060	-.058	.118	.014	-.046	.060	-0.062	-0.062	0
38.000	.229	-.241	.470	.169	-.175	.344	.113	-.105	.218	.052	-.042	.094	.012	-.020	.032			
38.500													.002	.002	0			
39.000	.200	-.244	.444	.135	-.171	.306	.079	-.091	.170	.021	-.013	.034						
39.500										.001	.001	0						
40.000	.166	-.238	.404	.093	-.165	.258	.033	-.077	.110									
41.000	.118	-.236	.354	.040	-.156	.196	-.024	-.064	.040									
41.500							-.056	-.056	0									
42.000	.067	-.227	.294	-.020	-.146	.126												
43.000	.010	-.214	.224	-.088	-.132	.044												
43.500				-.125	-.125	0												
44.000	-.052	-.198	.146															
45.000	-.124	-.178	.054															
45.500	-.164	-.164	0															

TABLE III.- COORDINATES FOR THE CAMBERED DELTA WING, INCHES

(a) Inboard portion of wing panel

x	y = 0			y = 2			y = 4			y = 8		
	Ordinates		t	Ordinates		t	Ordinates		t	Ordinates		t
	Top	Lower		Top	Lower		Top	Lower		Top	Lower	
8.700	0	0	0									
9.000	.540	-.540	1.080									
9.500	.728	-.728	1.456									
10.000	.835	-.835	1.670									
10.600	.920	-.920	1.840									
11.000	.955	-.955	1.910									
11.500	.987	-.987	1.974									
12.000	1.000	-1.000	2.000									
12.033				-0.044	-0.044	0						
12.500	1.000	-1.000	2.000	.121	-.125	.246						
13.000	1.000	-1.000	2.000	.251	-.199	.450						
13.500	.992	-.992	1.984	.350	-.256	.606						
14.000	.980	-.980	1.960	.429	-.299	.728						
14.500	.966	-.966	1.932	.486	-.336	.822						
15.000	.948	-.948	1.896	.531	-.361	.892						
15.367							-0.333	-0.333	0			
15.500	.930	-.930	1.860	.566	-.382	.948	-.301	-.337	.036			
16.000	.910	-.910	1.820	.591	-.399	.990	-.195	-.353	.158			
16.500	.888	-.888	1.776	.604	-.412	1.016	-.108	-.366	.258			
17.000	.867	-.867	1.734	.614	-.424	1.038	-.036	-.378	.342			
17.500	.844	-.844	1.688	.618	-.430	1.048	.024	-.386	.410			
18.000	.822	-.822	1.644	.619	-.435	1.054	.075	-.391	.466			
18.500	.800	-.800	1.600	.616	-.440	1.056	.120	-.392	.512			
19.000	.780	-.780	1.560	.611	-.445	1.056	.160	-.390	.550			
19.500	.765	-.765	1.530	.606	-.452	1.058	.193	-.393	.586			
20.000	.753	-.753	1.506	.601	-.461	1.062	.223	-.395	.618			
21.000	.735	-.735	1.470	.592	-.480	1.072	.277	-.397	.674			
22.000	.723	-.723	1.446	.587	-.497	1.084	.323	-.399	.722			
22.033										-0.476	-0.476	0
23.000	.723	-.723	1.446	.582	-.526	1.108	.368	-.404	.772	-.329	-.427	.098
24.000	.721	-.721	1.442	.573	-.555	1.128	.407	-.407	.814	-.212	-.398	.186
25.000	.719	-.719	1.438	.562	-.582	1.144	.441	-.409	.850	-.112	-.374	.262
26.000	.715	-.715	1.430	.551	-.603	1.154	.470	-.408	.878	-.024	-.352	.328
27.000	.710	-.710	1.420	.540	-.622	1.162	.497	-.405	.902	.054	-.332	.386
28.000	.706	-.706	1.412	.531	-.637	1.168	.521	-.403	.924	.126	-.310	.436
29.000	.704	-.704	1.408	.524	-.652	1.176	.545	-.401	.946	.194	-.290	.484
30.000	.704	-.704	1.408	.522	-.666	1.188	.571	-.397	.968	.253	-.273	.526
31.000	.707	-.707	1.414	.523	-.679	1.202	.601	-.391	.992	.311	-.257	.568
32.000	.716	-.716	1.432	.533	-.695	1.228	.633	-.389	1.022	.369	-.243	.612
33.000	.730	-.730	1.460	.548	-.712	1.260	.671	-.389	1.060	.427	-.231	.658
34.000	.739	-.739	1.478	.562	-.722	1.284	.706	-.382	1.088	.483	-.217	.700
35.000	.742	-.742	1.484	.574	-.722	1.296	.739	-.369	1.108	.533	-.199	.732
36.000	.739	-.739	1.478	.586	-.712	1.298	.769	-.349	1.118	.579	-.177	.756
37.000	.721	-.721	1.442	.589	-.683	1.272	.790	-.312	1.102	.616	-.146	.762
37.500	.706	-.706	1.412	.586	-.662	1.248	.798	-.288	1.086	.632	-.126	.758
38.000	.688	-.688	1.376	.582	-.638	1.220	.804	-.260	1.064	.647	-.103	.750
39.000	.643	-.643	1.286	.569	-.575	1.144	.809	-.195	1.004	.669	-.051	.720
40.000	.593	-.593	1.186	.560	-.500	1.060	.812	-.122	.934	.687	.007	.680
41.000	.535	-.535	1.070	.552	-.408	.960	.808	-.042	.850	.701	.073	.628
41.500	.506	-.506	1.012	.549	-.361	.910	.806	0	.806	.707	.107	.600
42.033	.474	-.474	.948	.547	-.307	.854	.805	.047	.758	.712	.144	.568
42.500	.439	-.439	.878	.535	-.249	.784	.793	.103	.690	.700	.200	.500
43.000	.400	-.400	.800	.521	-.185	.706	.779	.167	.612	.684	.258	.426
43.500	.365	-.365	.730	.514	-.122	.636	.771	.229	.542	.671	.315	.356
44.000	.332	-.332	.664	.508	-.062	.570	.765	.289	.476	.660	.372	.288
44.500	.295	-.295	.590	.500	.004	.496	.756	.354	.402	.646	.430	.216
45.000	.261	-.261	.522	.495	.067	.428	.752	.418	.334	.635	.489	.146
45.500	.225	-.225	.450	.490	.134	.356	.747	.485	.262	.623	.547	.076
46.000	.191	-.191	.382	.486	.198	.288	.745	.551	.194	.613	.609	.004
46.033										.613	.613	0
46.500	.155	-.155	.310	.481	.265	.216	.741	.619	.122			
47.000	.120	-.120	.240	.478	.332	.146	.740	.686	.054			
47.367							.738	.738	0			
47.500	.083	-.083	.166	.474	.400	.074						
48.000	.050	-.050	.100	.471	.467	.004						
48.033				.471	.471	0						
48.500	.008	-.008	.016									
48.700	0	0	0									

TABLE III.- COORDINATES FOR THE CAMBERED DELTA WING, INCHES - Concluded

(b) Outboard portion of wing panel

x	y = 12			y = 14			y = 16			y = 18			y = 19			y = 20		
	Ordinates		t	Ordinates		t	Ordinates		t	Ordinates		t	Ordinates		t	Ordinates		t
	Top	Lower		Top	Lower		Top	Lower		Top	Lower		Top	Lower		Top	Lower	
28.700	-0.281	-0.281	0															
29.000	-.233	-.253	.020															
30.000	-.109	-.195	.086															
31.000	-.006	-.152	.146															
32.000	.087	-.115	.202															
32.033				-0.154	-0.154	0												
33.000	.174	-.084	.258	-.021	-.079	.058												
34.000	.252	-.058	.310	.085	-.029	.114												
35.000	.323	-.033	.356	.180	.012	.168												
35.367							-0.008	-0.008	0									
36.000	.386	-.010	.396	.262	.048	.214	.083	.049	.034									
37.000	.441	.021	.420	.334	.080	.254	.193	.109	.084									
37.500	.467	.035	.432	.365	.097	.268	.239	.135	.104									
38.000	.490	.054	.436	.395	.115	.280	.284	.160	.124									
38.700										0.186	0.186	0						
39.000	.531	.093	.438	.448	.152	.296	.361	.207	.154	.232	.220	.012						
40.000	.565	.137	.428	.493	.191	.302	.425	.249	.176	.345	.295	.050						
40.367													0.302	0.302	0			
41.000	.586	.178	.408	.531	.233	.298	.477	.291	.186	.430	.354	.076	.408	.388	.020			
41.500	.598	.204	.394	.547	.255	.292	.501	.311	.190	.468	.382	.086	.460	.426	.034			
42.033	.612	.232	.380	.562	.278	.284	.523	.333	.190	.504	.410	.094	.510	.462	.048	0.442	0.442	0
42.367													.512	.512	0			
42.500	.595	.283	.312	.547	.329	.218	.509	.387	.122	.499	.471	.028						
42.700										.496	.496	0						
43.000	.577	.339	.238	.531	.385	.146	.494	.442	.052									
43.367							.482	.482	0									
43.500	.560	.392	.168	.514	.440	.074												
44.000	.543	.445	.098	.496	.492	.004												
44.033				.497	.497	0												
44.500	.526	.498	.028															
44.700	.519	.519	0															

TABLE IV.- COORDINATES FOR THE CAMBERED ARROW WING, INCHES

(a) Inboard portion of wing panel

x	y = 0			y = 2			y = 4			y = 8		
	Ordinates		t	Ordinates		t	Ordinates		t	Ordinates		t
	Top	Lower		Top	Lower		Top	Lower		Top	Lower	
0	0	0	0									
.500	.086	-.086	.172									
1.000	.171	-.171	.342									
2.000	.237	-.237	.474									
3.000	.304	-.304	.608									
4.000	.360	-.360	.720									
5.000	.395	-.395	.790									
5.750				-0.151	-0.151	0						
6.000	.408	-.408	.816	-.105	-.137	.032						
7.000	.426	-.426	.852	.020	-.132	.152						
8.000	.467	-.467	.934	.116	-.146	.262						
10.000	.534	-.534	1.068	.256	-.198	.454						
11.500							-0.386	-0.386	0			
12.000	.567	-.567	1.124	.342	-.248	.590	-.310	-.358	.048			
14.000	.610	-.610	1.220	.406	-.314	.720	-.101	-.319	.218			
16.000	.669	-.669	1.338	.460	-.398	.858	.057	-.319	.376			
17.500	.696	-.696	1.392	.483	-.451	.934	.162	-.316	.478			
18.000	.704	-.704	1.408	.489	-.469	.958	.183	-.325	.508			
19.000	.718	-.718	1.436	.500	-.502	1.002	.231	-.335	.566			
20.000	.731	-.731	1.462	.508	-.534	1.042	.277	-.345	.622			
22.000	.764	-.764	1.528	.525	-.603	1.128	.360	-.370	.730			
23.000										-0.403	-0.403	0
24.000	.814	-.814	1.628	.557	-.681	1.238	.442	-.406	.848	-.270	-.338	.068
26.000	.851	-.851	1.702	.583	-.743	1.326	.511	-.439	.950	-.075	-.271	.196
28.000	.877	-.877	1.754	.601	-.793	1.394	.568	-.466	1.034	.078	-.236	.314
30.000	.906	-.906	1.812	.627	-.837	1.464	.624	-.494	1.118	.205	-.217	.422
32.000	.948	-.948	1.896	.674	-.882	1.556	.689	-.525	1.214	.320	-.214	.534
33.333	[1].986	-.986	1.972	.718	-.914	1.632	.743	-.549	1.292	.392	-.220	.612
34.000	.955	-.955	1.910	.739	-.925	1.664	.768	-.558	1.326	.426	-.222	.648
35.000	.908	-.908	1.816	.770	-.936	1.706	.802	-.568	1.370	.474	-.226	.700
35.230	.898	-.898	1.796									
35.730				[1].780	-.932	1.712						
36.000	.852	-.852	1.704	.766	-.912	1.678	.816	-.556	1.372	.505	-.223	.728
37.000	.768	-.768	1.536	.710	-.828	1.538	.839	-.551	1.390	.538	-.224	.762
38.000	.642	-.642	1.284	.634	-.714	1.348	.852	-.532	1.384	.564	-.220	.784
38.150							[1].856	-.530	1.386			
39.000	.508	-.508	1.016	.547	-.583	1.130	.798	-.446	1.244	.589	-.215	.804
40.000	.387	-.387	.774	.465	-.451	.916	.722	-.334	1.056	.612	-.208	.820
40.500				.417	-.377	.794	.683	-.275	.958	.614	-.196	.810
41.000				.372	-.304	.676	.640	-.212	.852	.635	-.203	.838
41.532				.317	-.217	.534	.592	-.144	.736	.650	-.206	.856
41.750				.309	-.193	.502						
42.000							.571	-.097	.668	[1].668	-.210	.878
43.000							.523	.003	.520	[1].703	-.221	.924
43.500							.500	.054	.446			
45.000										.582	-.048	.630
47.000										.464	.130	.334

[1]Ridge

TABLE IV.- COORDINATES FOR THE CAMBERED ARROW WING, INCHES - Concluded

(b) Outboard portion of wing panel

x	y = 12			y = 16			y = 19			y = 20		
	Ordinates		t	Ordinates		t	Ordinates		t	Ordinates		t
	Top	Lower		Top	Lower		Top	Lower		Top	Lower	
34.500	-0.420	-0.420	0									
35.000	-.346	-.376	.030									
36.000	-.234	-.318	.084									
37.000	-.143	-.279	.136									
38.000	-.062	-.244	.182									
39.000	.008	-.218	.226									
40.000	.068	-.198	.266									
40.500	.096	-.190	.286									
41.000	.121	-.181	.302									
41.532	.148	-.176	.324									
42.000	.172	-.174	.346									
43.000	.221	-.171	.392									
45.000	.309	-.177	.486									
46.000				-0.437	-0.437	0						
47.000	.386	-.192	.578	-.300	-.346	.046						
47.825	[1].402	-.214	.616									
49.000	.341	-.103	.444	-.121	-.259	.138						
50.500	.243	.018	.225									
51.000				.012	-.218	.230						
52.660				[1].101	-.207	.308						
53.000				.083	-.175	.258						
54.000				.030	-.082	.112						
54.625							-0.446	-0.446	0			
55.000							-.385	-.403	.018			
56.000							-.267	-.331	.064			
56.280							[1]-.242	-.320	.078			
56.625							-.242	-.270	.028			
57.500										-0.451	-0.451	0

[1]Ridge

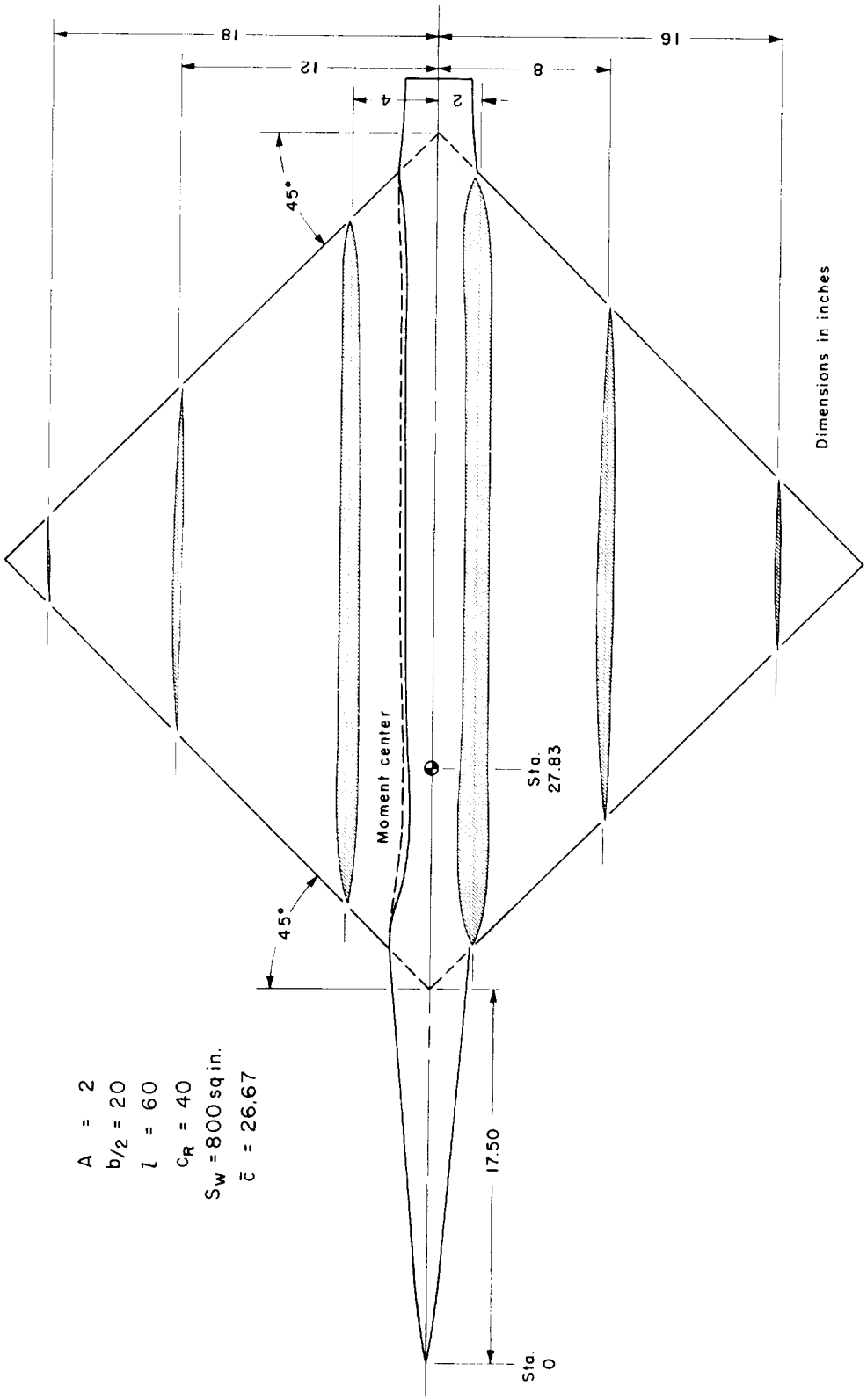

(a) Cambered diamond model.

Figure 1.- Sketches of the models, showing wing cross sections at selected spanwise stations.

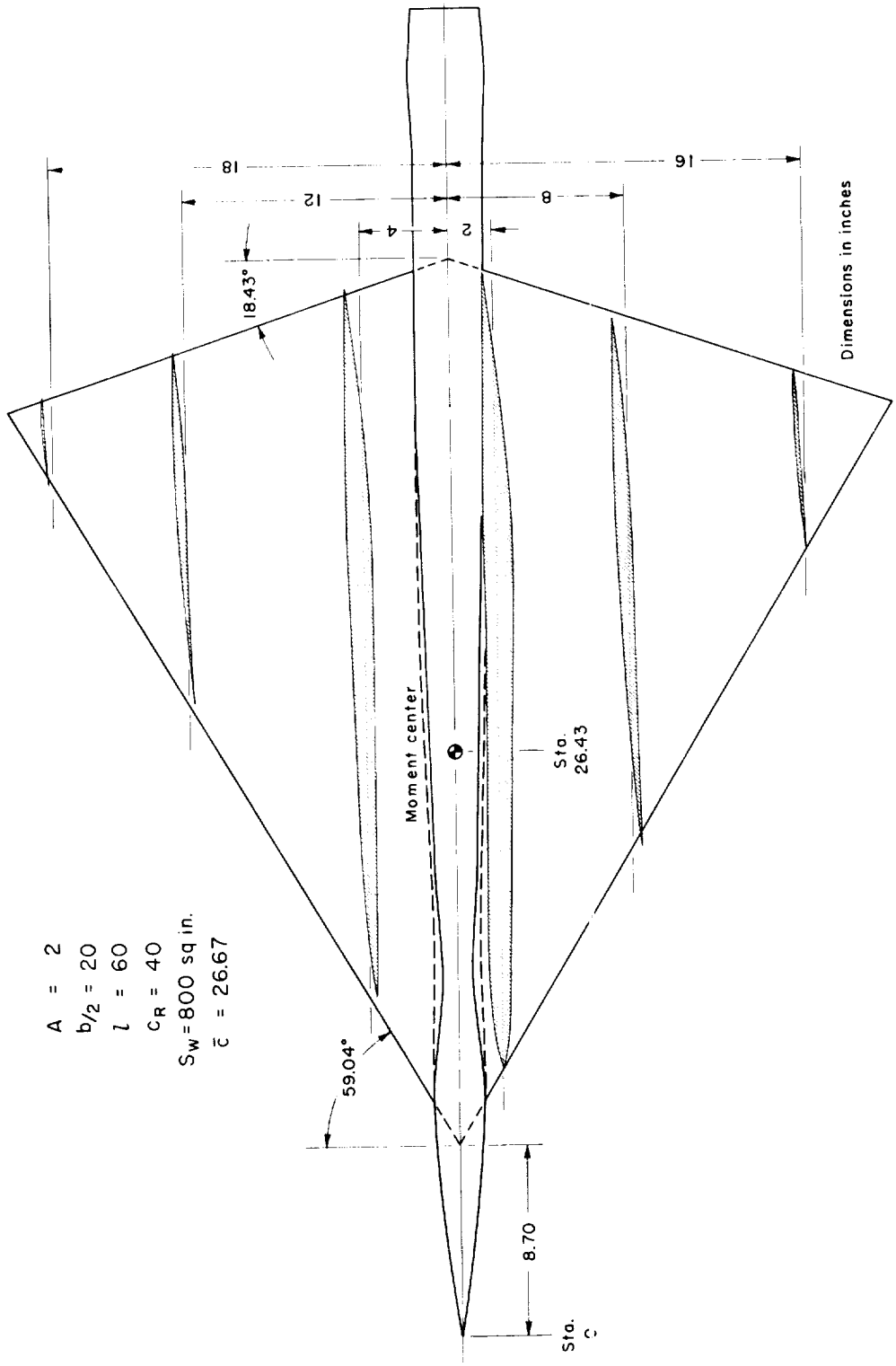

(b) Cambered delta model.

Figure 1.- Continued.

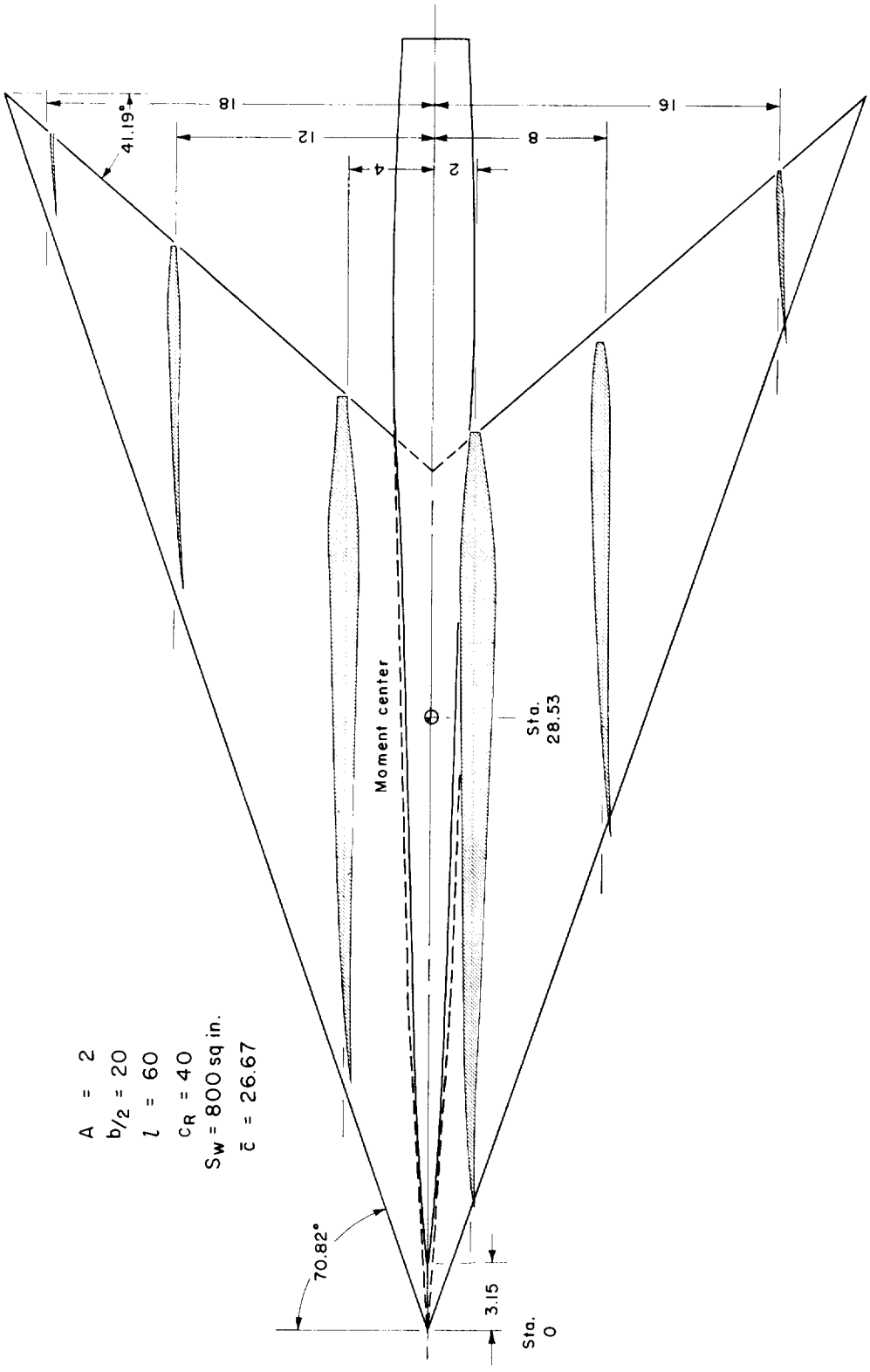

(c) Cambered arrow model.

Figure 1.- Concluded.

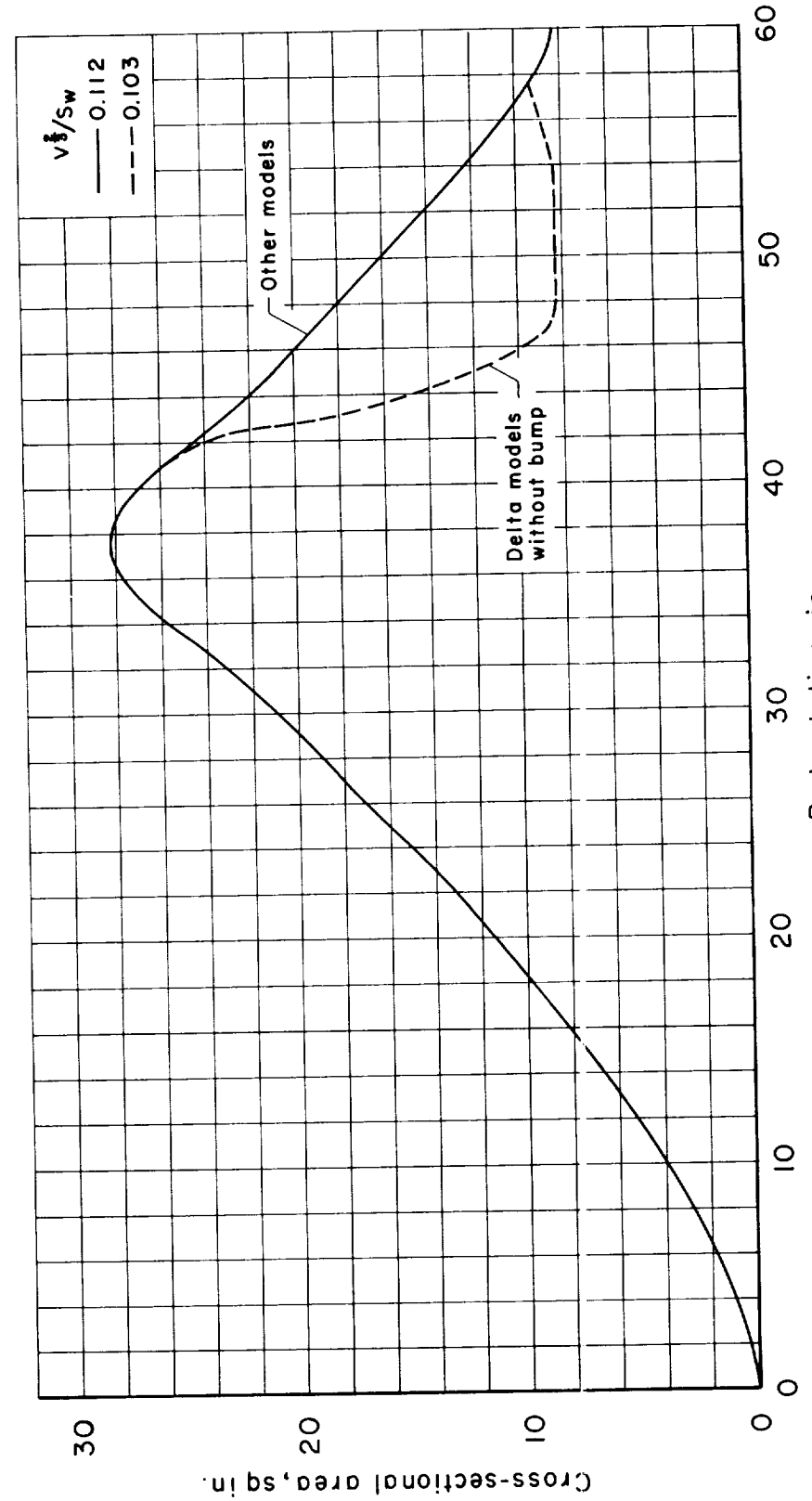

Figure 2.- The design area distribution used for most of the models as derived in reference 1 and modified for the delta models without the body bump.

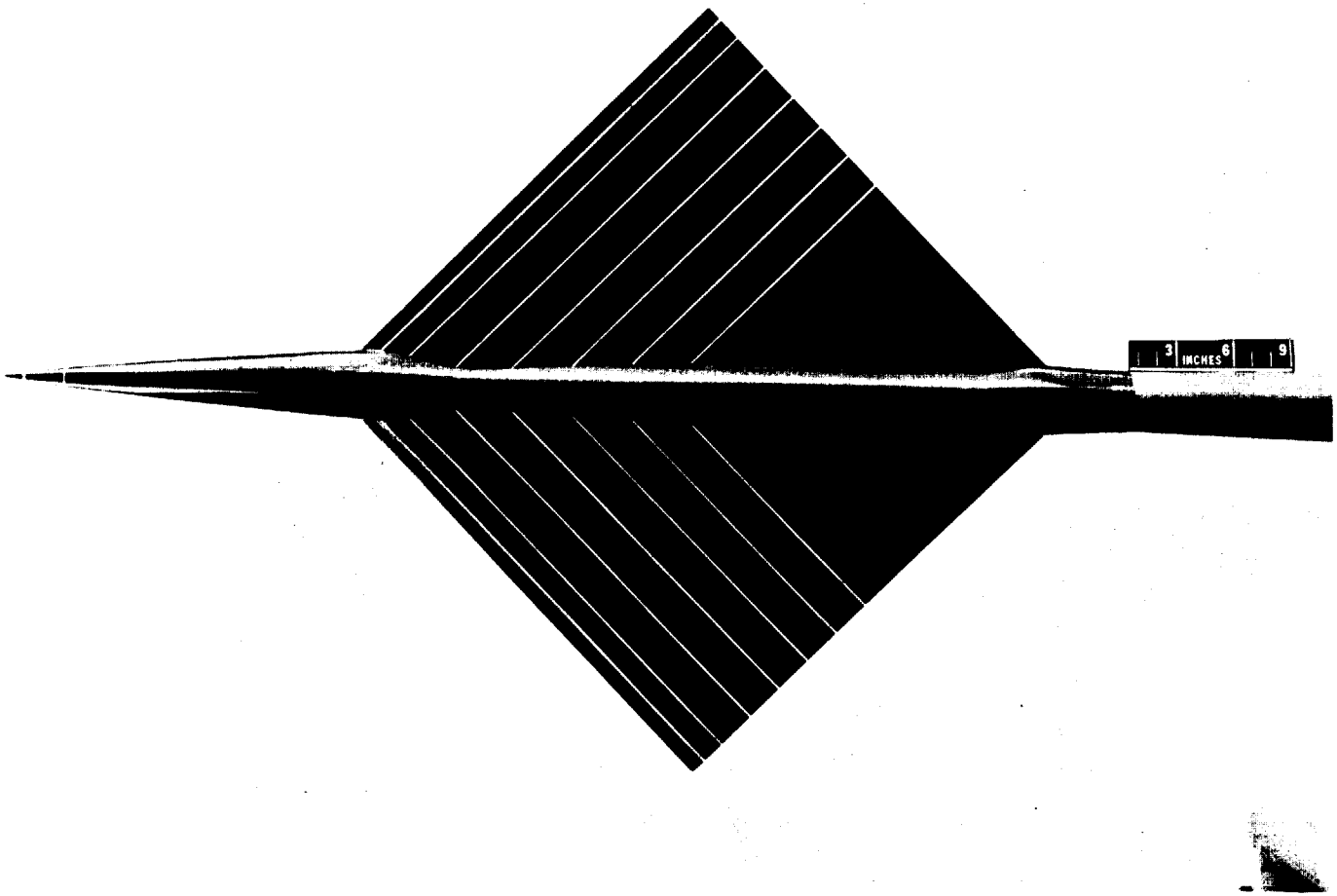

A-25265

(a) Cambered diamond model.

Figure 3.- Photographs showing the model plan forms.

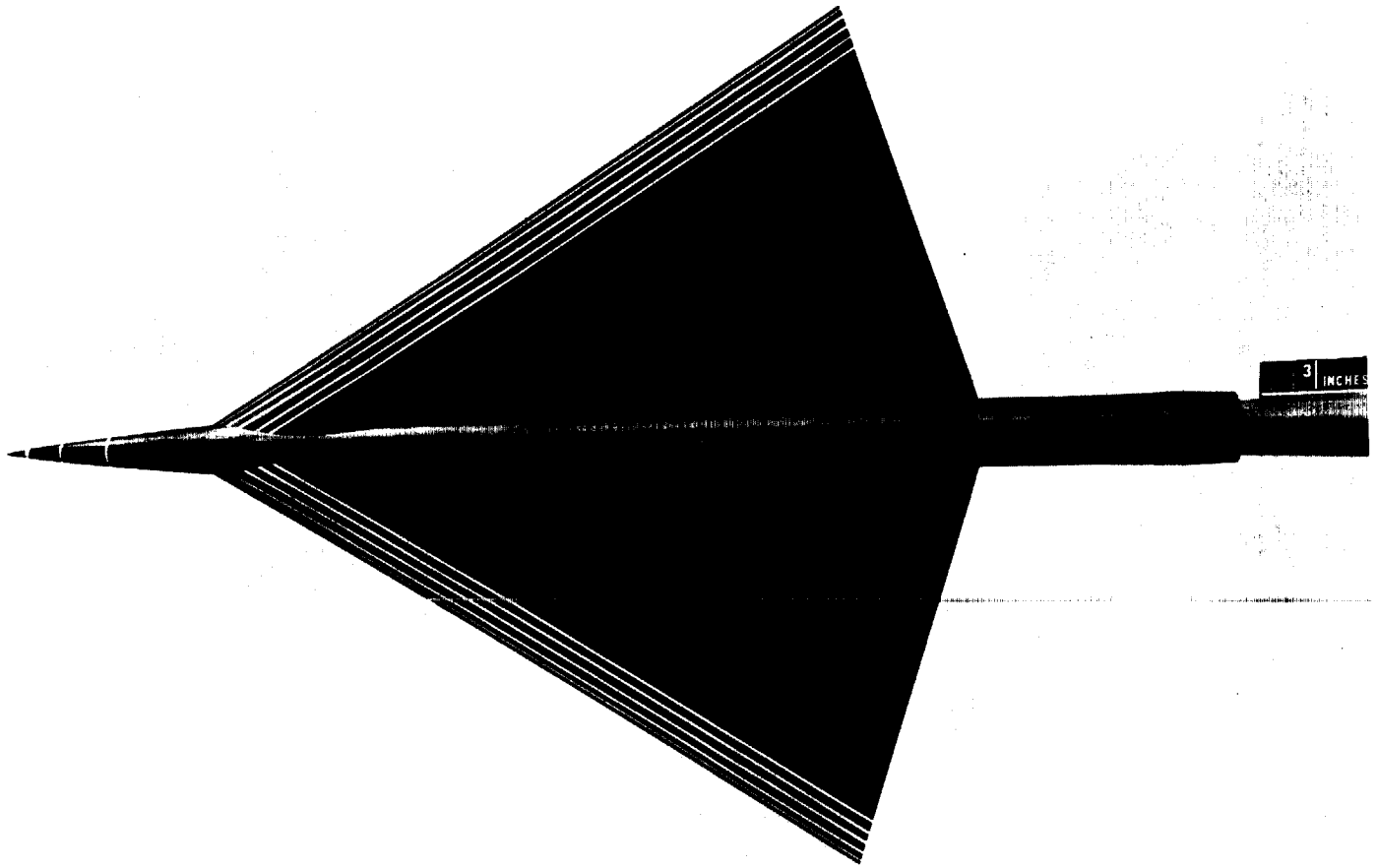

A-25421

(b) Cambered delta model.

Figure 3.- Continued.

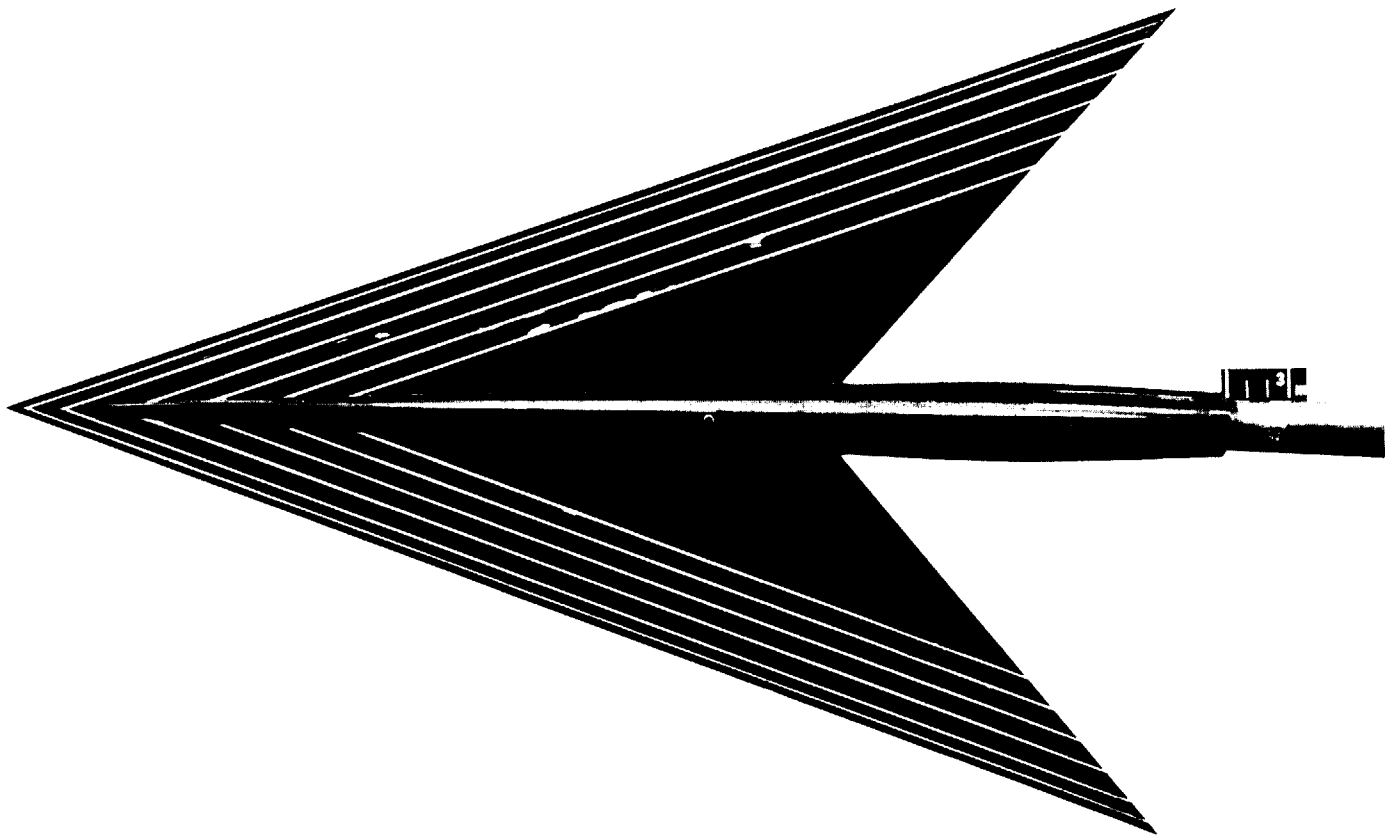

A-25898

(c) Arrow model.

Figure 3.- Concluded.

A-24091

(a) Arrow model in the 14-foot transonic test section.

Figure 4.- Photographs of the high-speed test regions of the transonic and supersonic wind tunnels with models mounted for testing.

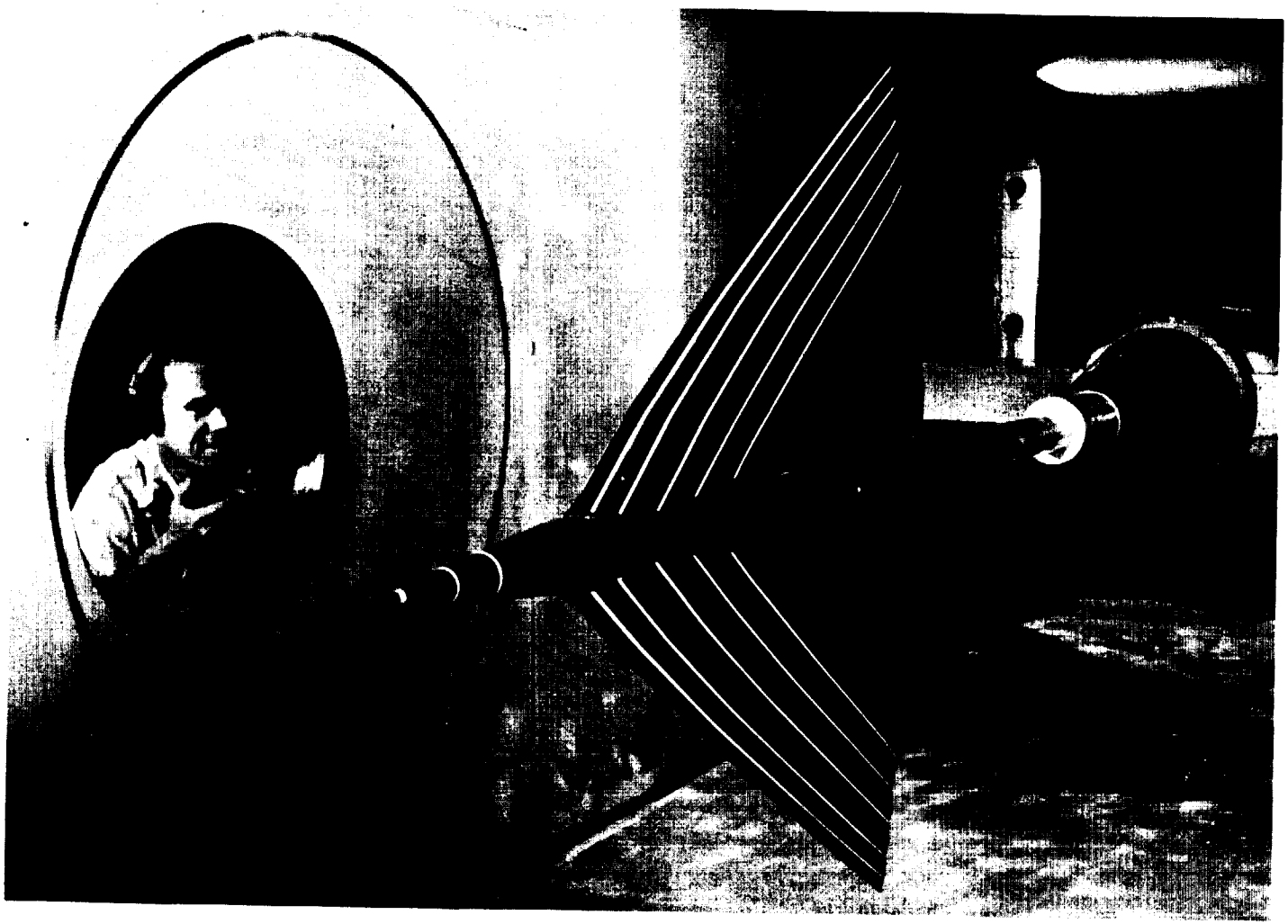

A-25865

(b) Cambered delta model in the 9- by 7-foot supersonic test section.

Figure 4.- Continued.

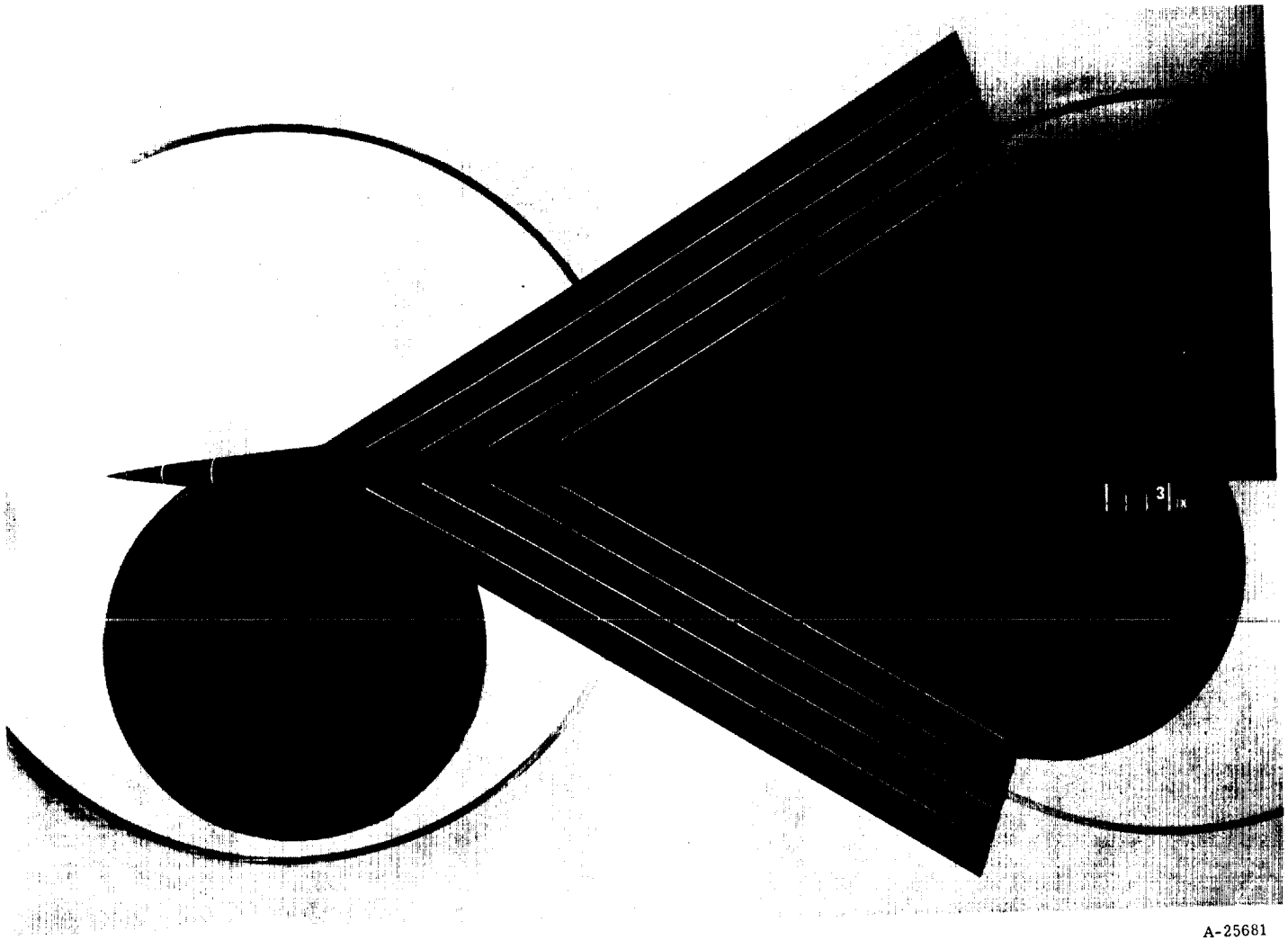

(c) Cambered delta model in the 8- by 7-foot supersonic test section.

Figure 4.- Concluded.

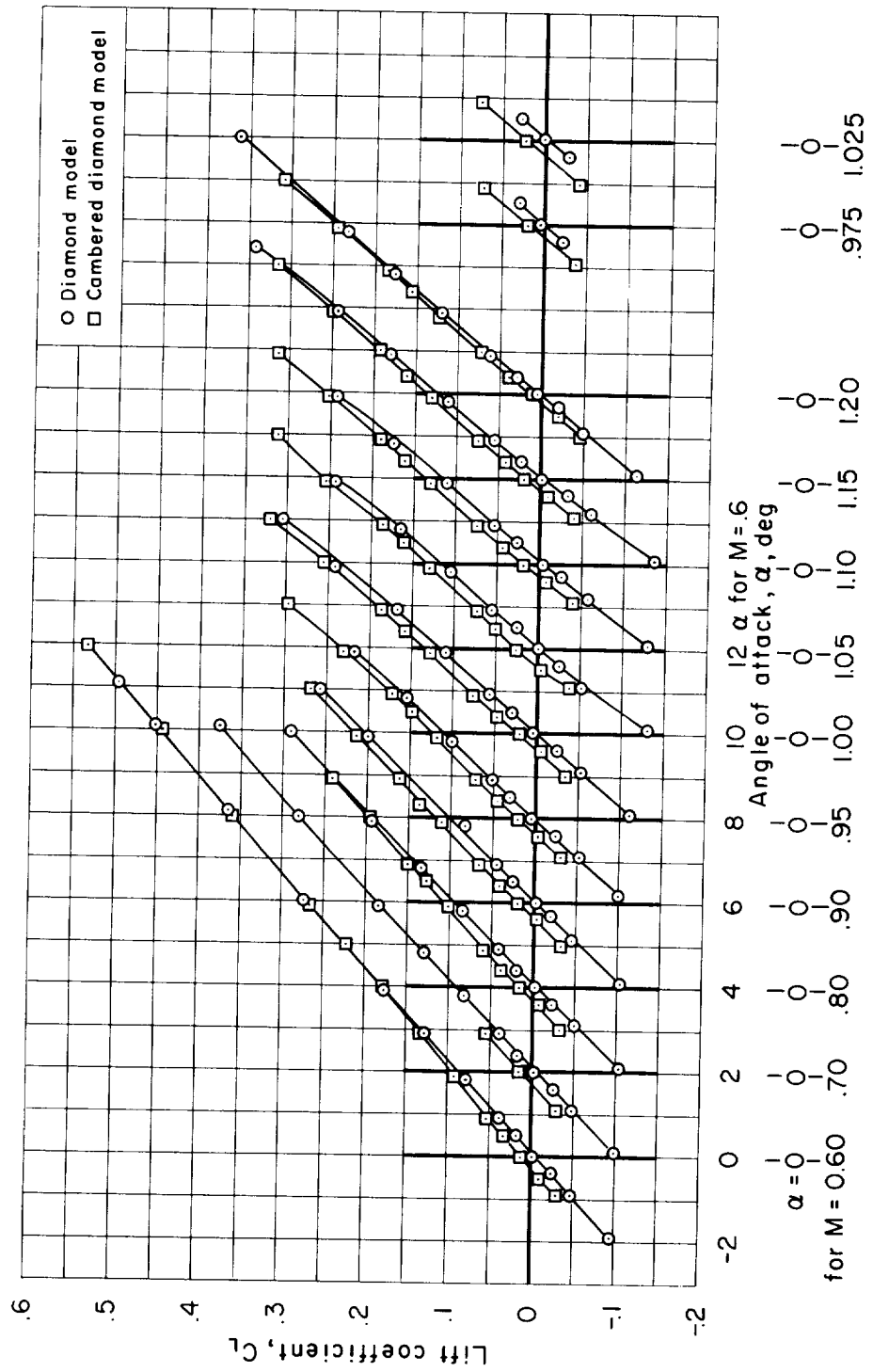

(a) C_L vs. α

Figure 5.- Transonic aerodynamic characteristics for the diamond and cambered diamond models with transition fixed as determined from tests in the Ames 14-Foot Transonic Wind Tunnel (R/ft = 3,500,000 to 4,000,000).

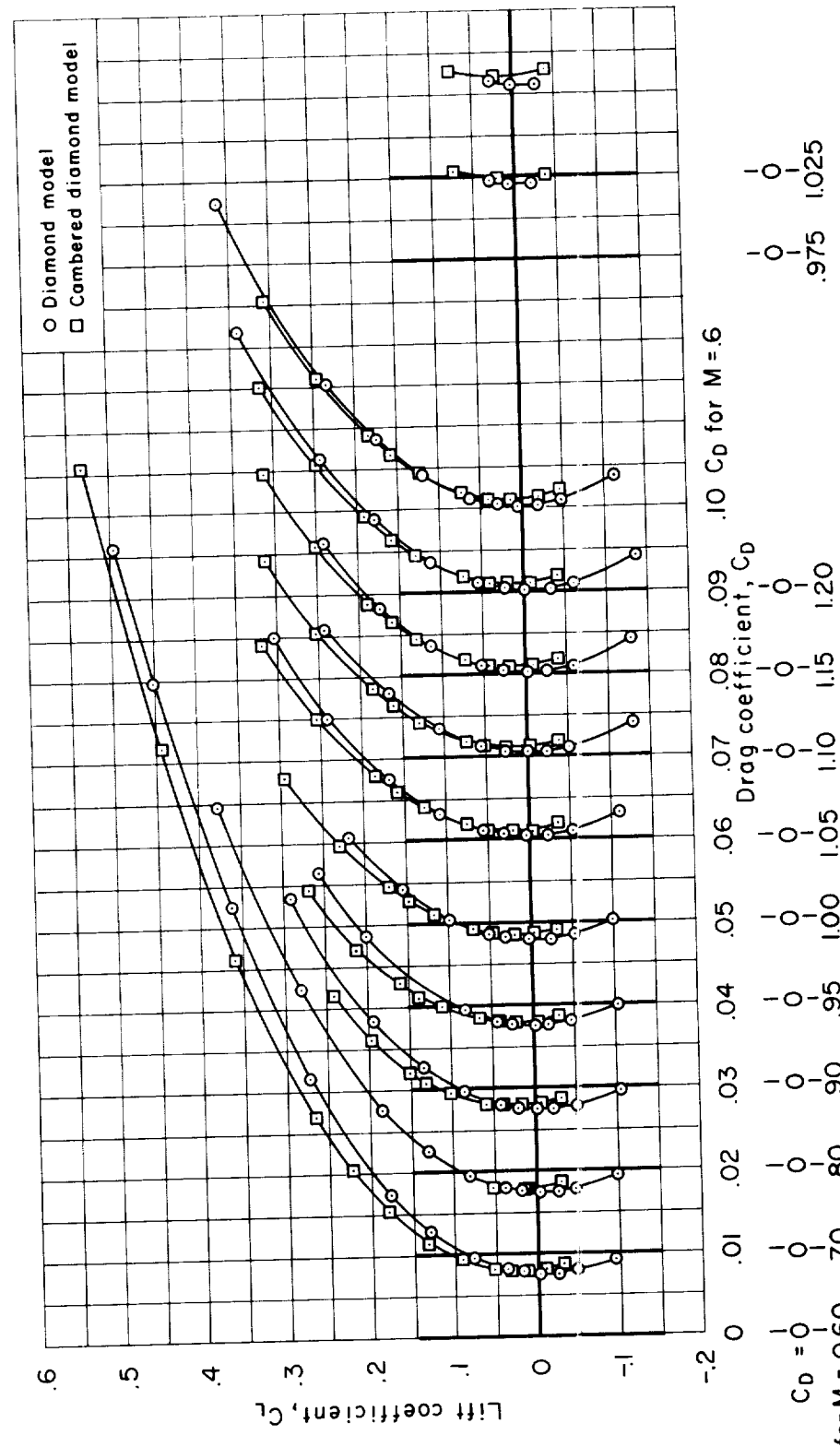

(b) C_L vs. C_D

Figure 5.- Continued.

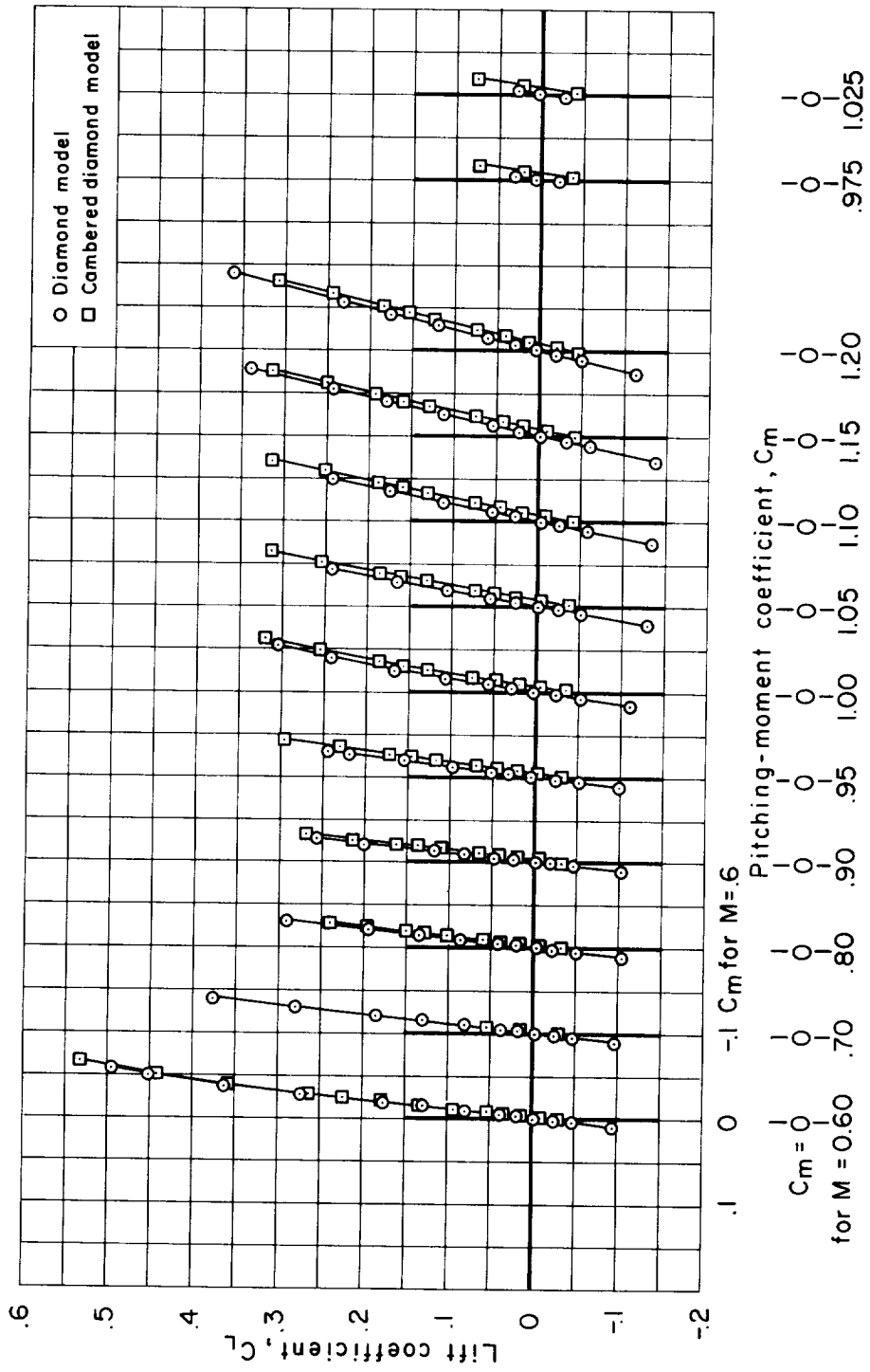

(c) C_L vs. C_m

Figure 5.- Concluded.

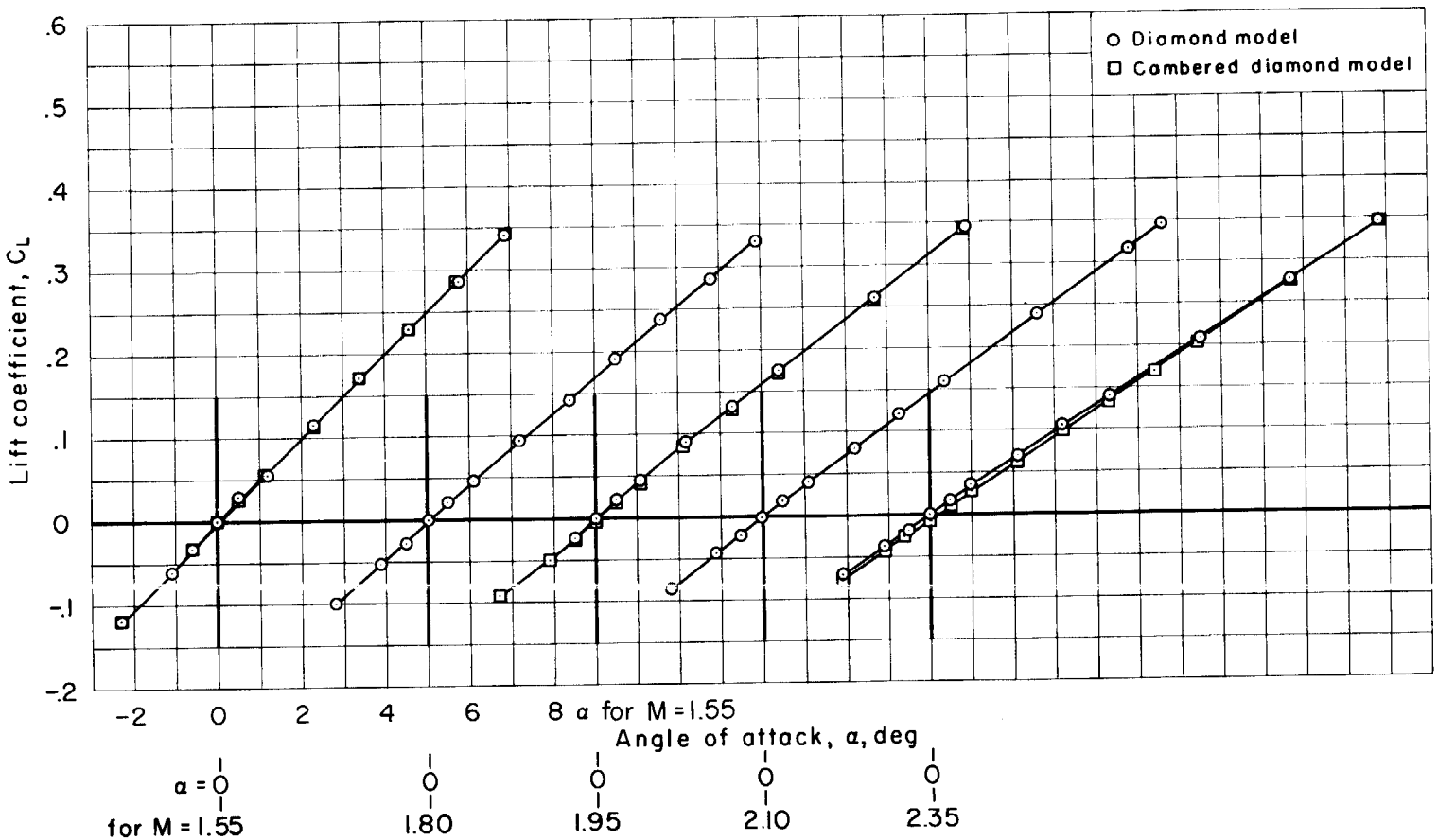

(a) C_L vs. α

Figure 6.- Supersonic aerodynamic characteristics for the diamond and cambered diamond models with transition fixed as determined from tests in the 9- by 7-foot supersonic test section of the Ames Unitary Plan Wind Tunnel (R/ft = 3,000,000).

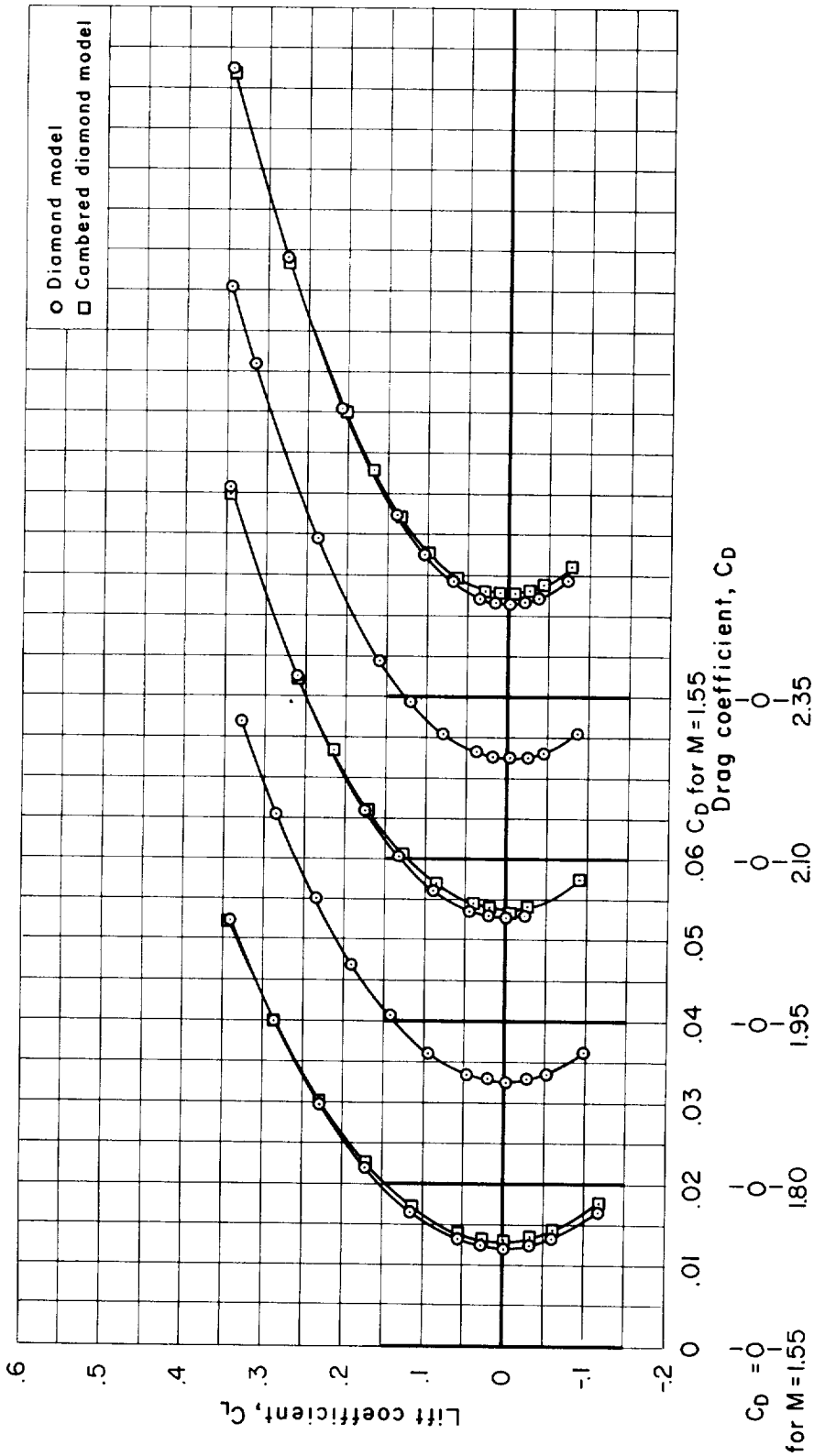

(b) C_L vs. C_D

Figure 6.- Continued.

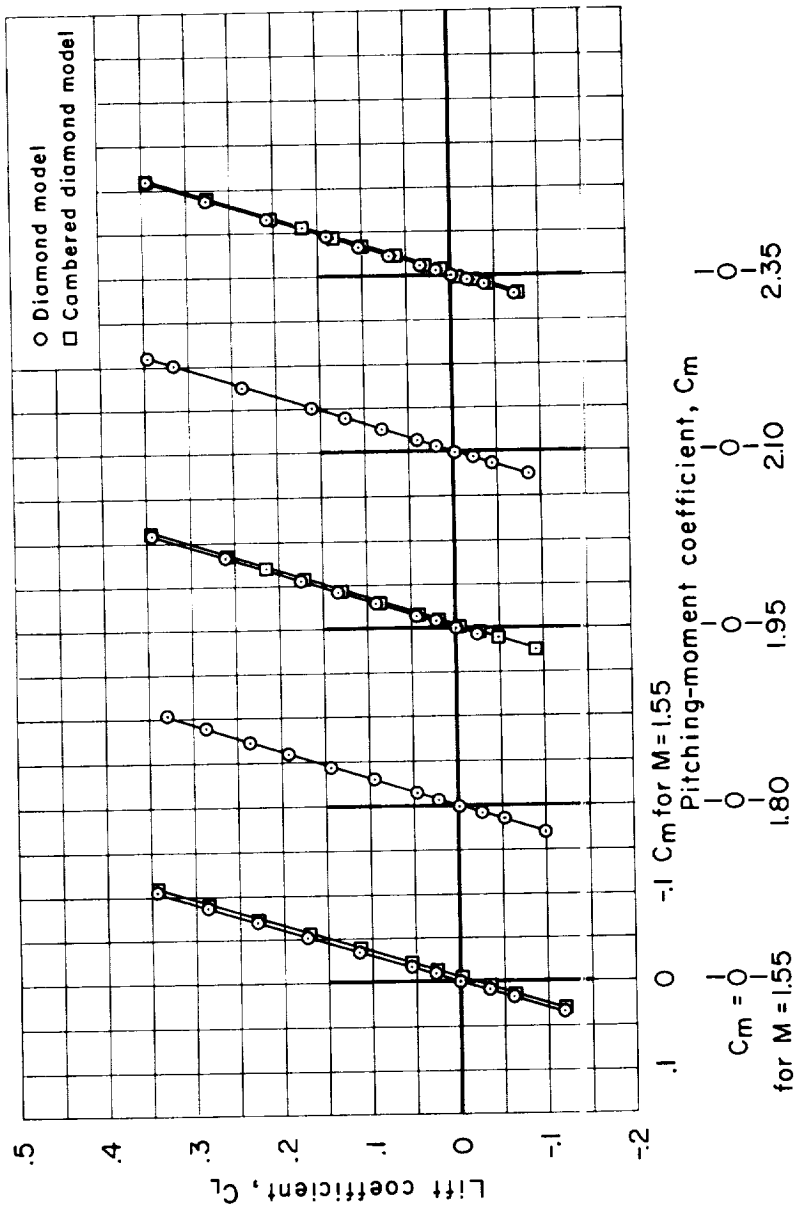

(c) C_L vs. C_m

Figure 6.- Continued.

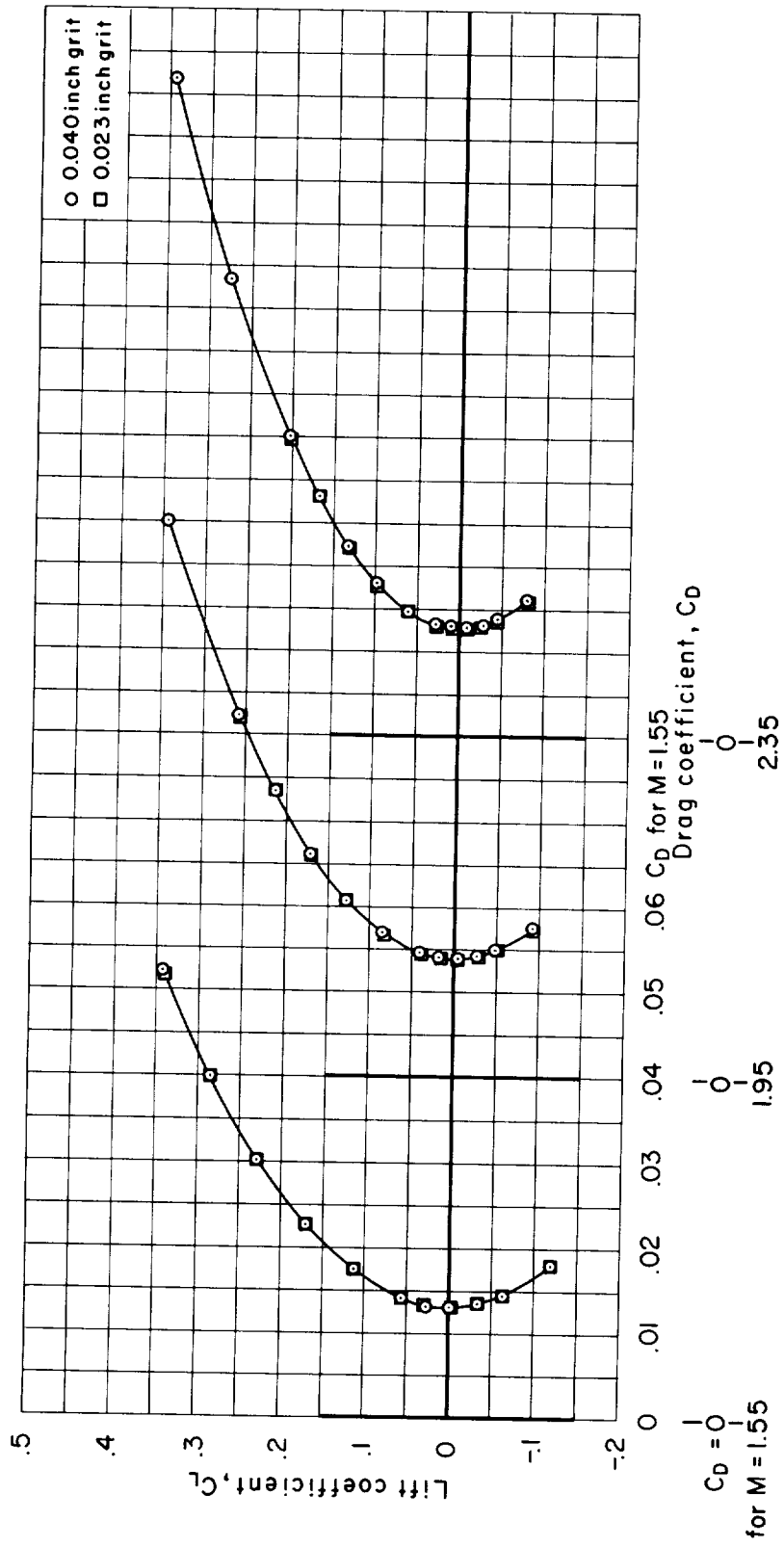

(d) C_L vs. C_D for the cambered diamond model with two different sizes of grit.

Figure 6.- Concluded.

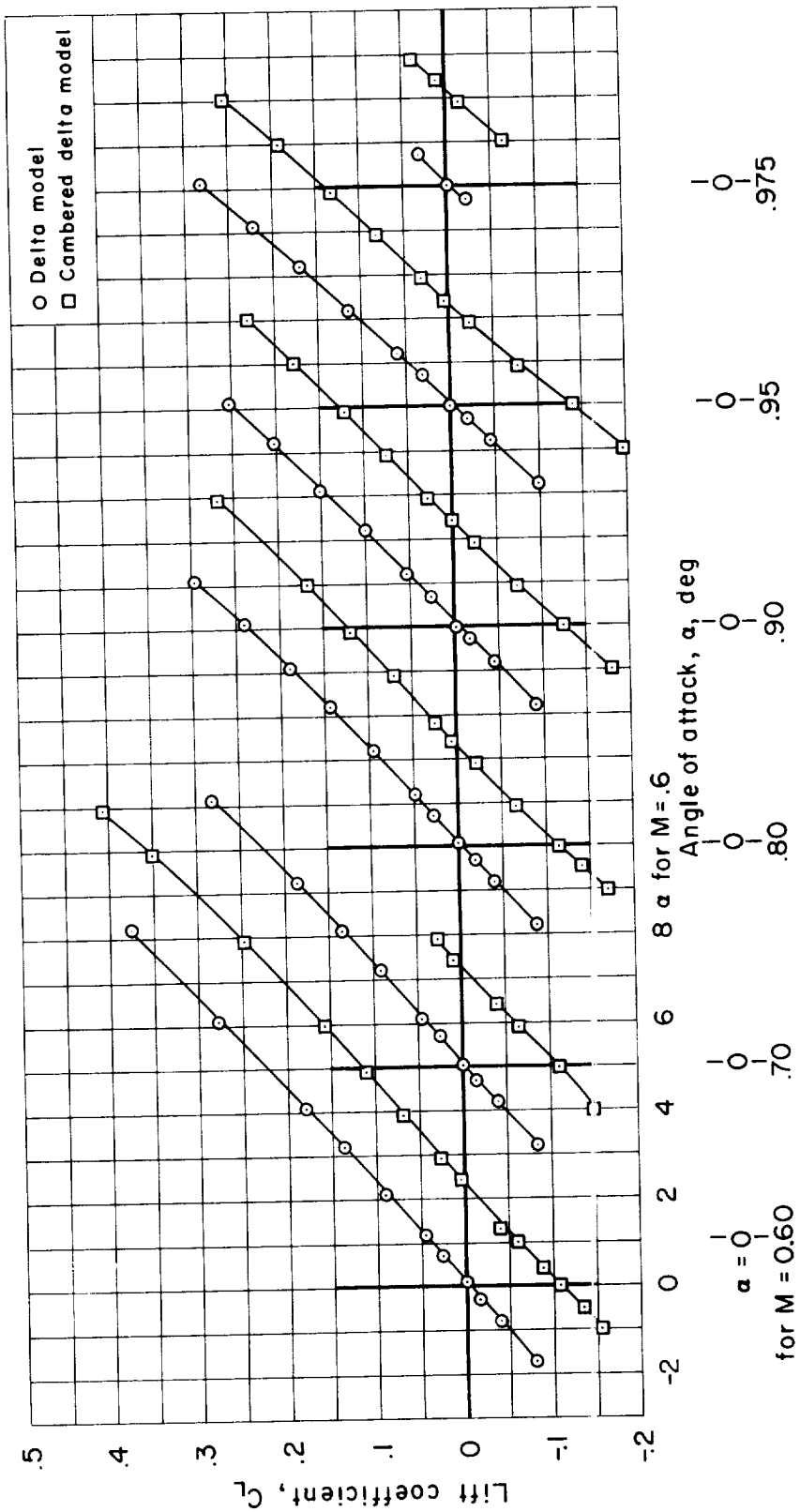

(a) C_L vs. α, M=0.60 to 0.975

Figure 7.- Transonic aerodynamic characteristics for the delta and cambered delta models with transition fixed as determined from tests in the Ames 14-Foot Transonic Wind Tunnel (R/ft = 3,500,000 to 4,000,000).

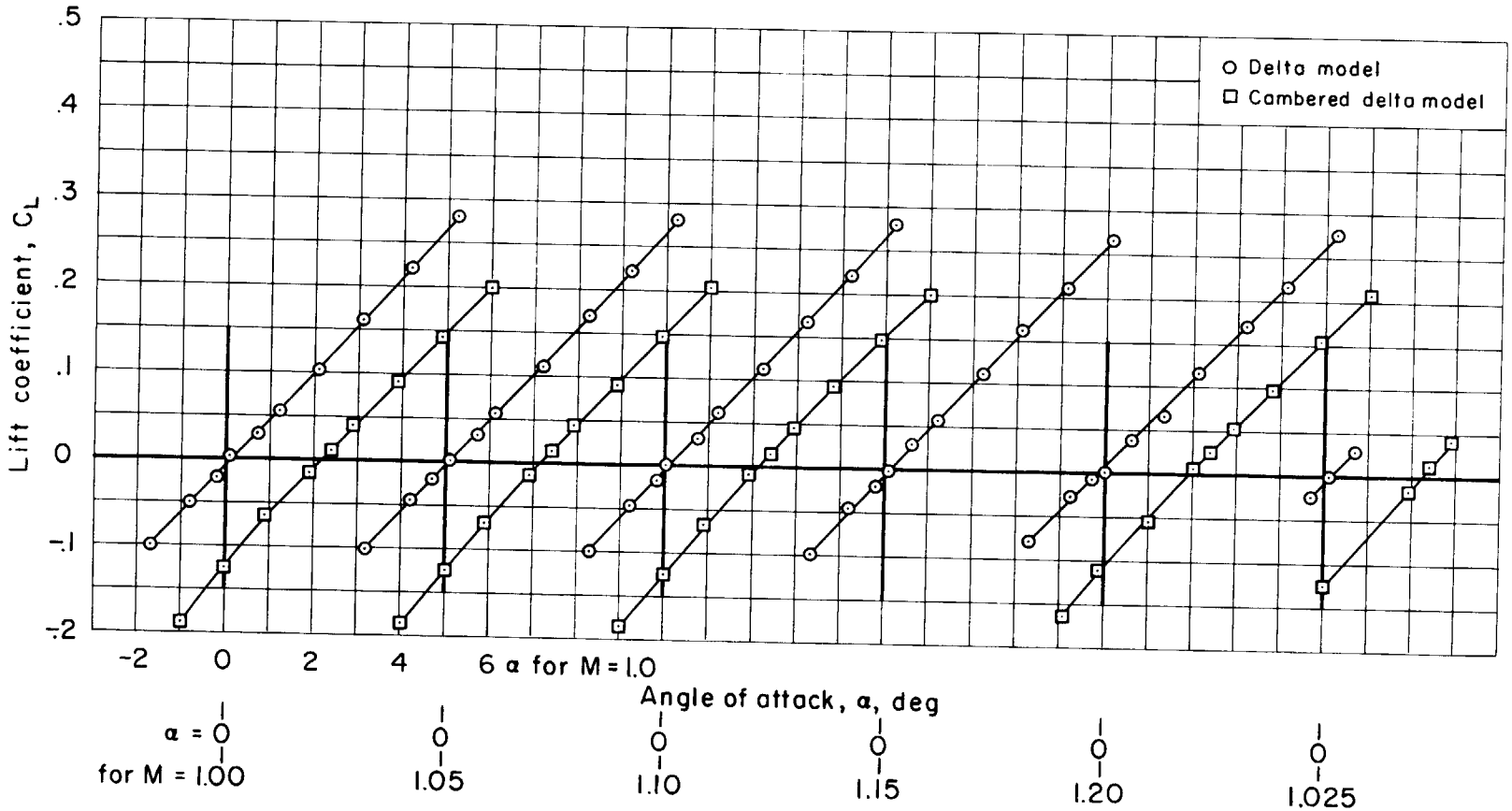

(b) C_L vs. α, M=1.00 to 1.20

Figure 7.- Continued.

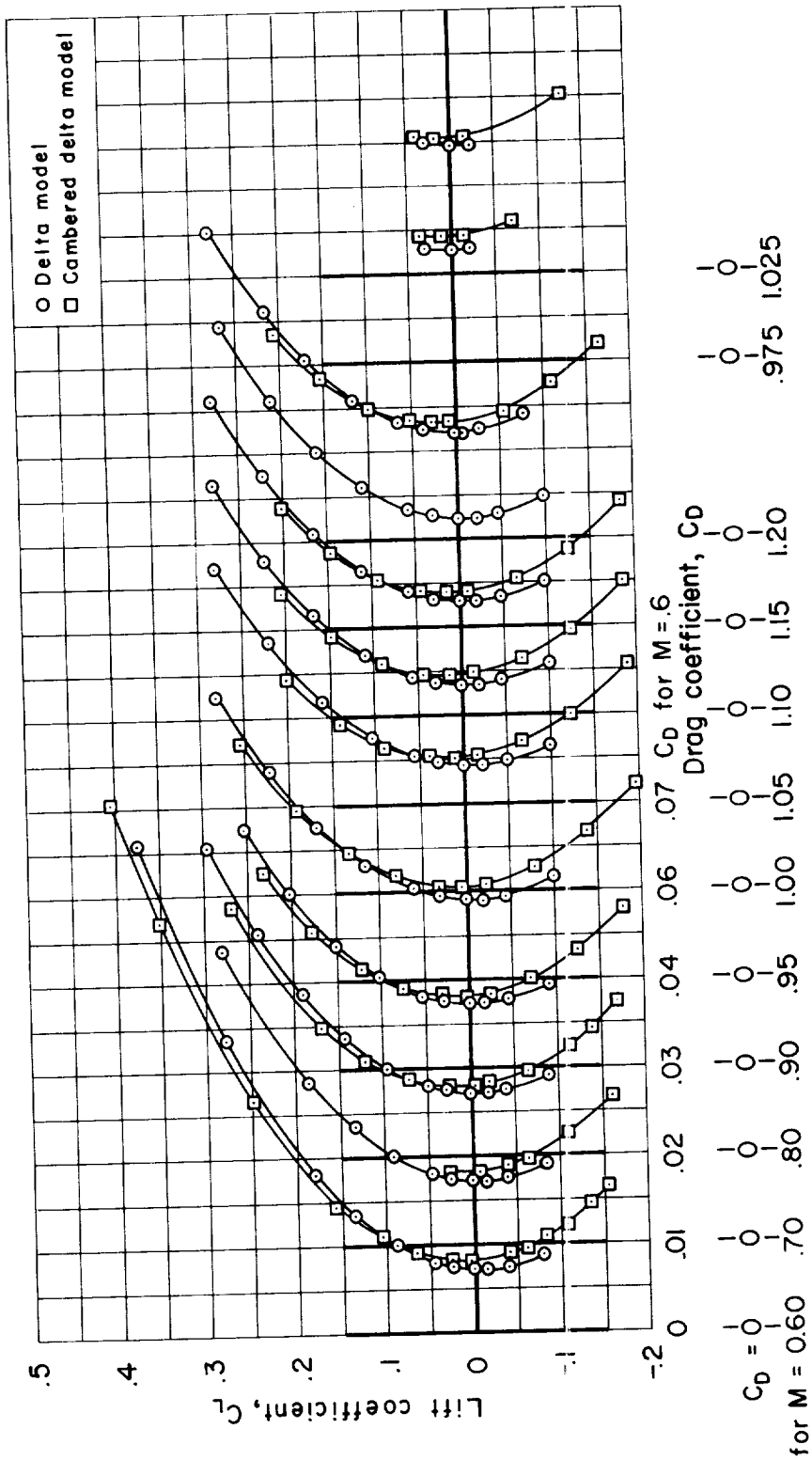

(c) C_L vs. C_D

Figure 7.- Continued.

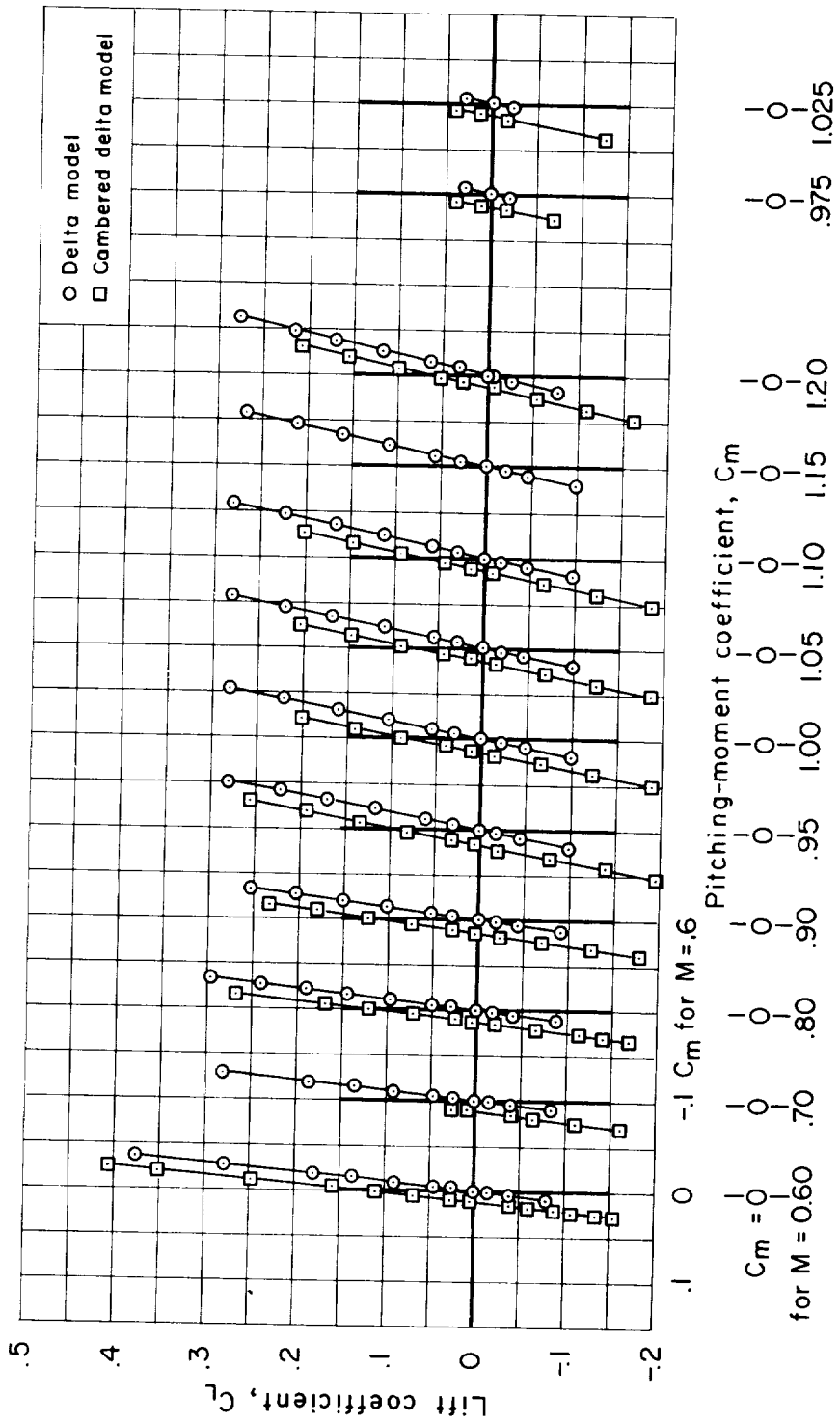

(d) C_L vs. C_m

Figure 7.- Concluded.

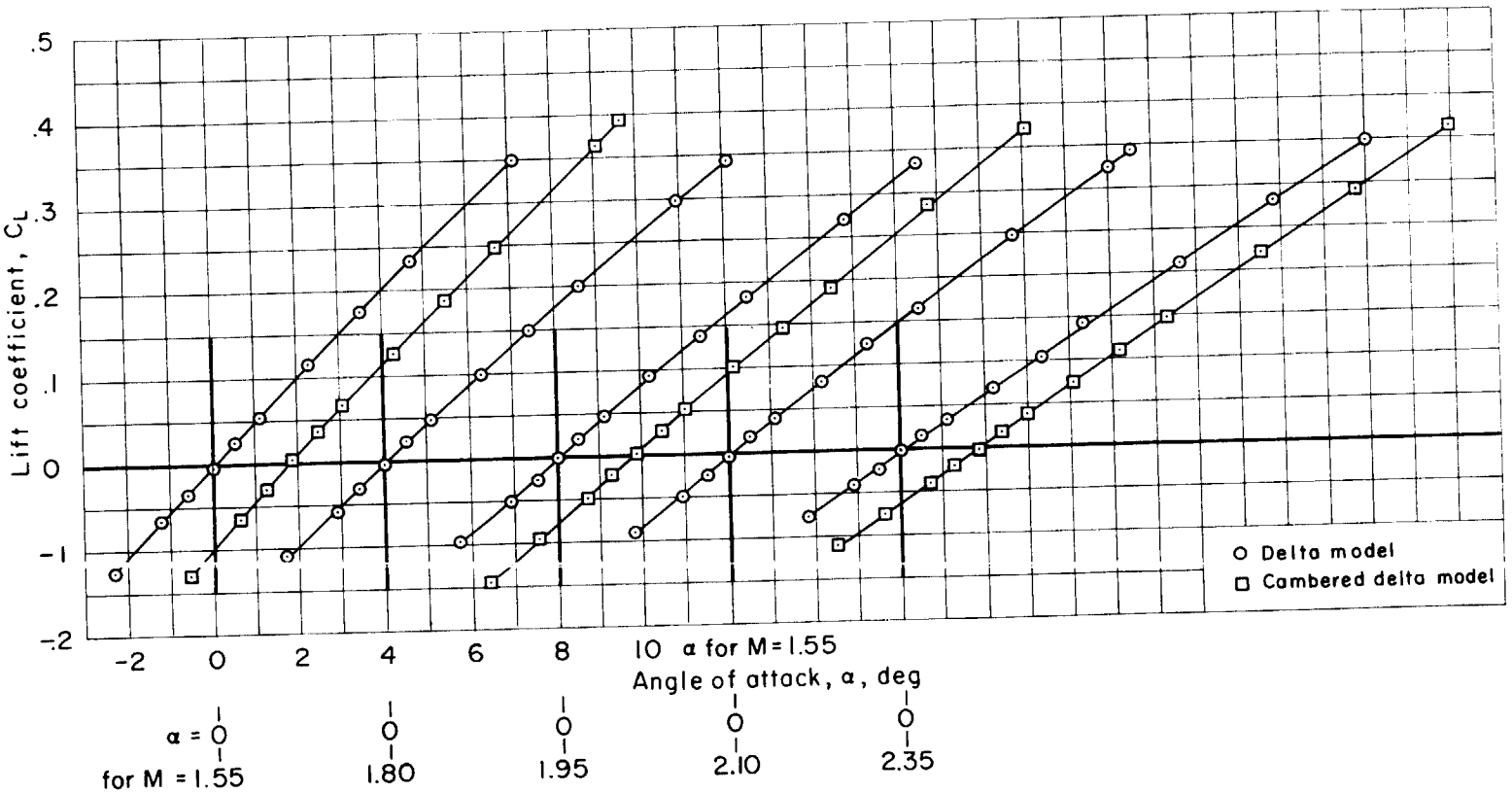

(a) C_L vs. α

Figure 8.- Supersonic aerodynamic characteristics for the delta and cambered delta models with transition fixed as determined from tests in the 9- by 7-foot supersonic test section of the Ames Unitary Plan Wind Tunnel (R/ft = 3,000,000).

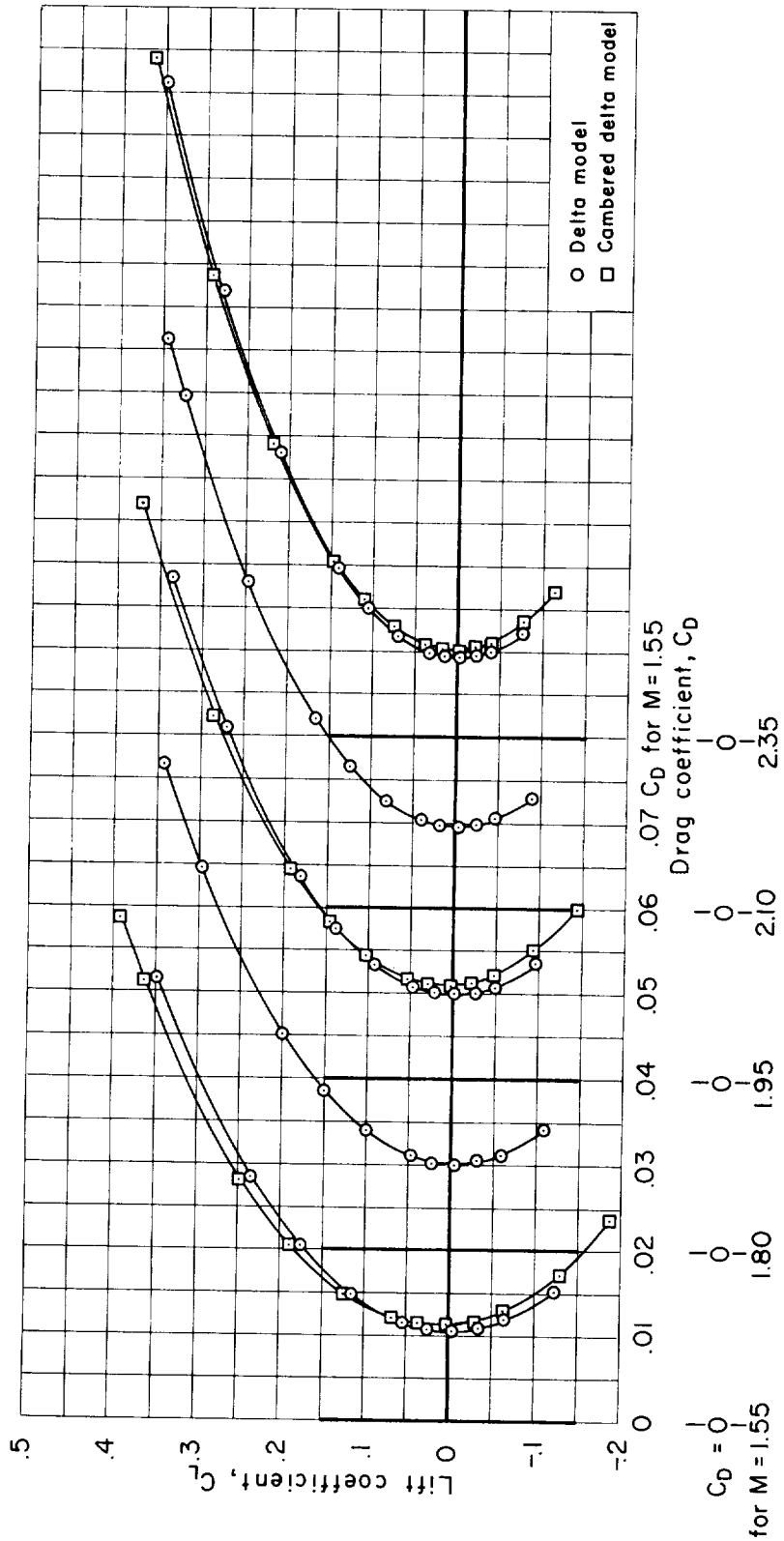

(b) C_L vs. C_D

Figure 8.- Continued.

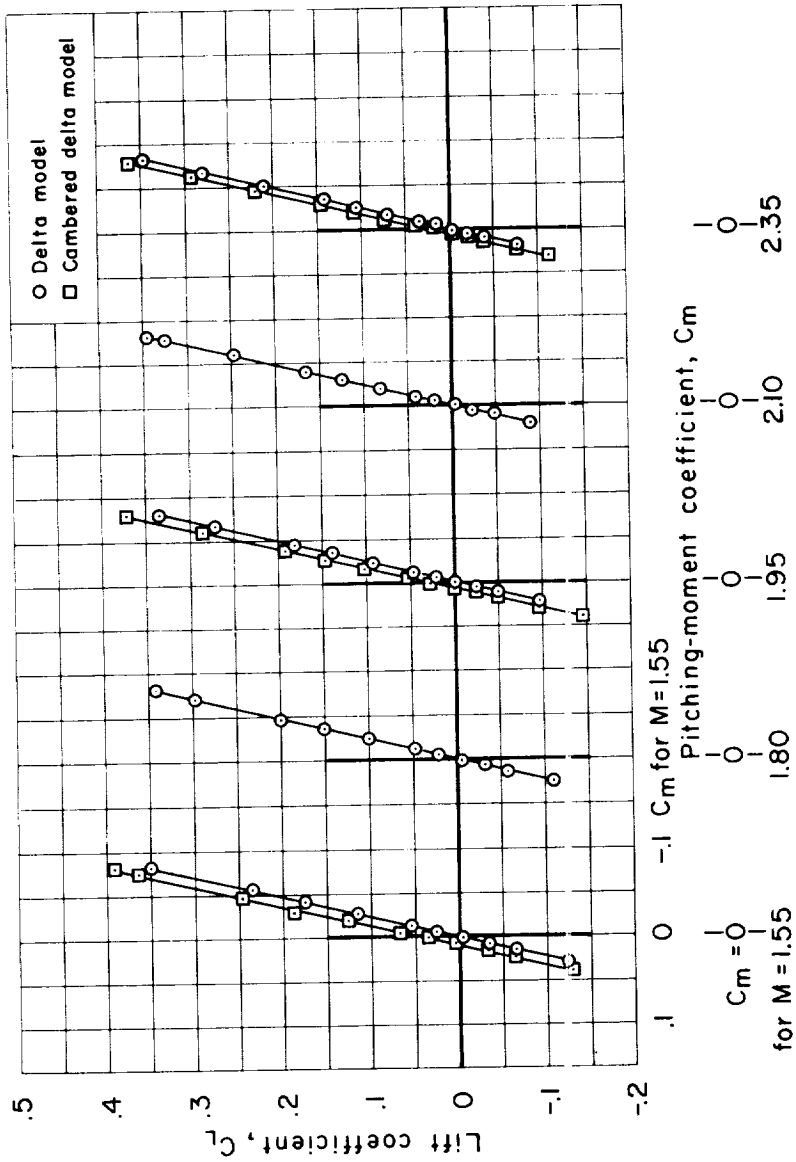

(c) C_L vs. C_m

Figure 8.- Concluded.

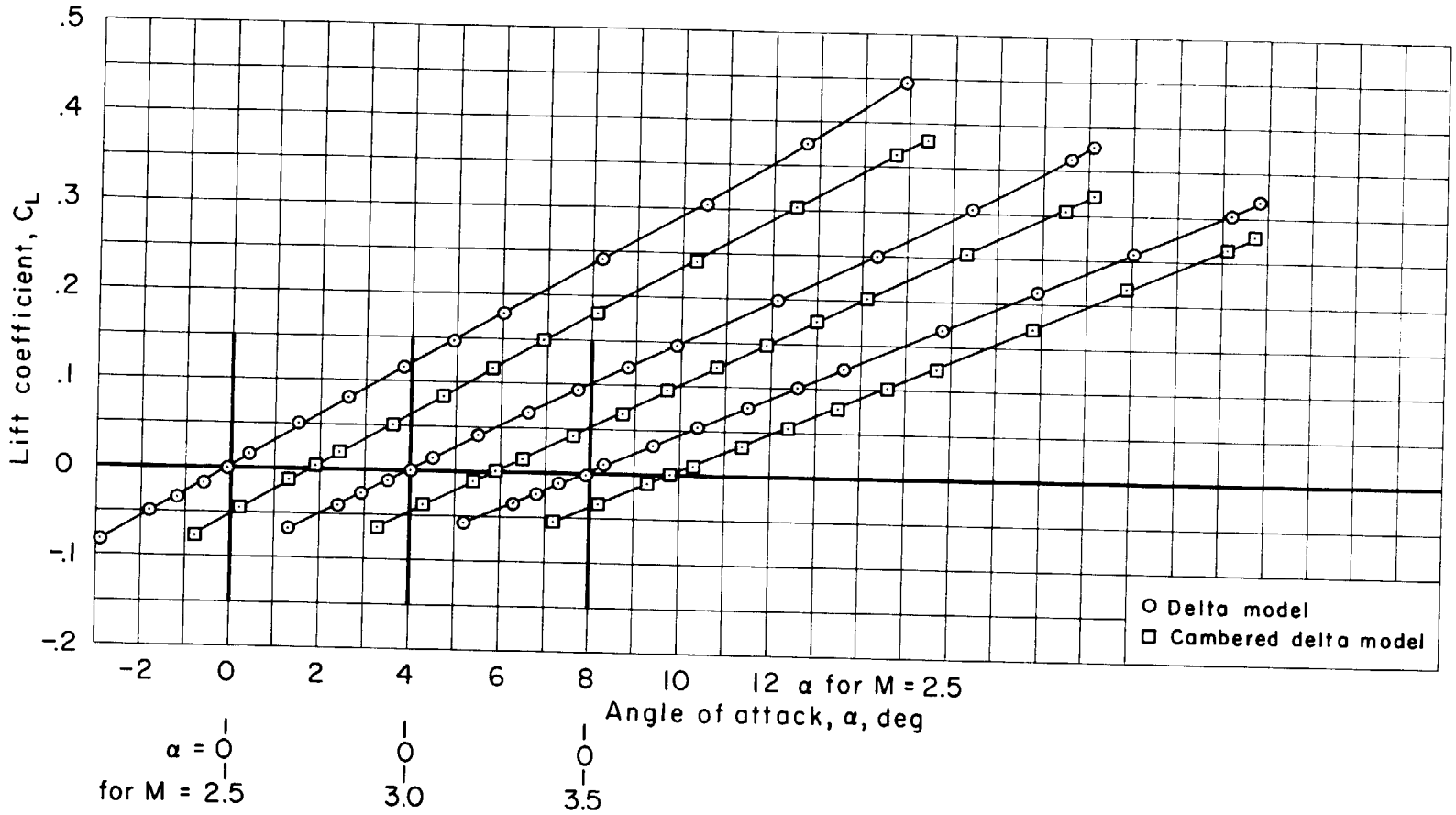

(a) C_L vs. α

Figure 9.- Supersonic aerodynamic characteristics for the delta and cambered delta models with transition fixed as determined from tests in the 8- by 7-foot supersonic test section of the Ames Unitary Plan Wind Tunnel (R/ft = 2,000,000).

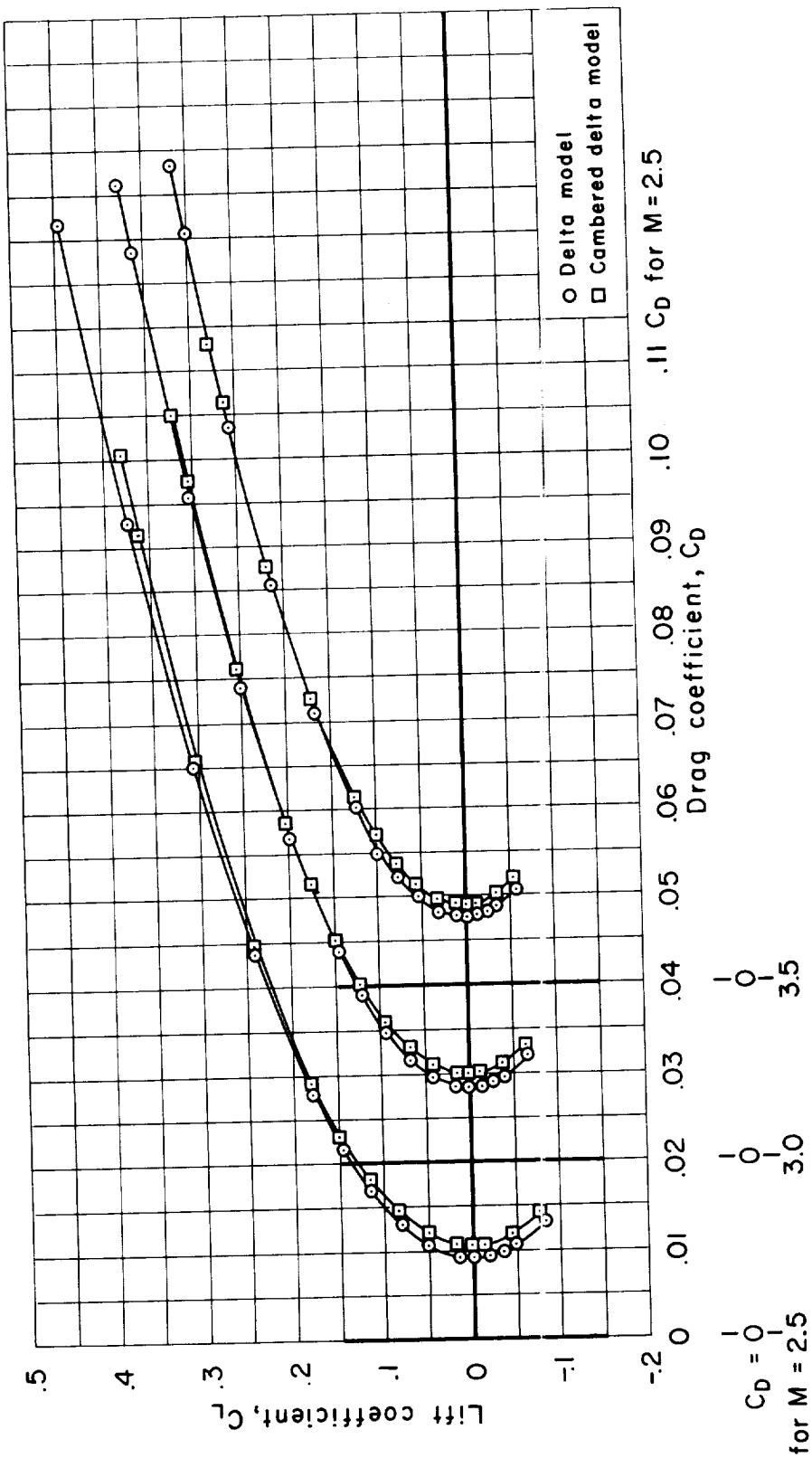

(b) C_L vs. C_D

Figure 9.- Continued.

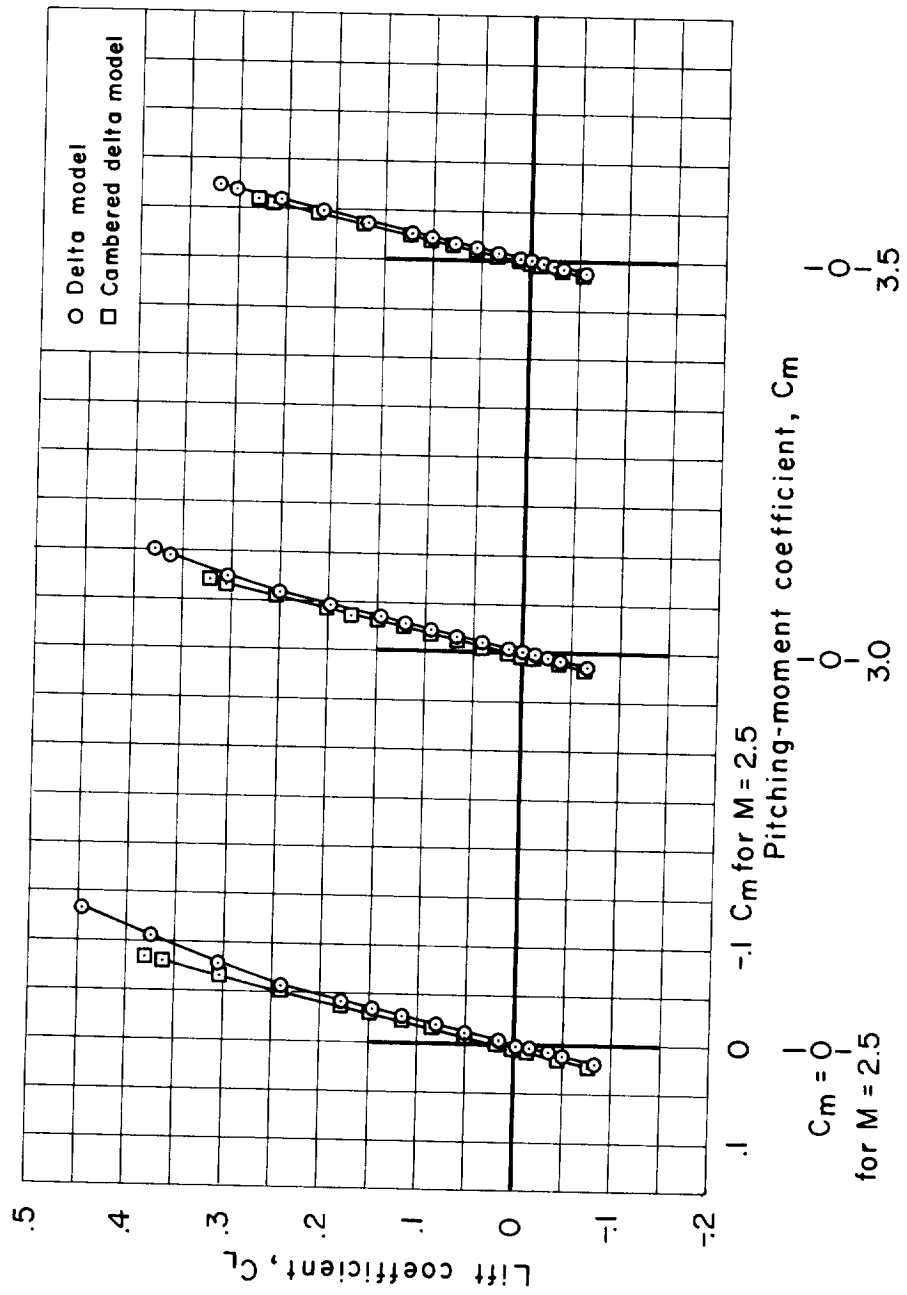

(c) C_L vs. C_m

Figure 9.- Concluded.

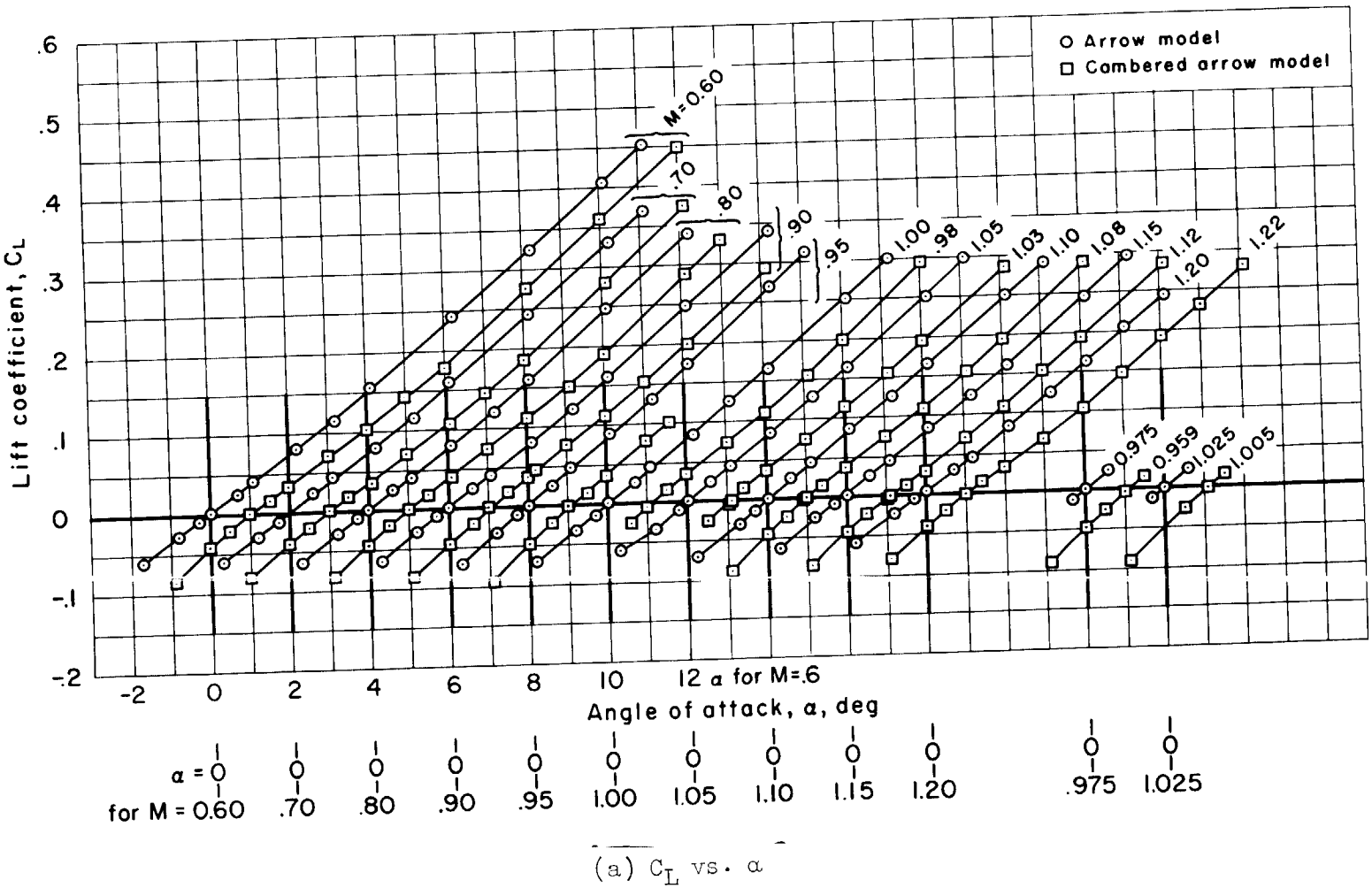

(a) C_L vs. α

Figure 10.- Transonic aerodynamic characteristics for the arrow and cambered arrow models with transition fixed as determined from tests in the Ames 14-Foot Transonic Wind Tunnel (R/ft = 3,500,000 to 4,000,000).

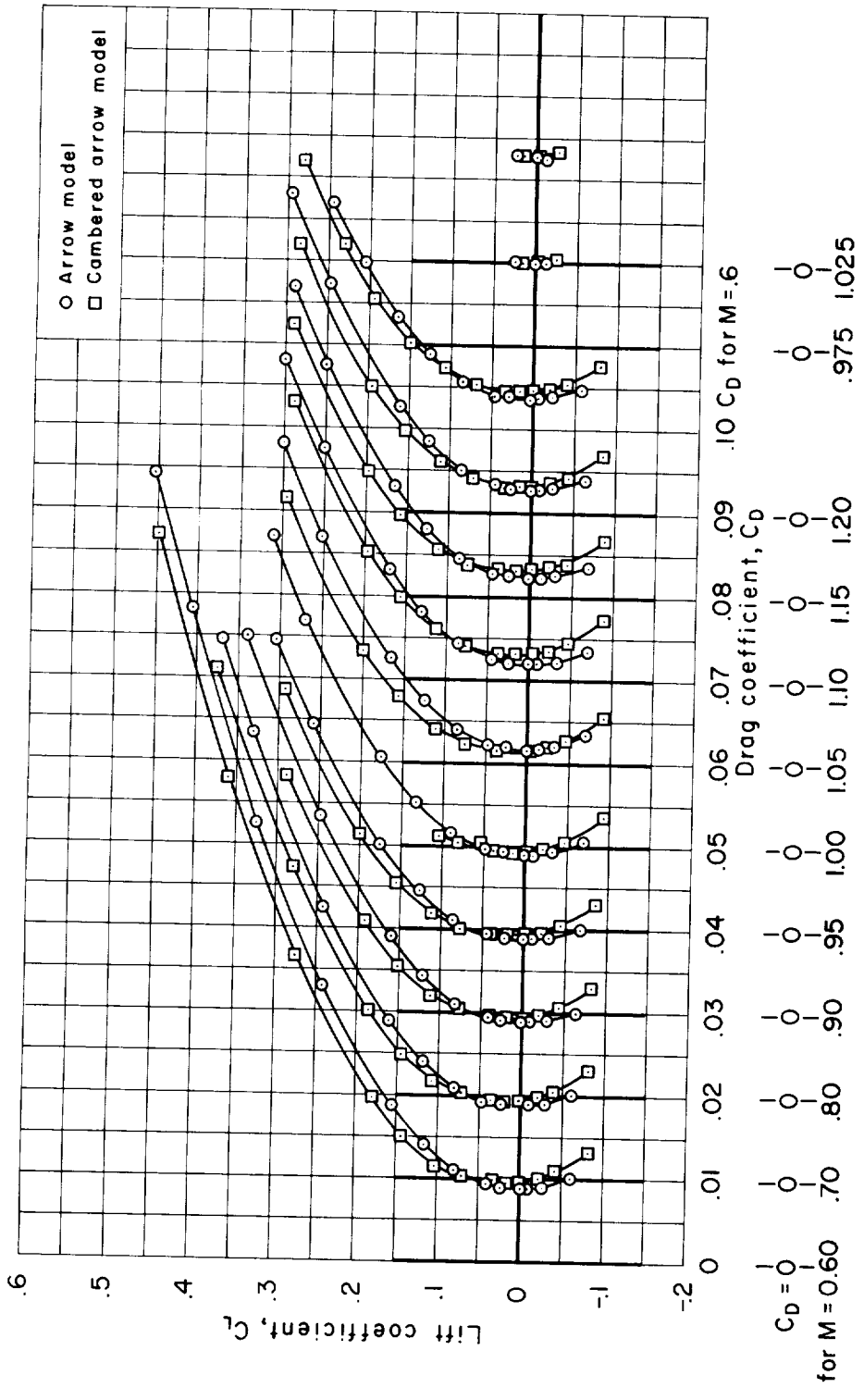

(b) C_L vs. C_D

Figure 10.- Continued.

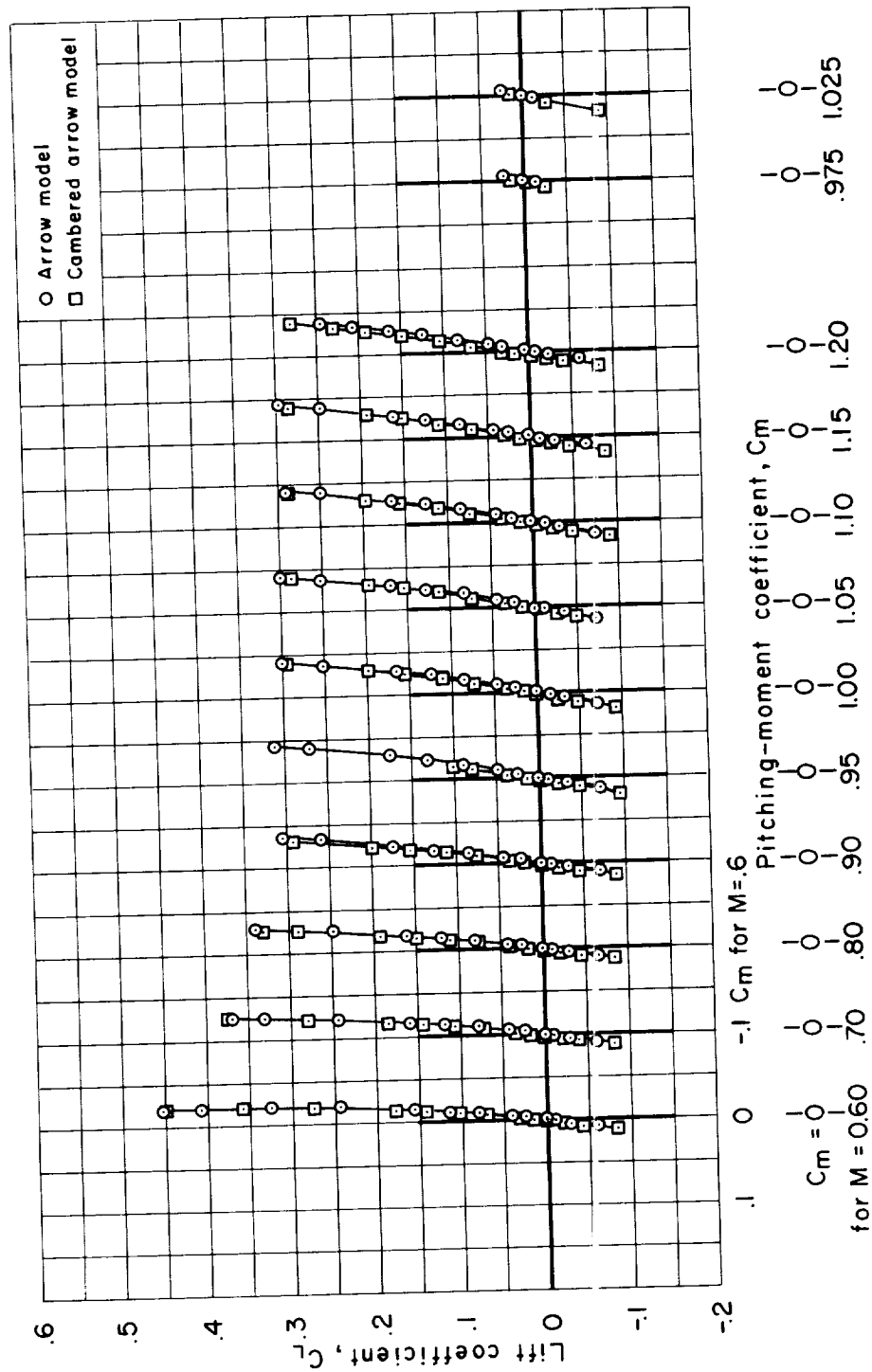

(c) C_L vs. C_m

Figure 10.- Continued.

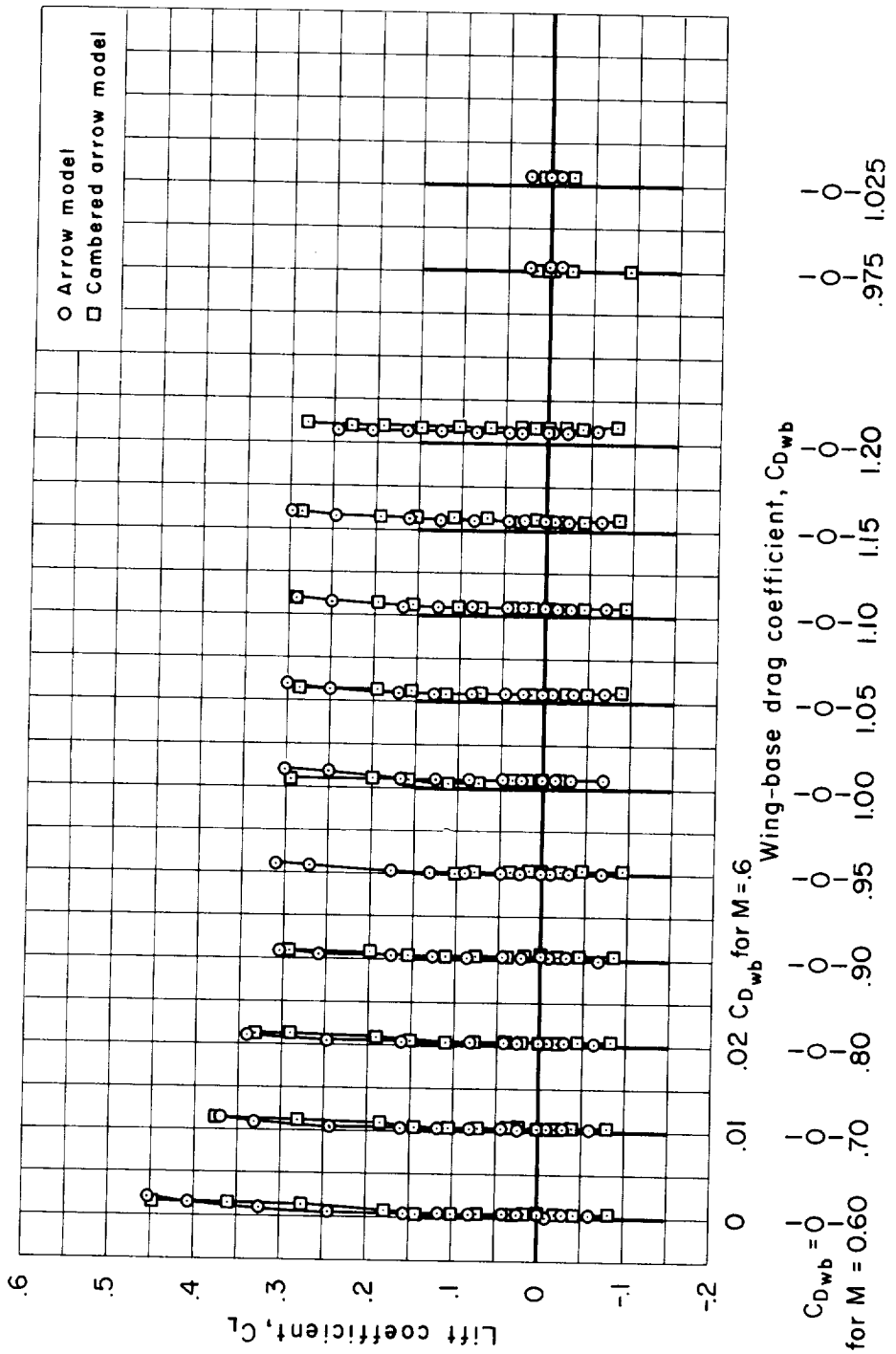

(d) C_L vs. $C_{D_{wb}}$

Figure 10.- Concluded.

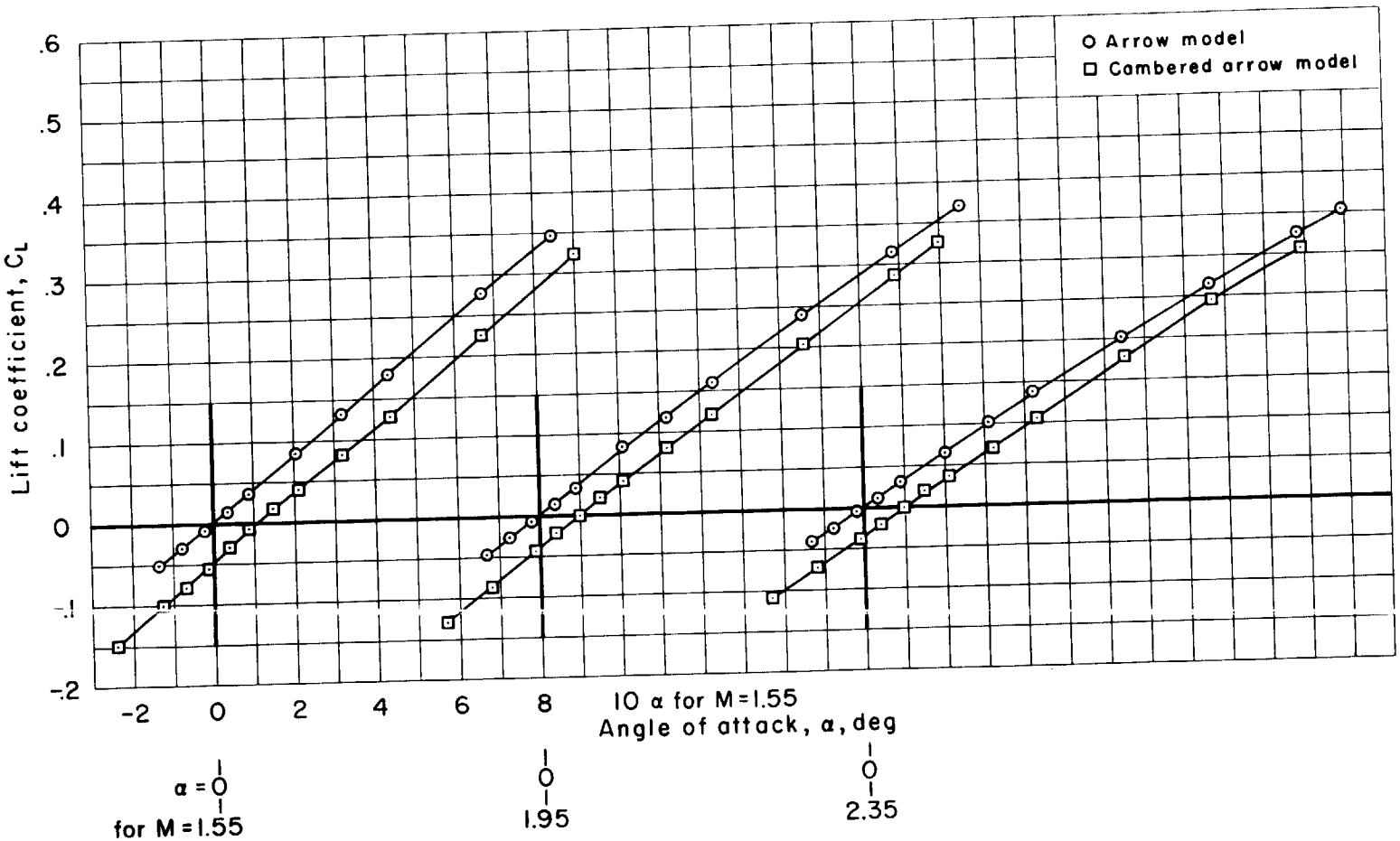

(a) C_L vs. α

Figure 11.- Supersonic aerodynamic characteristics for the arrow and cambered arrow models with transition fixed as determined from tests in the 9- by 7-foot supersonic test section of the Ames Unitary Plan Wind Tunnel (R/ft = 3,000,000).

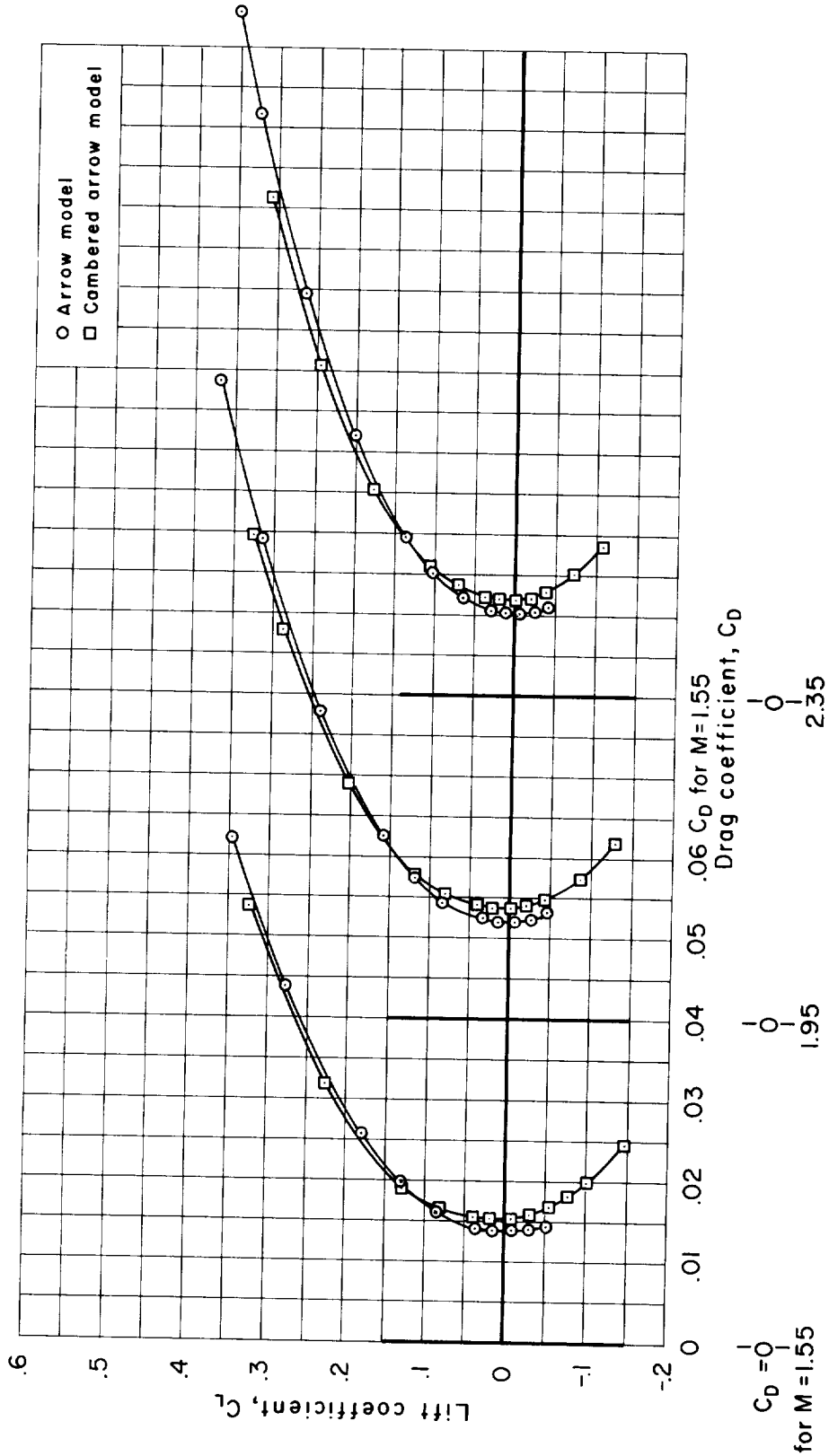

(b) C_L vs. C_D

Figure 11.- Continued.

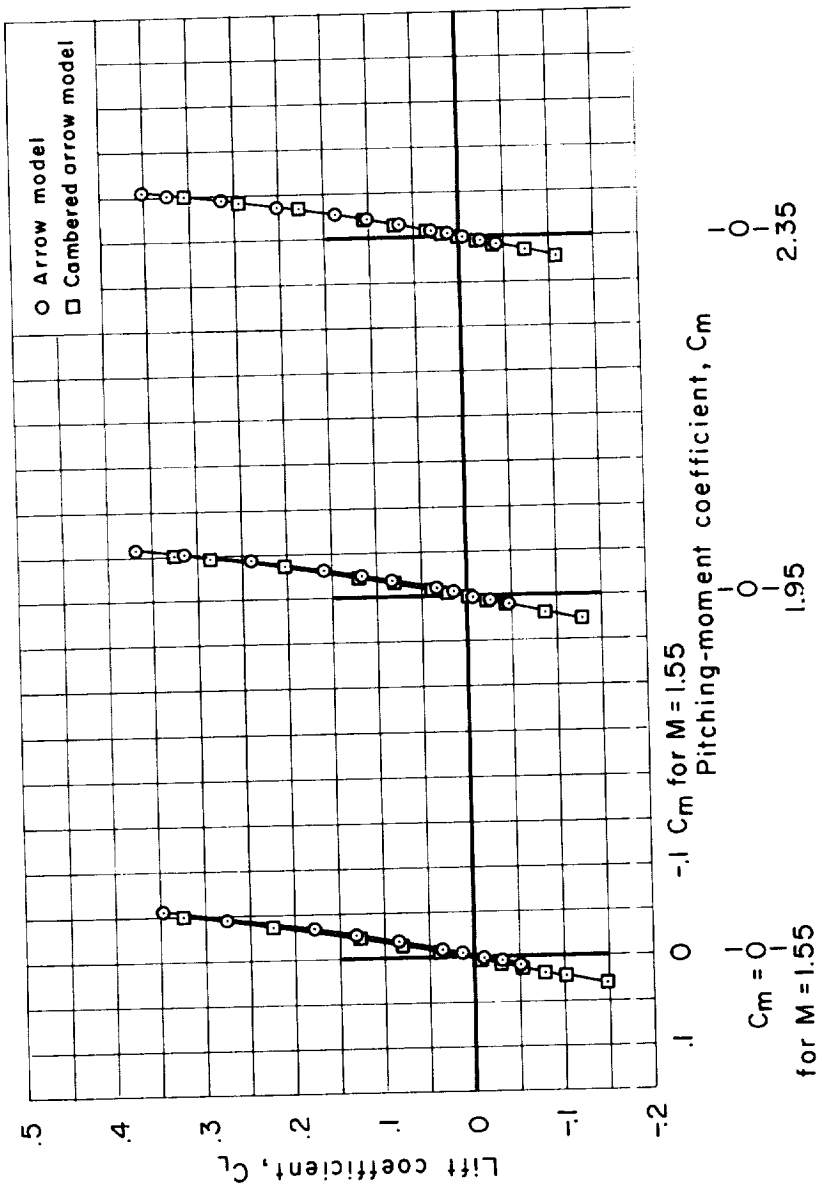

(c) C_L vs. C_m

Figure 11.- Concluded.

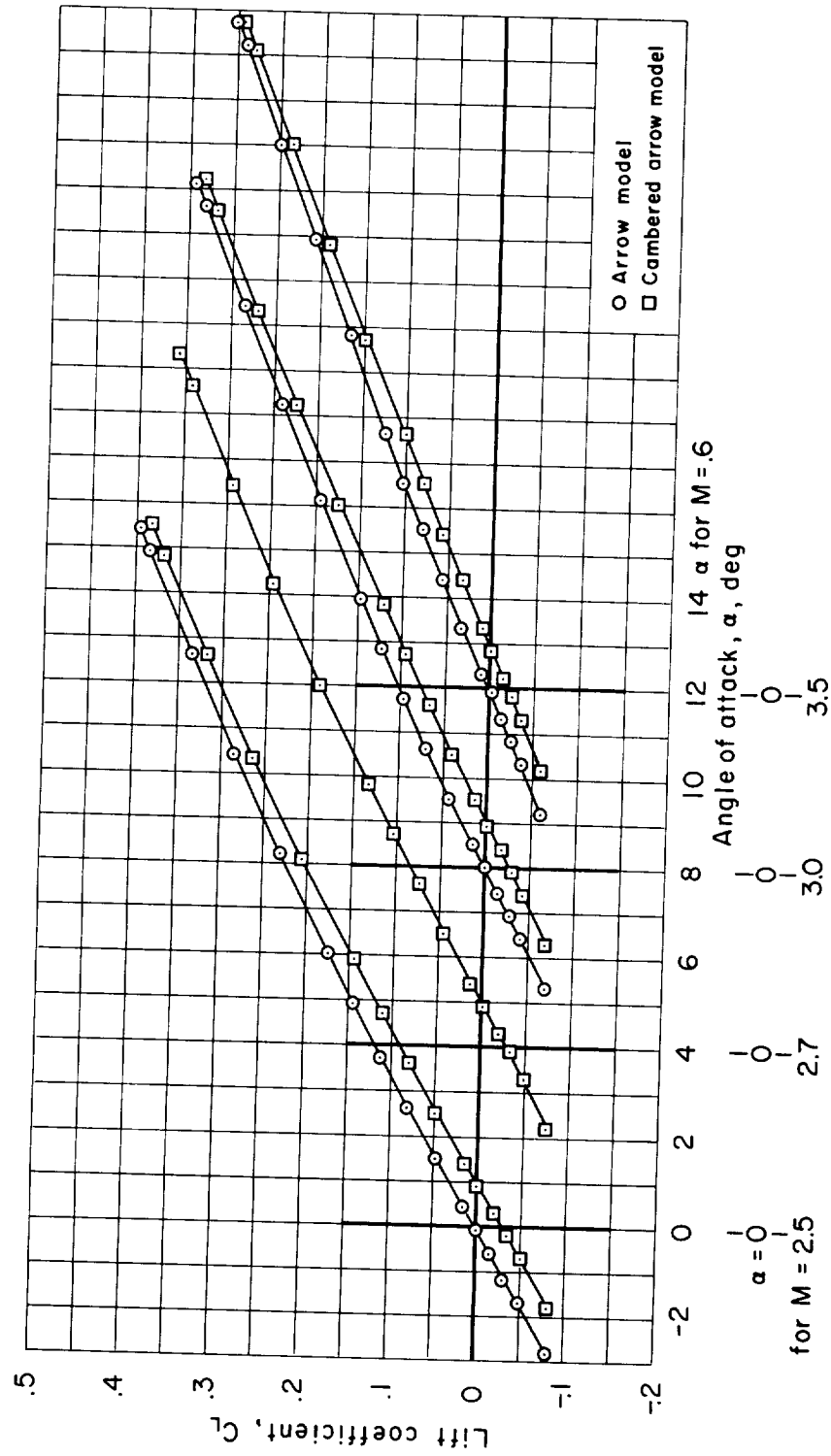

(a) C_L vs. α

Figure 12.- Supersonic aerodynamic characteristics for the arrow and cambered arrow models as determined from tests in the 8- by 7-foot supersonic test section of the Ames Unitary Plan Wind Tunnel (R/ft = 2,000,000).

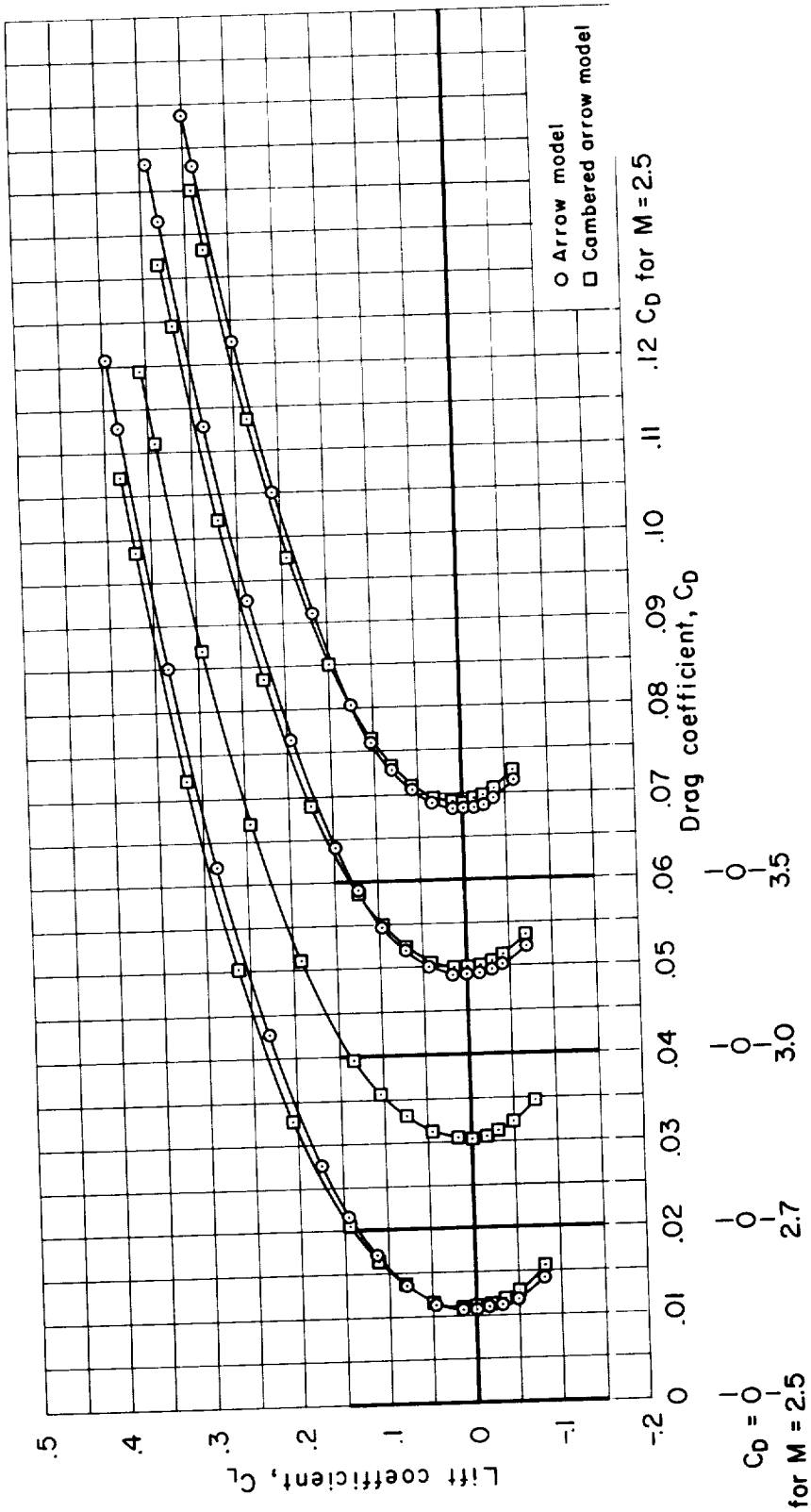

(b) C_L vs. C_D

Figure 12.- Continued.

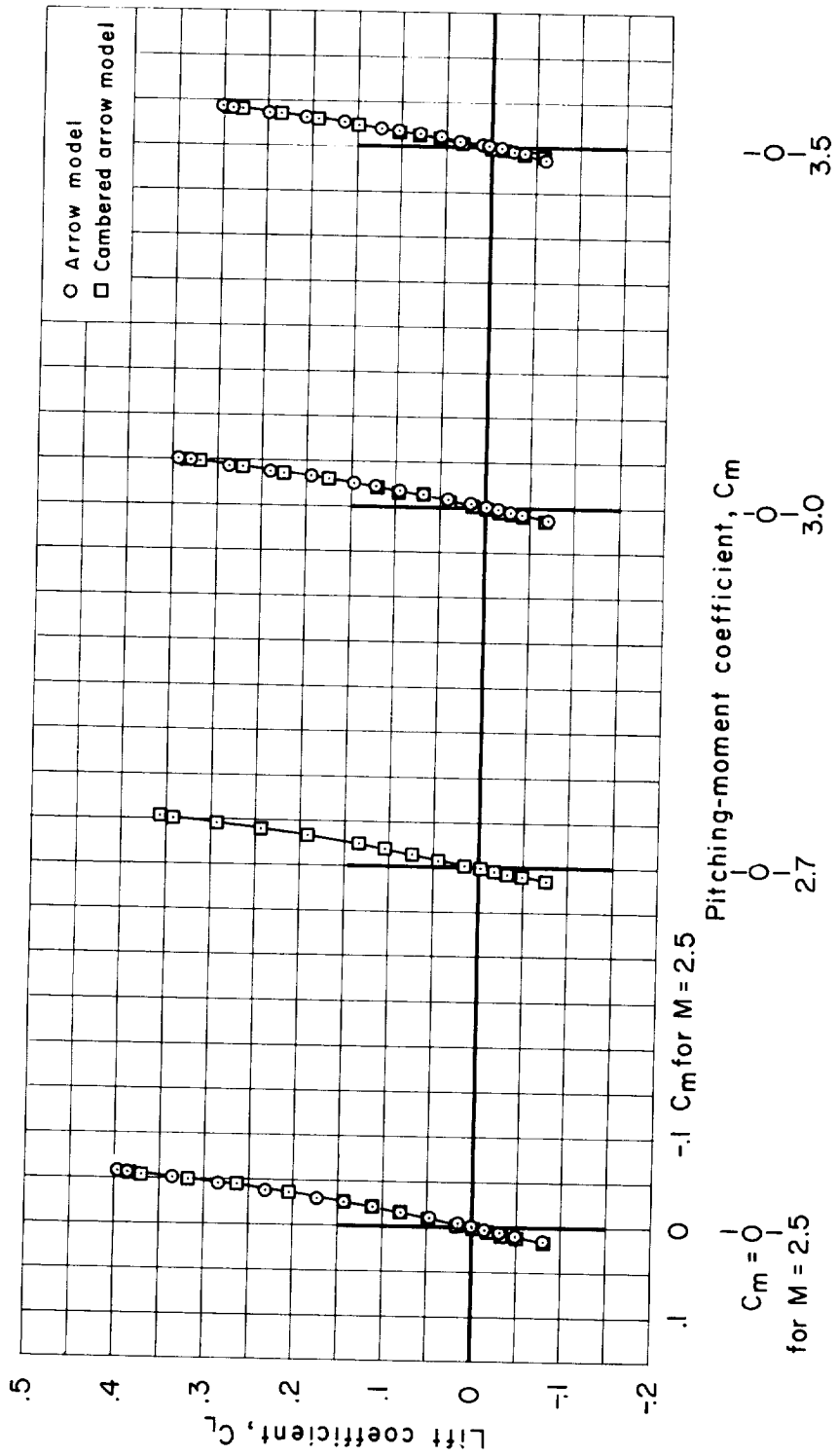

(c) C_L vs. C_m

Figure 12.- Concluded.

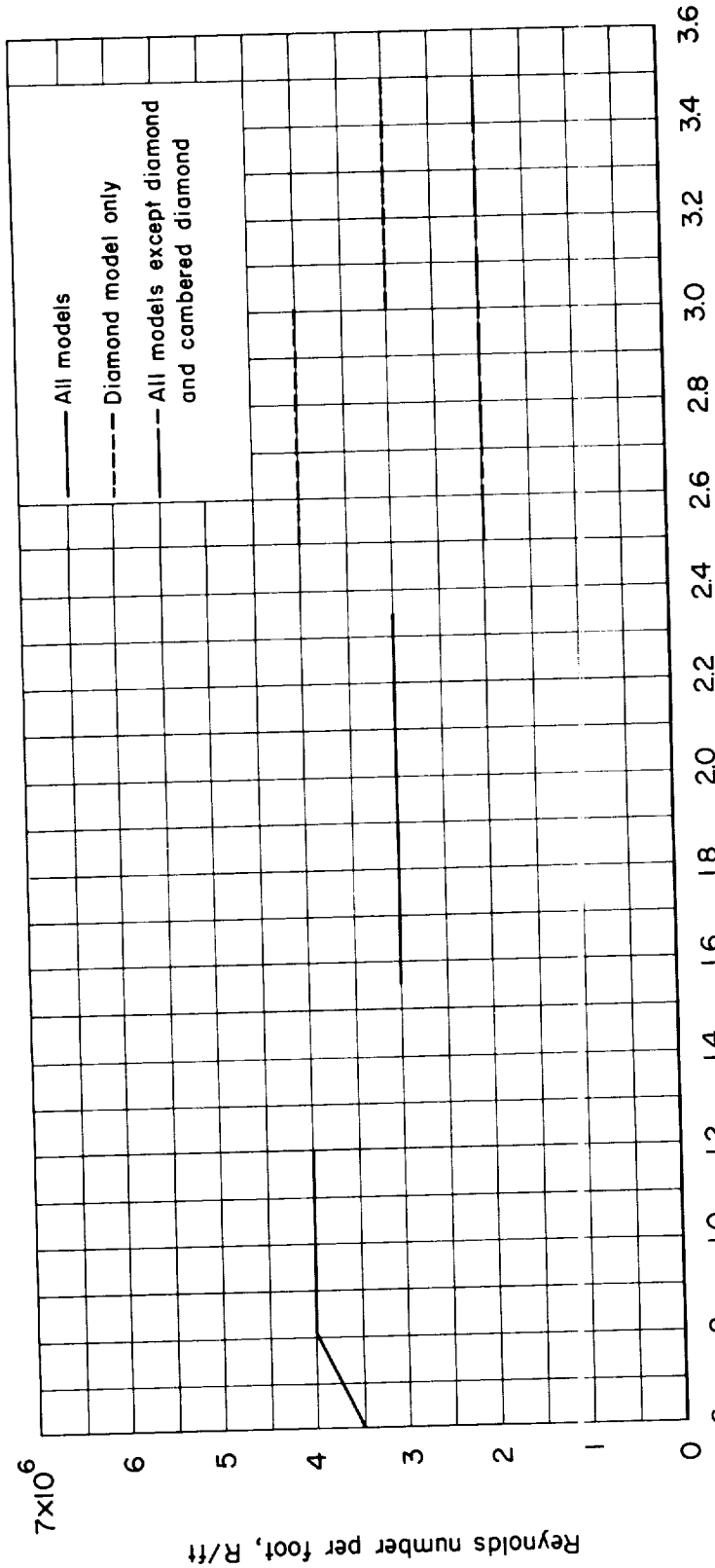

Figure 13.- Reynolds number per foot variation with Mach number for the models investigated.

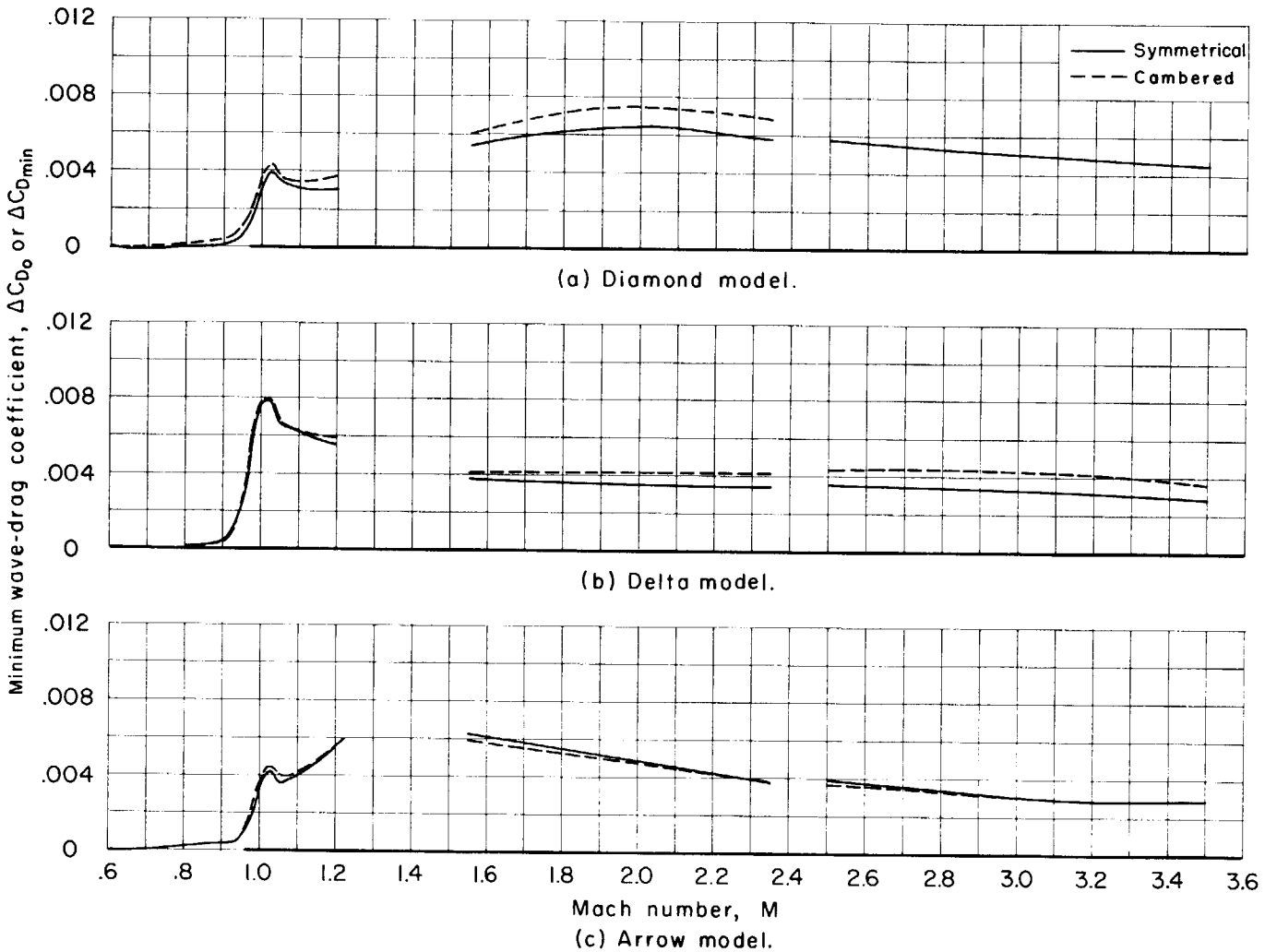

Figure 14.- Experimental zero-lift or minimum wave-drag coefficients for the symmetrical and cambered models.

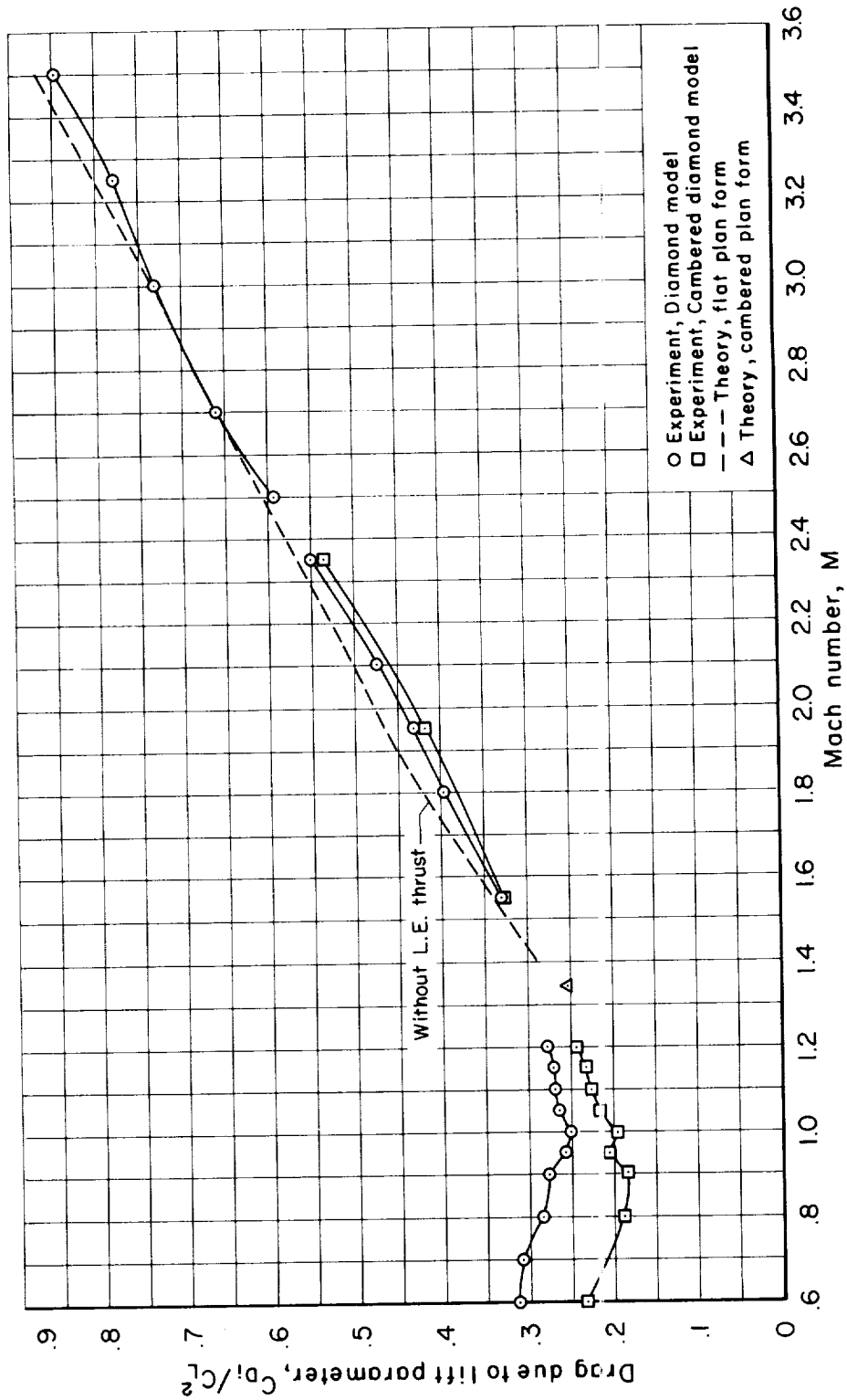

(a) Diamond models.

Figure 15.- Experimental values of drag due to lift parameter for the symmetrical and cambered models compared with theoretical values for flat plate wings of the same plan form with and without leading-edge thrust.

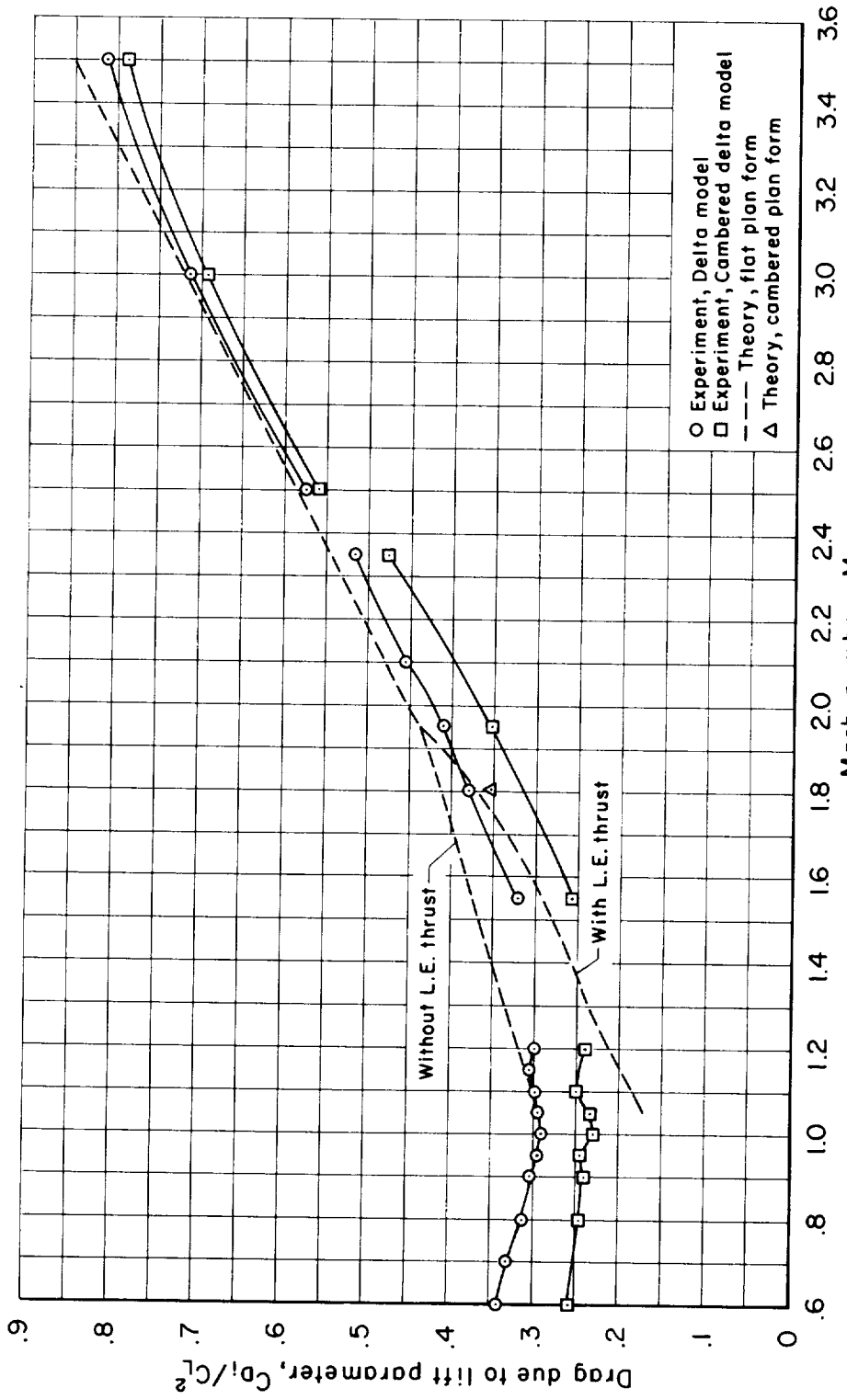

(b) Delta models.

Figure 15.- Continued.

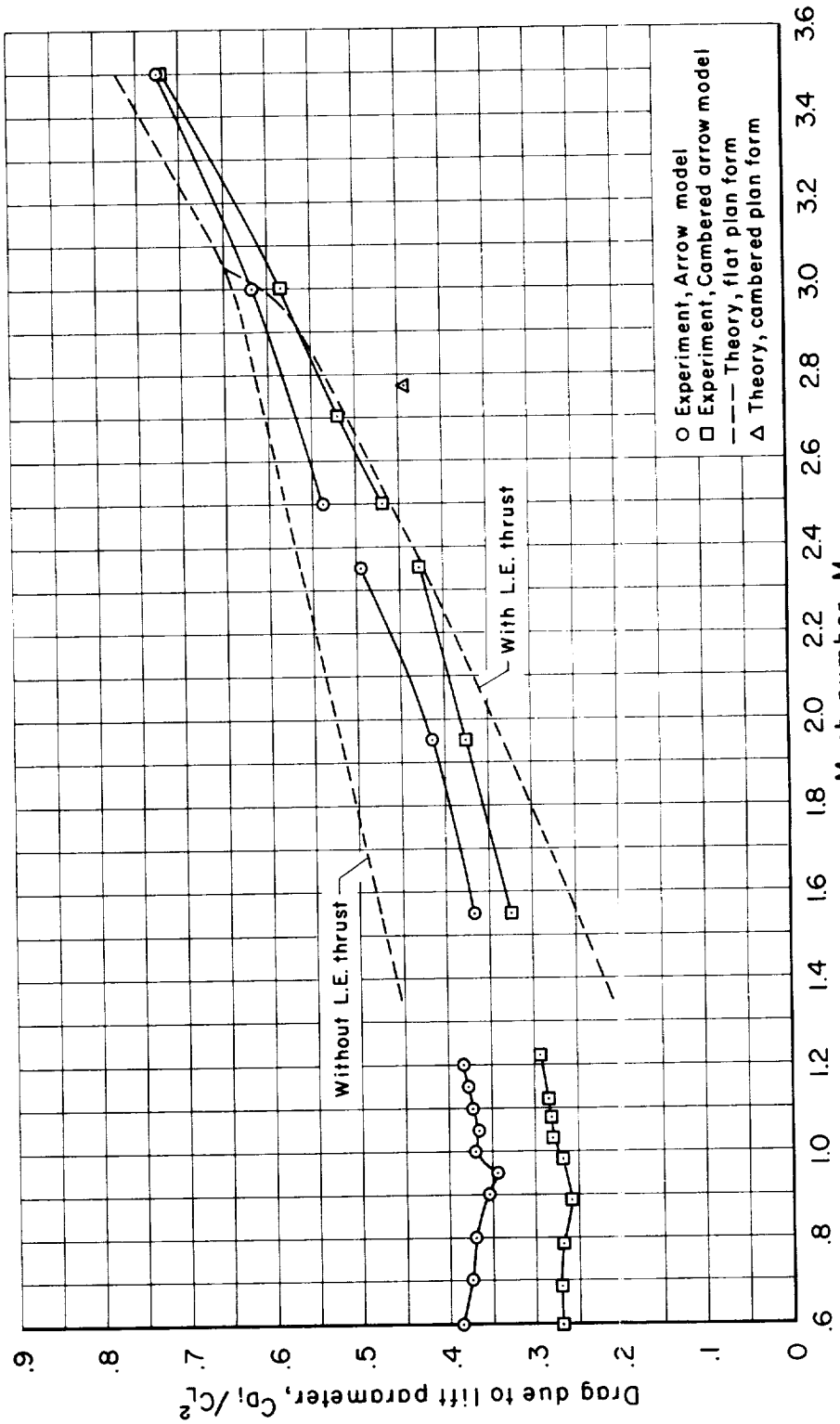

(c) Arrow models.

Figure 15.- Concluded.

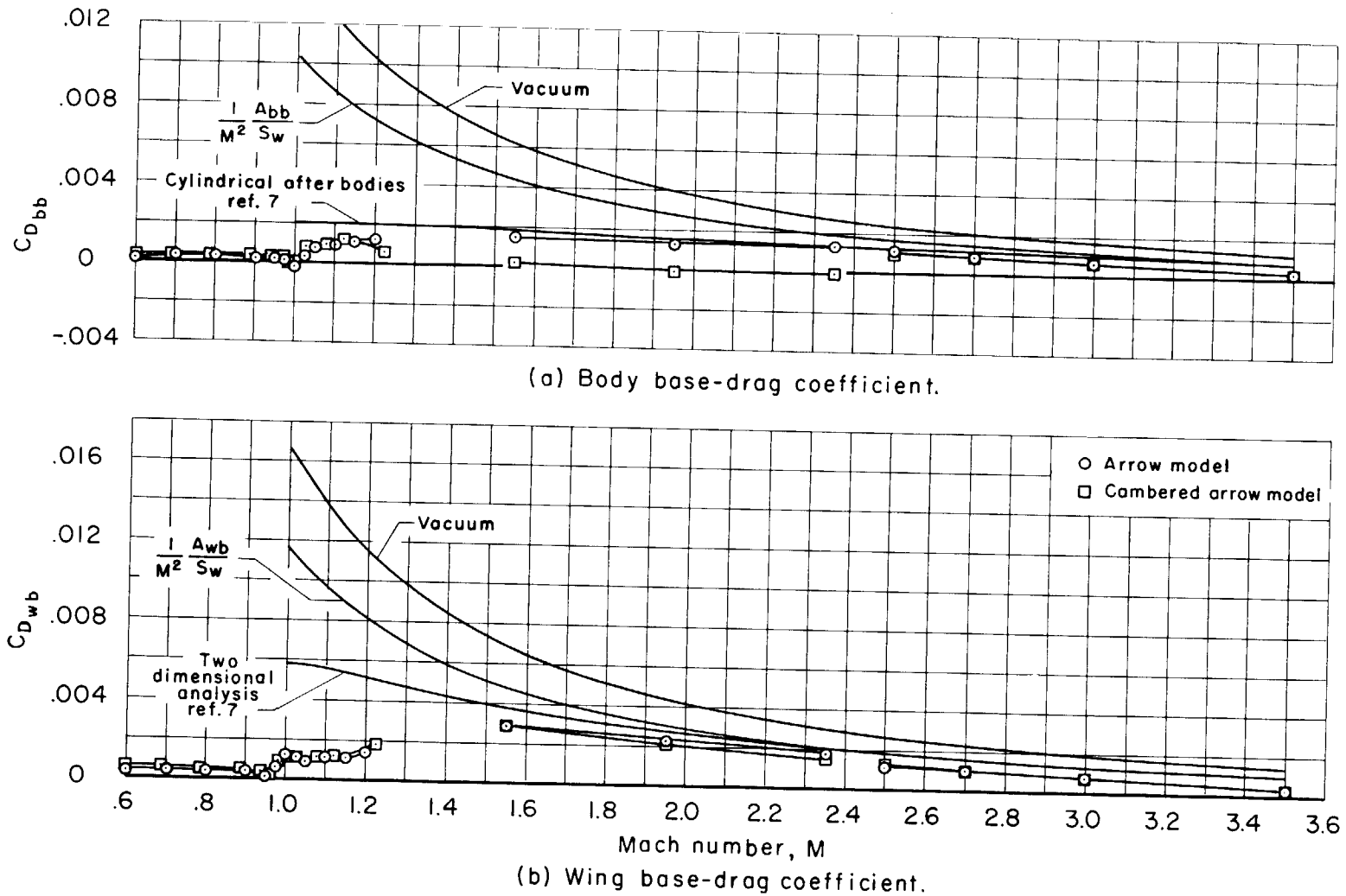

Figure 16.- Variation of wing and body base-drag coefficients with Mach number for the arrow and cambered arrow models.

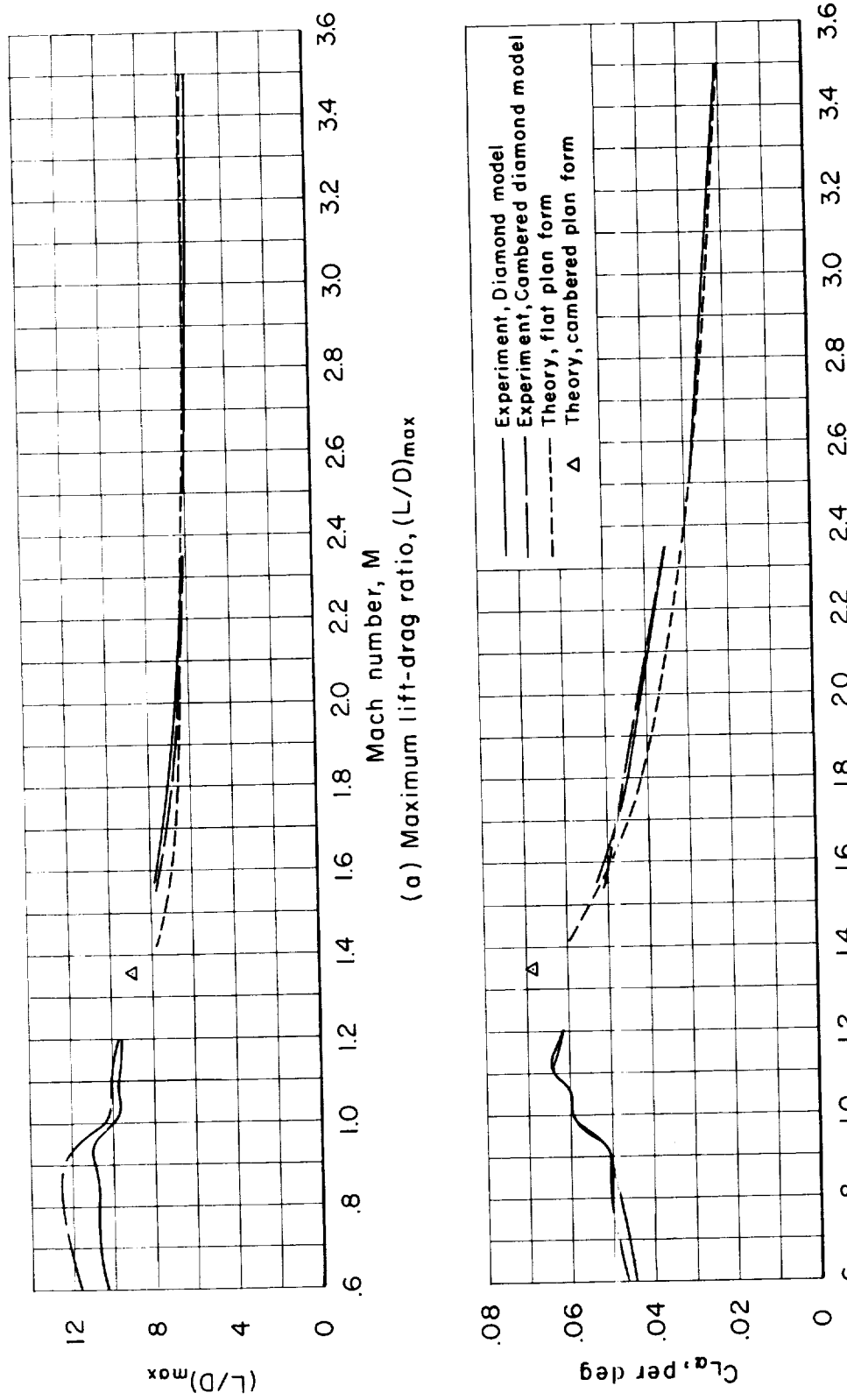

Figure 17.- Aerodynamic trends with Mach number for the diamond and cambered diamond models as indicated by experiment and theory; transition fixed.

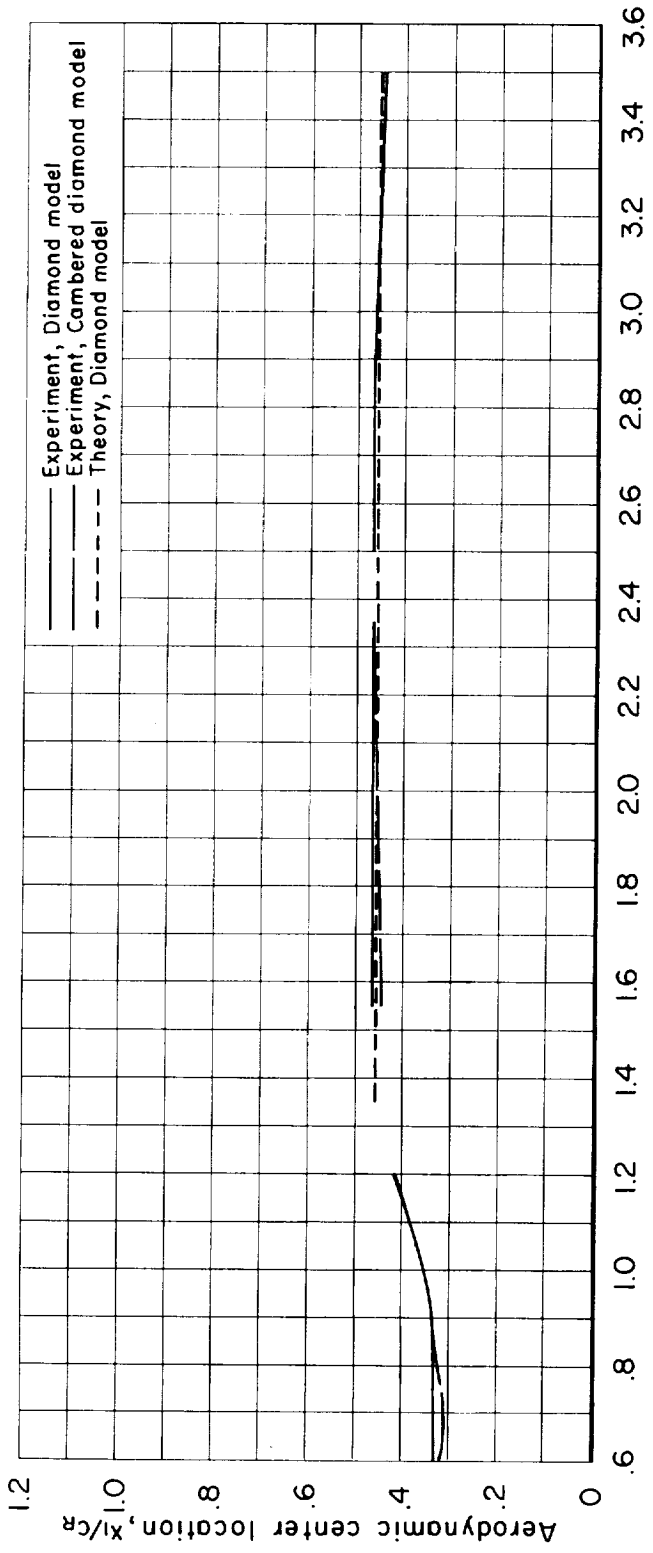

(c) Aerodynamic center location, x_l/c_R

Figure 17.- Concluded.

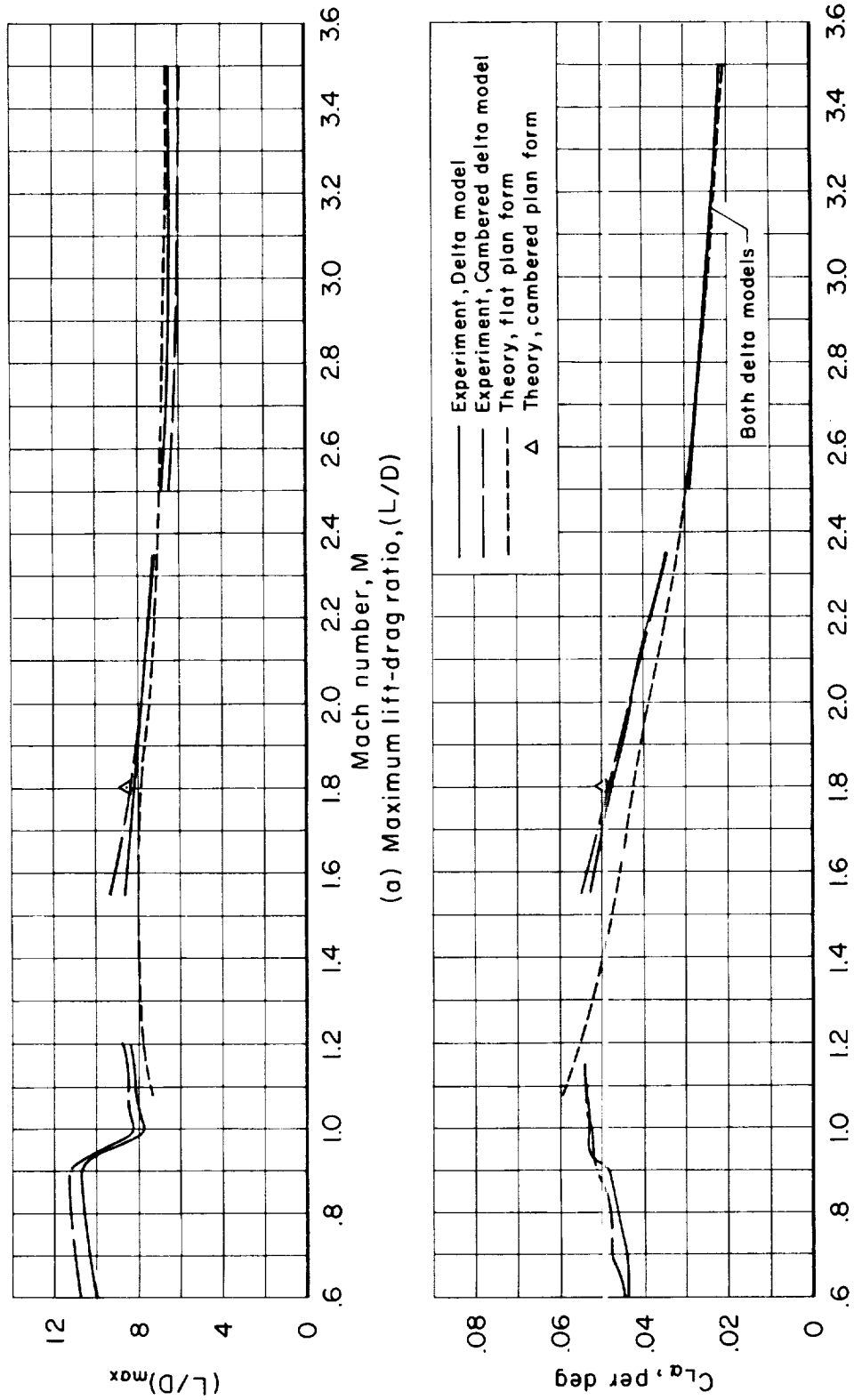

Figure 18.- Aerodynamic trends with Mach number for the delta and cambered delta models as indicated by experiment and theory; transition fixed.

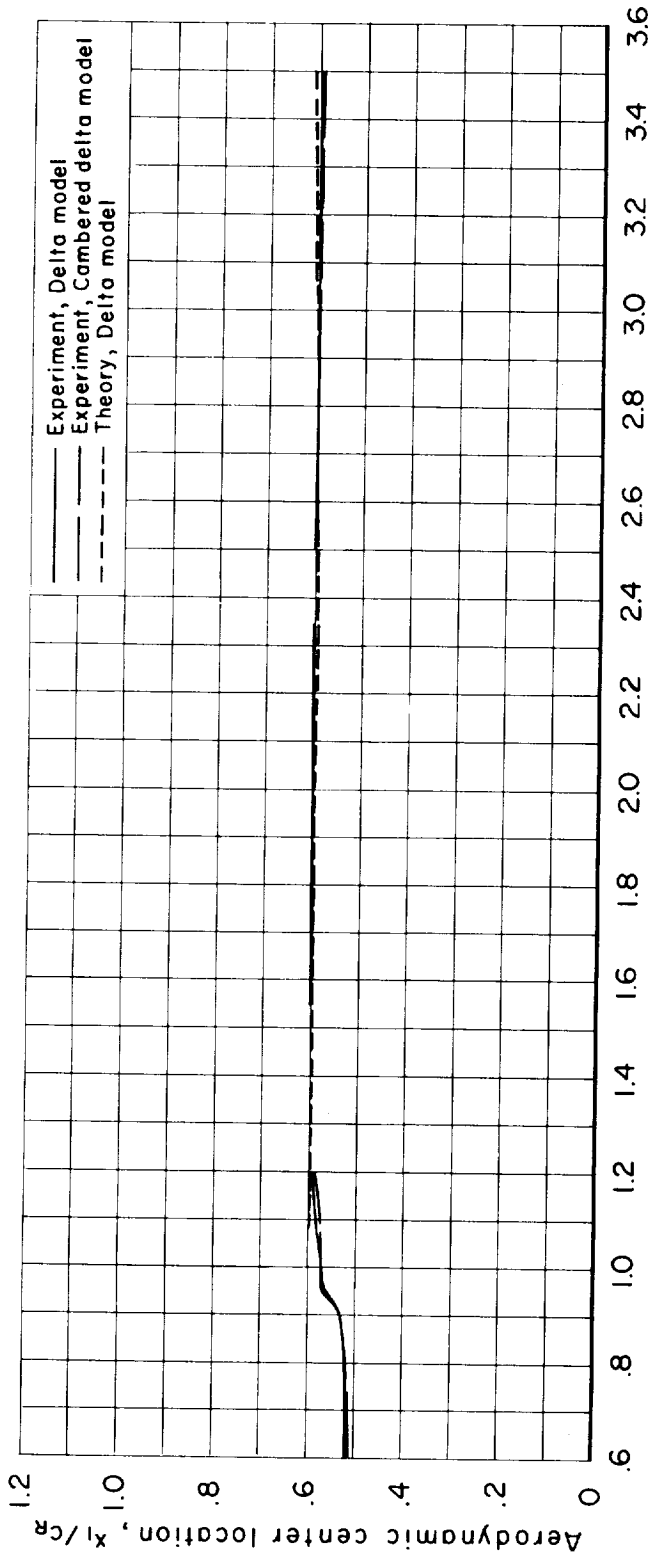

(c) Aerodynamic center location, x_1/c_R

Figure 18.- Concluded.

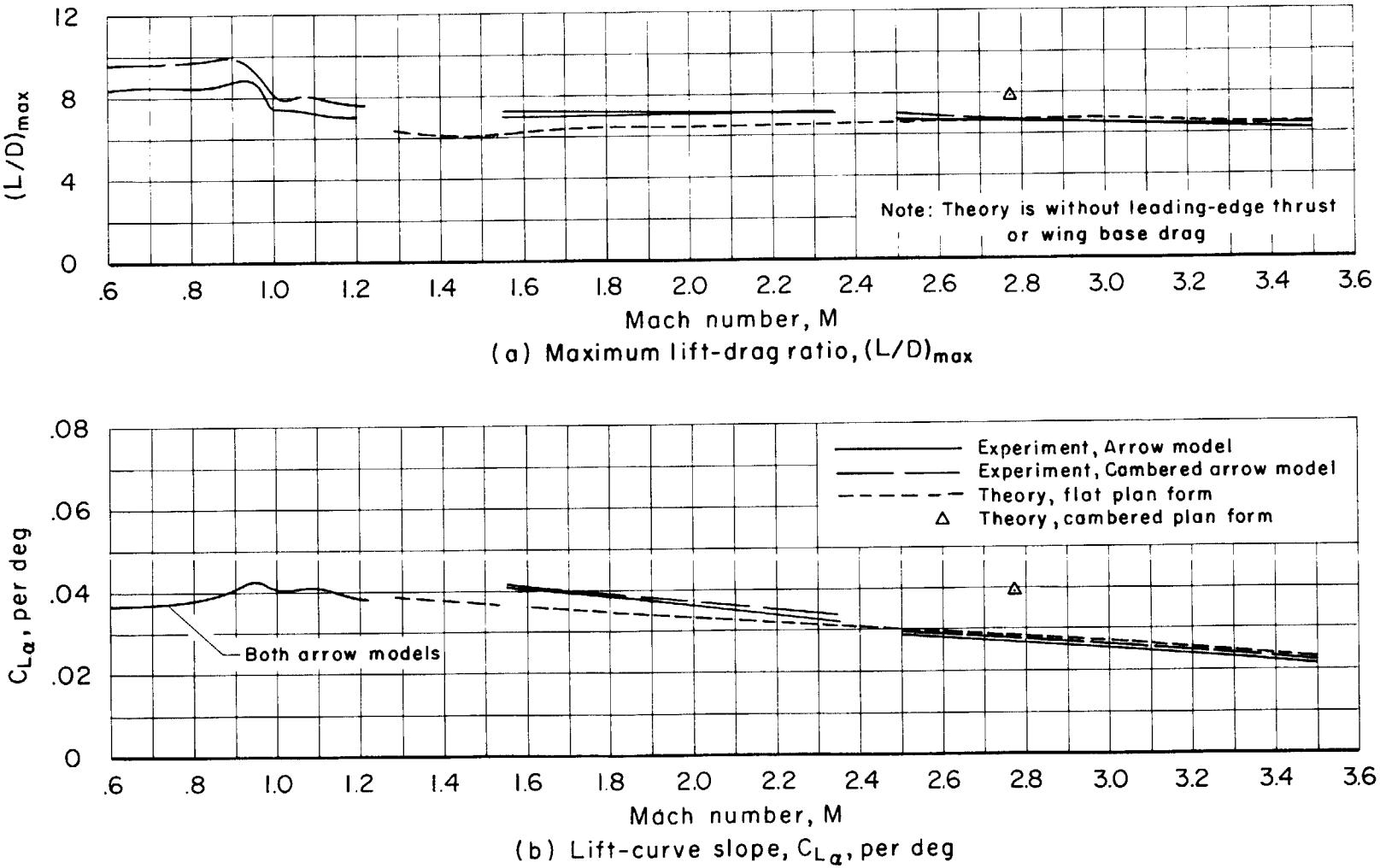

Figure 19.- Aerodynamic trends with Mach number for the arrow and cambered arrow models as indicated by experiment and theory; transition fixed.

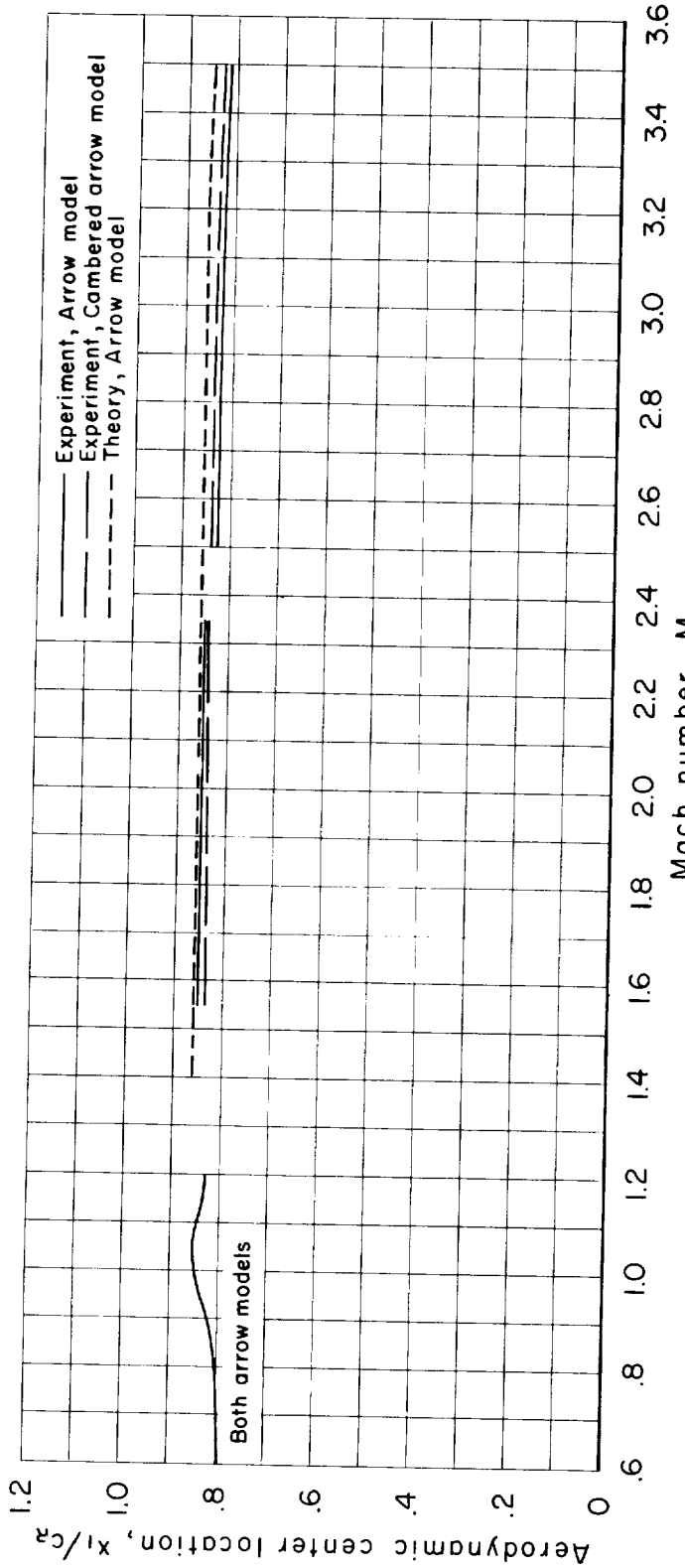

(c) Aerodynamic center location, x_1/c_R

Figure 19.- Concluded.

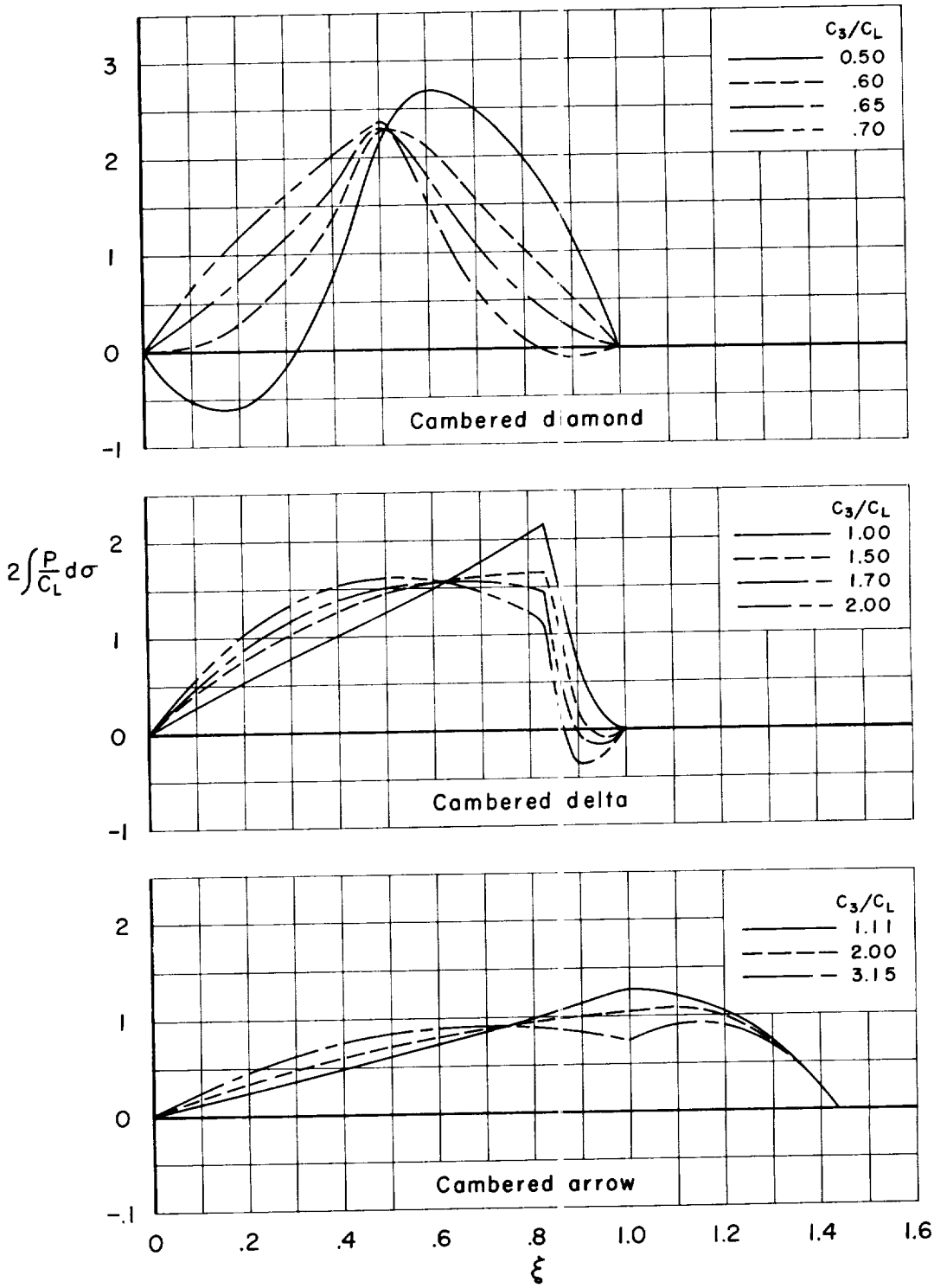

Figure 20.- Design parameters (C_3/C_L) considered for the cambered plan forms in selecting the chordwise lift distribution.

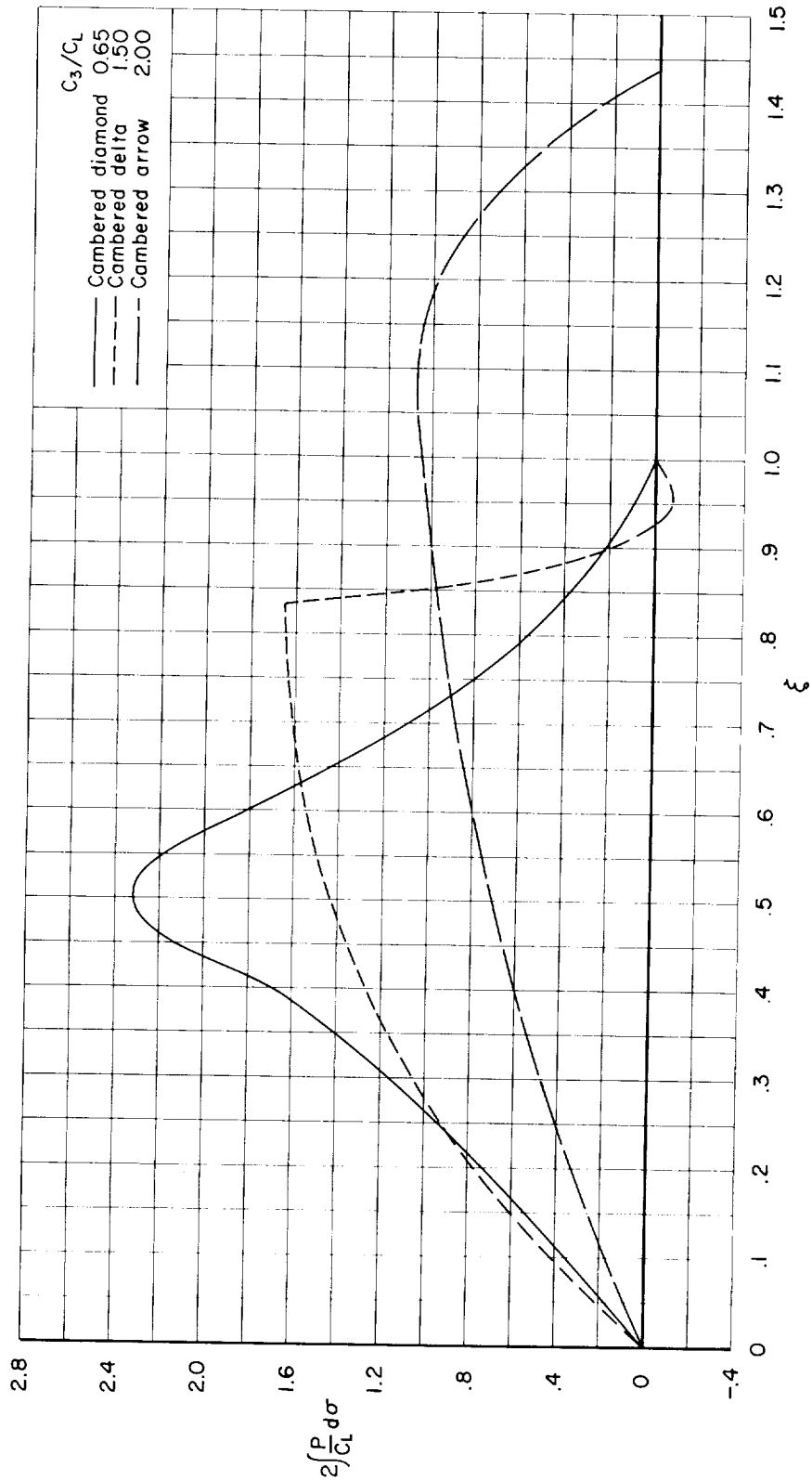

Figure 21.- Chordwise lift distributions selected from among those shown in figure 20 for the cambered plan forms.

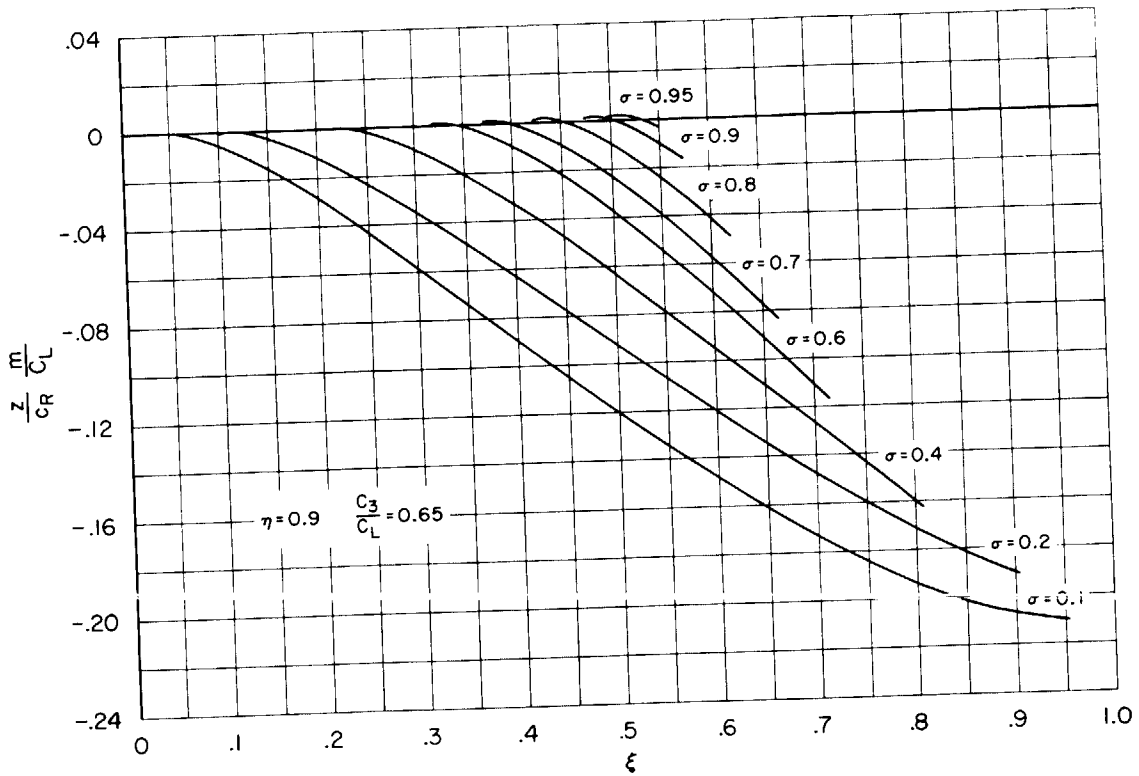

(a) Cambered diamond model.

Figure 22.- Mean camber lines at selected spanwise stations of the cambered models prior to corrections for dihedral and center-line incidence.

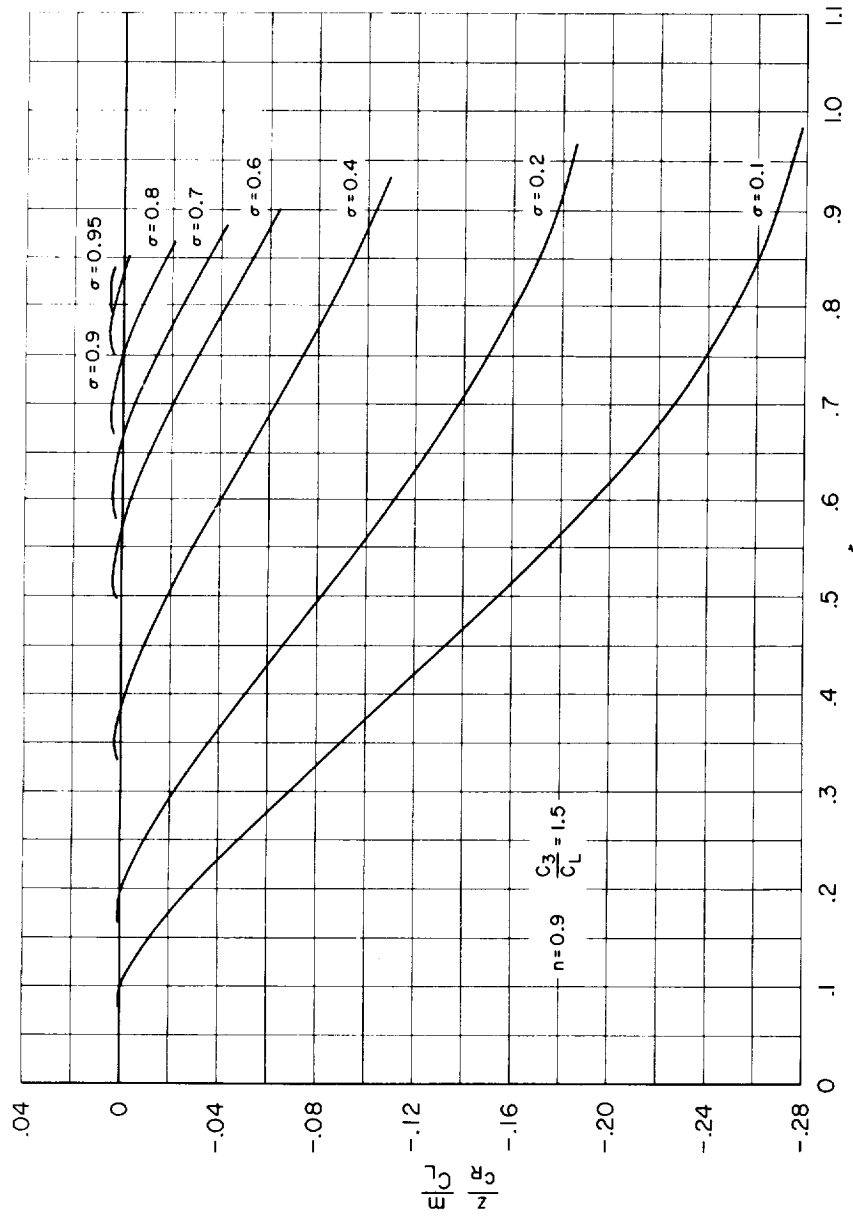

(b) Cambered delta model.

Figure 22.- Continued.

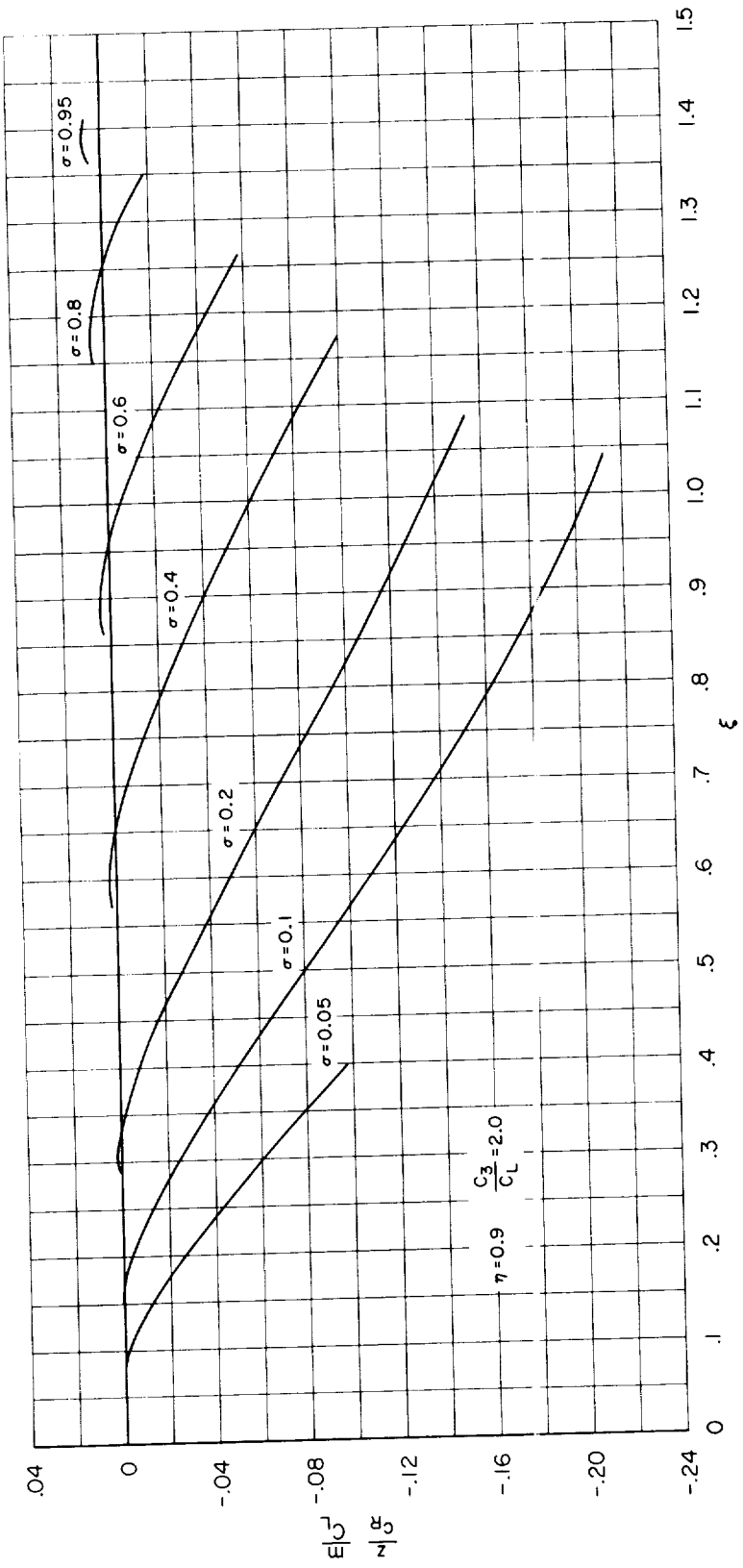

(c) Cambered arrow model.

Figure 22.- Concluded.

NASA TM X-390
National Aeronautics and Space Administration.
INVESTIGATION AT MACH NUMBERS OF 0.60 TO 3.50 OF BLENDED WING-BODY COMBINATIONS WITH CAMBERED AND TWISTED WINGS WITH DIAMOND, DELTA, AND ARROW PLAN FORMS.
George H. Holdaway and Jack A. Mellenthin.
October 1960. 76p.
(NASA TECHNICAL MEMORANDUM X-390)

(Title, Unclassified)

The wing camber and twist were computed to result in nearly elliptical spanwise and chordwise lifting pressure distribution for each plan form and thus to obtain low drag due to lift at Mach numbers for which the velocities normal to the wing leading edge were subsonic. Elliptical chordwise load distributions were not possible for the plan forms and design conditions selected, so these distributions were somewhat different for each plan form. The wings had an aspect ratio of 2 with leading-edge sweeps of 45.00°,
(over)

Copies obtainable from NASA, Washington

I. Holdaway, George H.
II. Mellenthin, Jack A.
III. NASA TM X-390

(Initial NASA distribution: 3, Aircraft.)

NASA

NASA TM X-390
National Aeronautics and Space Administration.
INVESTIGATION AT MACH NUMBERS OF 0.60 TO 3.50 OF BLENDED WING-BODY COMBINATIONS WITH CAMBERED AND TWISTED WINGS WITH DIAMOND, DELTA, AND ARROW PLAN FORMS.
George H. Holdaway and Jack A. Mellenthin.
October 1960. 76p.
(NASA TECHNICAL MEMORANDUM X-390)

(Title, Unclassified)

The wing camber and twist were computed to result in nearly elliptical spanwise and chordwise lifting pressure distribution for each plan form and thus to obtain low drag due to lift at Mach numbers for which the velocities normal to the wing leading edge were subsonic. Elliptical chordwise load distributions were not possible for the plan forms and design conditions selected, so these distributions were somewhat different for each plan form. The wings had an aspect ratio of 2 with leading-edge sweeps of 45.00°,
(over)

Copies obtainable from NASA, Washington

I. Holdaway, George H.
II. Mellenthin, Jack A.
III. NASA TM X-390

(Initial NASA distribution: 3, Aircraft.)

NASA

NASA TM X-390
National Aeronautics and Space Administration.
INVESTIGATION AT MACH NUMBERS OF 0.60 TO 3.50 OF BLENDED WING-BODY COMBINATIONS WITH CAMBERED AND TWISTED WINGS WITH DIAMOND, DELTA, AND ARROW PLAN FORMS.
George H. Holdaway and Jack A. Mellenthin.
October 1960. 76p.
(NASA TECHNICAL MEMORANDUM X-390)

(Title, Unclassified)

The wing camber and twist were computed to result in nearly elliptical spanwise and chordwise lifting pressure distribution for each plan form and thus to obtain low drag due to lift at Mach numbers for which the velocities normal to the wing leading edge were subsonic. Elliptical chordwise load distributions were not possible for the plan forms and design conditions selected, so these distributions were somewhat different for each plan form. The wings had an aspect ratio of 2 with leading-edge sweeps of 45.00°,
(over)

Copies obtainable from NASA, Washington

I. Holdaway, George H.
II. Mellenthin, Jack A.
III. NASA TM X-390

(Initial NASA distribution: 3, Aircraft.)

NASA

NASA TM X-390
National Aeronautics and Space Administration.
INVESTIGATION AT MACH NUMBERS OF 0.60 TO 3.50 OF BLENDED WING-BODY COMBINATIONS WITH CAMBERED AND TWISTED WINGS WITH DIAMOND, DELTA, AND ARROW PLAN FORMS.
George H. Holdaway and Jack A. Mellenthin.
October 1960. 76p.
(NASA TECHNICAL MEMORANDUM X-390)

(Title, Unclassified)

The wing camber and twist were computed to result in nearly elliptical spanwise and chordwise lifting pressure distribution for each plan form and thus to obtain low drag due to lift at Mach numbers for which the velocities normal to the wing leading edge were subsonic. Elliptical chordwise load distributions were not possible for the plan forms and design conditions selected, so these distributions were somewhat different for each plan form. The wings had an aspect ratio of 2 with leading-edge sweeps of 45.00°,
(over)

Copies obtainable from NASA, Washington

I. Holdaway, George H.
II. Mellenthin, Jack A.
III. NASA TM X-390

(Initial NASA distribution: 3, Aircraft.)

NASA

NASA TM X-390

59.04°, and 70.82° and trailing-edge sweeps of
-45.00°, -18.43°, and 41.19° for the models identified
as diamond, delta, and arrow, respectively.

NASA

Copies obtainable from NASA, Washington

NASA TM X-390

59.04°, and 70.82° and trailing-edge sweeps of
-45.00°, -18.43°, and 41.19° for the models identified
as diamond, delta, and arrow, respectively.

NASA

Copies obtainable from NASA, Washington

NASA TM X-390

59.04°, and 70.82° and trailing-edge sweeps of
-45.00°, -18.43°, and 41.19° for the models identified
as diamond, delta, and arrow, respectively.

NASA

Copies obtainable from NASA, Washington

NASA TM X-390

59.04°, and 70.82° and trailing-edge sweeps of
-45.00°, -18.43°, and 41.19° for the models identified
as diamond, delta, and arrow, respectively.

NASA

Copies obtainable from NASA, Washington